On the Sample Complexity of One Hidden Layer Networks with Equivariance, Locality and Weight Sharing

Anonymous authors
Paper under double-blind review

Abstract

Weight sharing, equivariance, and local filters, as in convolutional neural networks, are believed to contribute to the sample efficiency of neural networks. However, it is not clear how each one of these design choices contribute to the generalization error. Through the lens of statistical learning theory, we aim to provide an insight into this question by characterizing the relative impact of each choice on the sample complexity. We obtain lower and upper sample complexity bounds for a class of single hidden layer networks. It is shown that the gain of equivariance is directly manifested in the bound, while getting a similar increase for weight sharing depends on the sharing mechanism. Among our results, we obtain a completely dimension-free bound for equivariant networks for a class of pooling operations. We show that the bound depends merely on the norm of filters, which is tighter than using the spectral norm of the respective matrix. We also characterize the trade-off in sample complexity between the parametrization of filters in spatial and frequency domains, particularly when spatial filters are localized as in vanilla convolutional neural networks.

1 Introduction

In recent years, equivariant neural networks have gained particular interest within the machine learning community thanks to their inherent ability to preserve certain transformations in the input data, thereby providing a form of inductive bias that aligns with many real-world problems. Indeed, equivariant networks have shown remarkable performance in various applications, ranging from computer vision to molecular chemistry, where data often exhibit specific forms of symmetry. Equivariant networks are closely related to their more traditional counterparts, Convolutional Neural Networks (CNNs). CNNs are a particular class of neural networks that achieve equivariance to translation. The convolution operation in CNNs ensures that the response to a particular feature is the same, regardless of its spatial location in the input data. However, the concept of equivariance extends beyond just translation, accommodating a broader spectrum of transformations such as rotations, reflections, and scaling, among others. Group Convolutional Neural Networks (GCNNs) Cohen and Welling (2016a) are the typical example of equivariant neural networks. The inductive bias introduced by equivariance, in the form of symmetry preservation, offers an intuitive connection to their generalization capabilities. By encoding prior knowledge about the structure of the data, equivariant networks can efficiently exploit the inherent symmetries, reducing sample complexity and improving generalization performance. This ability to generalize from a limited set of examples is crucial to their success. Their mathematical foundation is grounded in group representation theory, which provides a powerful framework to understand and design neural networks that are equivariant or invariant to the action of a group of transformations.

Besides the inductive bias of data symmetry, the generalization benefits of CNNs and GCNNs are attributed additionally to the weight-sharing, implemented by the convolution operation, and the locality, implemented by the smaller filter size. In this paper, we study the impact of equivariance, weight-sharing, and locality on generalization within the framework of statistical learning theory. Our focus will be on neural networks with one hidden layer. Similar to works like Vardi et al. (2022); Magen and Shamir (2023), we believe that this study provides a first step toward a better understanding of deeper networks. Getting dimension-free generalization error bounds constitutes an important line of research in the literature. Following this line of

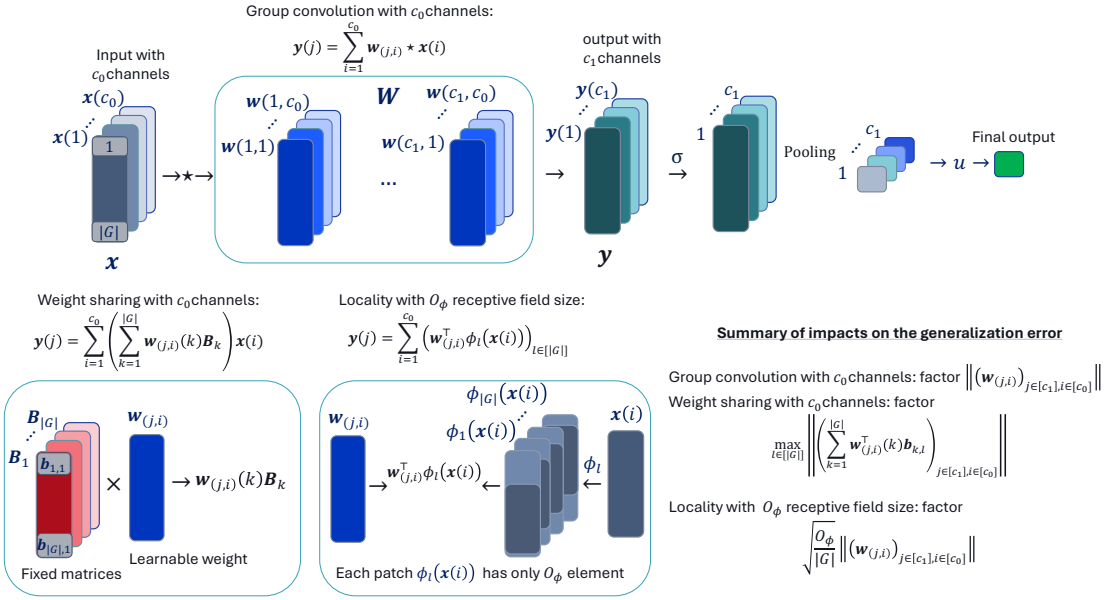

Figure 1: Visualization of the network architectures with equivariance, locality and weight sharing. On the right, we also summarize how each choice impacts the generalization error in our theory.

work, we provide various dimension-free and norm-based bounds for one hidden layer networks. See Appendix J.1 for discussions on the desiderata of learning theory.

Contributions. We consider a class of one hidden layer networks where the first layer is a multi-channel equivariant layer followed by point-wise non-linearity, a pooling layer, and the final linear layer. We assume that the ℓ_2-norm of the parameters of each layer is bounded. For architectures based on group convolution with point-wise non-linearity, we provide generalization bounds for various pooling operations that are completely dimension-free. We obtain a similar norm-based bound for general equivariant networks. We also provide a lower bound on Rademacher complexity that shows the tightness of our bound. We show that no gain is observed if the analysis is conducted for the networks parameterized in the frequency domain. When the equivariant layer is replaced by a layer with, not necessarily equivariant, weight-sharing, we provide as well a dimension-free bound. By studying the bound, it can be seen that some particular weight-sharing schemes, although not all of them, can provide similar generalization guarantees. Next, we provide another bound for networks with local filters and show that the locality can bring additional gain on top of equivariance. We will then show that there is a trade-off between locality in the spatial domain and frequency domain, important for band-limited inputs. The trade-off is characterized by the uncertainty principle. Finally, we provide the numerical verification of our bounds. The generalization bounds are all obtained using Rademacher complexity analysis. We relegate all proofs to the appendix.

Notations. We introduce some of the notations used throughout the paper. We define $[n] := \{1, \dots, n\}$ for $n \in \mathcal{N}$. The term $\|\cdot\|$ refers to the ℓ_2-norm, which for the space of matrices is the Frobenius norm. The spectral norm of a matrix $\boldsymbol{A}$ is denoted by $\|\boldsymbol{A}\|_{2\to 2}$. A positively homogeneous activation function $\sigma(\cdots)$ is a function that satisfies $\sigma(\lambda x) = \lambda \sigma(x)$ for all $\lambda \geq 0$. The loss functions are assumed to be 1-Lipschitz. The matrix of the training data is denoted by $\boldsymbol{X} = [\boldsymbol{x}_1 \dots \boldsymbol{x}_m]$. The terms $\mathcal{L}(h)$ and $\hat{\mathcal{L}}(h)$ denotes, respectively, the test and the training error.

2 Preliminaries

Convolution: a simple example. We start with a simple example of familiar convolutional neural networks, indulging some of the subtleties needed for our later discussions. For an RGB image input, each

convolution filter will slide over the input image and act on its receptive field by simple multiplication. If we just translate the pixels of the input image, ignoring the *corner* pixels, the output of the previous convolution operation would just get translated as well. The act of translation is an example of a *group action*, and the fact that the convolution output is shifted by this act is an example of equivariance property[1]. In what follows, we work with a generalized notion of action captured by group theory, which studies objects like translation and rotation that can combine and have an inverse element.

We introduce key concepts from group and representation theories necessary to present our main results in Appendix A. In the rest of this work, we will generally assume a *compact* group G. Note that this includes any *finite* group. For the most part, we will consider *Abelian* groups, i.e., commutative groups (such as planar rotations or periodic translations).

Equivariance. Given two spaces $\mathcal{X}, \mathcal{Y}$ carrying an action of a group G, a function $\phi : \mathcal{X} \to \mathcal{Y}$ is said to be **equivariant** with respect to G if $\phi(g.x) = g.\phi(x)$ for any $x \in \mathcal{X}$, i.e. if ϕ commutes with the group's action. For example, the spaces $\mathcal{X}, \mathcal{Y}$ could be vector spaces, and the group action $. : G \times \mathcal{X} \to \mathcal{X}$ could be a linear function.

Group Convolution. If G is a *finite* group, the most popular design choice to construct equivariant networks relies on the **group convolution** operator Cohen and Welling (2016a), thereby generalizing typical convolutional neural networks (CNNs). Specifically, given an input signal $x : G \to \mathbb{R}$ over G and a filter $w : G \to \mathbb{R}$, the group convolution produces another output signal $y : G \to \mathbb{R}$ defined as:

$$y(g) = (w \circledast_G x)(g) := \sum_{h \in G} w(g^{-1}h)x(h) \ . \tag{1}$$

Note that the signals x, w, y can be represented as vectors $\boldsymbol{x}, \boldsymbol{w}, \boldsymbol{y} \in \mathbb{R}^{|G|}$; hence, the convolution operation can be expressed as $\boldsymbol{y} = \boldsymbol{W}\boldsymbol{x}$, where $\boldsymbol{W} \in \mathbb{R}^{|G| \times |G|}$ is a group-circulant matrix encoding G-convolution with the filter $\boldsymbol{w}$.

Like in classical CNNs, one typically considers multi-channel input signals $x : G \to \mathbb{R}^{c_0}$, filters $w : G \to \mathbb{R}^{c_1 \times c_0}$ and output signals $y : G \to \mathbb{R}^{c_1}$. We represent a multi-channel signal $x : G \to \mathbb{R}^{c_0}$ as a stack of features over the group G, namely, a tensor $(\boldsymbol{x}(1), \ldots, \boldsymbol{x}(c_0))$ of shape $|G| \times c_0$ (i.e. with c_0 channels and each $\boldsymbol{x}(i) \in \mathbb{R}^{|G|}$). Then, a convolution layer consists of c_1 convolutional filters $\{\boldsymbol{w}_j, j \in [c_1]\}$, each of size $|G| \times c_0$, parametrized by per-channel convolutions $\boldsymbol{w}_{(j,i)} \in \mathbb{R}^{|G|}, i \in [c_0]$; the convolution operation, which yields the output channel j, is given by

$$\boldsymbol{y}(j) = \sum_{i=1}^{c_0} \boldsymbol{w}_{(j,i)} \circledast_G \boldsymbol{x}(i) \in \mathbb{R}^{|G|}, j \in [c_1]$$

In summary, a group convolution layer can be visualized as

$$\overbrace{\left[\begin{array}{c|c|c|c} \boldsymbol{W}_{(1,1)} & \boldsymbol{W}_{(2,1)} & \cdots & \boldsymbol{W}_{(c_0,1)} \\ \hline \boldsymbol{W}_{(1,2)} & \boldsymbol{W}_{(2,2)} & \cdots & \boldsymbol{W}_{(c_0,2)} \\ \hline \vdots & \vdots & \ddots & \vdots \\ \hline \boldsymbol{W}_{(1,c_1)} & \boldsymbol{W}_{(2,c_1)} & \cdots & \boldsymbol{W}_{(c_0,c_1)} \end{array}\right]}^{\boldsymbol{W}} \cdot \overbrace{\left[\begin{array}{c} \boldsymbol{x}(1) \in \mathbb{R}^{|G|} \\ \hline \boldsymbol{x}(2) \in \mathbb{R}^{|G|} \\ \hline \vdots \\ \hline \boldsymbol{x}(c_0) \in \mathbb{R}^{|G|} \end{array}\right]}^{\boldsymbol{x}} = \overbrace{\left[\begin{array}{c} \boldsymbol{y}(1) \in \mathbb{R}^{|G|} \\ \hline \boldsymbol{y}(2) \in \mathbb{R}^{|G|} \\ \hline \vdots \\ \hline \boldsymbol{y}(c_1) \in \mathbb{R}^{|G|} \end{array}\right]}^{\boldsymbol{y}} \tag{2}$$

Here, any $\boldsymbol{W}_{(i,j)} \in \mathbb{R}^{|G| \times |G|}$ block is a group circulant matrix corresponding to G, which encodes a G-convolution parameterised by a filter $\boldsymbol{w}_{i,j} \in \mathbb{R}^{|G|}$. Note that the output of the convolution is a $|G| \times c_1$ signal, i.e. it contains a different value $y(g, j)$ for each group element $g \in G$ and output channel $j \in [c_1]$.

Note also that the group G naturally acts on a signal $x : G \to \mathbb{R}^c$ as $g : x \mapsto g.x$, with $[g.x](h) = x(g^{-1}h)$. Then, one can show that the group convolution operator above is equivariant with respect to this action on its input and output, i.e. $w \circledast_G g.x = g.(w \circledast_G x)$. Additionally, it is well known, e.g. Cohen et al. (2018); Kondor and Trivedi (2018), that group convolutions with learnable filters in this form parameterize the most

[1]We would like to emphasize again that the example is not perfect. First, the convolution in CNN is really a cross-correlation. Second, the conventional CNNs are only approximately translation equivariant because of the finite input size and the corner pixels.

general linear equivariant maps between feature spaces of signals over a compact group G. Finally, GCNN typically uses an activation function applied point-wise on the convolution output. In our 1-layer architecture, a first convolution layer is followed by a pointwise activation layer and, then, a per-channel - average or max - pooling layer, which produces c_1 invariant features. These final features are mixed with the final linear layer $\boldsymbol{u}$. See Figure 1 for more details. The final network is then given as:

$$h_{\boldsymbol{u},\boldsymbol{w}}(\boldsymbol{x}) := \boldsymbol{u}^\top P \circ \sigma \begin{pmatrix} \sum_{i=1}^{c_0} \boldsymbol{w}_{(1,i)} \circledast_G \boldsymbol{x}(i)) \\ \vdots \\ \sum_{i=1}^{c_0} \boldsymbol{w}_{(c_1,i)} \circledast_G \boldsymbol{x}(i)) \end{pmatrix} \tag{3}$$

where $P(\cdot)$ is the pooling operation, and $\boldsymbol{w} := (\boldsymbol{w}_{(j,i)})_{j\in[c_1],i\in[c_0]}$ is the concatenation of all kernels.

3 Related Works

Equivariant and Geometric Deep Learning Previous works attempted to improve machine learning models by leveraging prior knowledge about the symmetries and the geometry of a problem Bronstein et al. (2021). A variety of design strategies have been explored in the literature to achieve group equivariance, for example via equivariant MLPs Shawe-Taylor (1993; 1989); Finzi et al. (2021), group convolution Cohen and Welling (2016a); Kondor and Trivedi (2018); Bekkers et al. (2018), Lie group convolution Bekkers (2020); Finzi et al. (2020), steerable convolution Cohen and Welling (2016b); Cohen et al. (2018); Worrall et al. (2017); Weiler et al. (2018b;a); Thomas et al. (2018); Weiler and Cesa (2019); Fuchs et al. (2020); Brandstetter et al. (2021); Cesa et al. (2022) and, very recently, by using geometric algebra Ruhe et al. (2023); Brehmer et al. (2023), to only mention a few. Other previous approaches include Mallat (2012); Dieleman et al. (2016); Defferrard et al. (2019). Some of these ideas have also been used to generalize convolution beyond groups to more generic manifolds via the framework of Gauge equivariance Cohen et al. (2019); Weiler et al. (2021). While equivariance is generally considered a powerful inductive bias leading to improved data efficiency, this large selection of equivariant designs raises the following question: what impact different architectural choices have on performance and to what extent do they aid generalization?

Generalization Properties of Equivariant networks Some previous works tried to answer some aspects of this question. Shawe-Taylor (1991) is of the first works studying the relation between invariance and generalization. For example, Sokolić et al. (2017a) extend the robustness-based generalization bounds found in Sokolić et al. (2017b) by assuming the set of transformations of interest change the inputs drastically, thereby proving that the generalization error of a G-invariant classifier scales $1/\sqrt{|G|}$, where $|G|$ is the cardinality of the finite equivariance group G. Bietti and Mairal (2019) study the stability of some particular compact group equivariant models and also describe an associated Rademacher complexity and generalization bound. Lyle et al. (2020) investigate the effect of invariance under the lenses of the PAC-Bayesian framework but do not provide an explicit bound. Later, Elesedy and Zaidi (2021) use VC-dimension analysis and derive more concrete bounds. Elesedy (2022) studies compact-group equivariance in PAC learning framework and equates learning with equivariant hypotheses and learning on a reduced data space of orbit representatives to obtain a sample complexity bound. Sannai et al. (2021) propose a similar idea, proving that equivariant models work in a reduced space, the Quotient Feature Space (QFS), whose volume directly affect the generalization error. While the result relaxes the robustness assumption in Sokolić et al. (2017a), the final bound is suboptimal with respect to the sample size. PAC learnability under transformation invariance is also studied in Shao et al. (2022). Zhu et al. (2021) characterize the generalization benefit of invariant models using an argument based on the covering number induced by a set of transformations. More recently, Behboodi et al. (2022) leverages a representation-theoretic construction of equivariant networks and provides a norm-based PAC-Bayesian generalization bound inspired by Neyshabur et al. (2018). Finally, Petrache and Trivedi (2023) considers a more general setting, allowing for approximate, partial, and misspecified equivariance and studying how the relation between data and model equivariance error impacts generalization.

Generalization in generic neural networks Many works in the literature have previously investigated the generalization properties of deep learning methods. Zhang et al. (2017) first noted that a model trained on random labels can achieve small training error while producing arbitrarily large generalization errors. This

result raised a new challenge in the field since popular uniform complexity measures such as VC-dimensions are inconsistent with this finding. This inspired many recent works which tried to explain generalization in terms of other quantities, such as margin or norms of the learnable weights; a few nonexhaustive examples are Wei and Ma (2019); Sokolić et al. (2017b); Neyshabur et al. (2018); Arora et al. (2018); Bartlett et al. (2017); Golowich et al. (2018); Dziugaite and Roy (2018a); Long and Sedghi (2019); Vardi et al. (2022); Ledent et al. (2021); Valle-Pérez and Louis (2020). The PAC Bayesian framework is a particularly popular method and has been applied to neural networks in many previous works, e.g. see Neyshabur et al. (2018); Biggs and Guedj (2022); Dziugaite and Roy (2017; 2018b;a); Dziugaite et al. (2020); Lotfi et al. (2022). Jiang et al. (2020) perform a thorough experimental comparison of many complexity measures and identifies some failure cases; see also Nagarajan and Kolter (2019); Koehler et al. (2021); Negrea et al. (2021) for further discussion on uniform complexity measures and their limitations. The norm-based bounds can still be tight and informative for shallow networks considered in this work.

Generalization bounds for Convolutional neural networks As one of the most popular deep learning architectures, convolutional neural networks (CNNs) have received particular attention in the literature. Generalization studies on CNNs are especially relevant for our work since we focus significantly on equivariance to finite and abelian groups, which can often be realized via periodic convolution. Pitas et al. (2019); Long and Sedghi (2019); Vardi et al. (2022); Ledent et al. (2021) previously studied these architectures. In particular, Graf et al. (2022) recently established two covering-numbers-based bounds for convolution models.

4 Sample Complexity Bounds For Equivariant Networks

We consider the group convolutional networks as defined in eq. 3. We assume that the input to the network is bounded as $\|\boldsymbol{x}\| \leq b_x$[2]. Consider the following hypothesis space:

$$\mathcal{H} := \{h_{\boldsymbol{u},\boldsymbol{w}} : \|\boldsymbol{u}\| \leq M_1, \|\boldsymbol{w}\| \leq M_2\}, \tag{4}$$

where $\boldsymbol{u} \in \mathbb{R}^{c_1}, \boldsymbol{w} \in \mathbb{R}^{c_0 c_1 |G|}$. The hypothesis space is the group convolution network class that has bounded Euclidean norm on the kernels. For this network, we derive dimension-free bounds.

Since the pooling operation is a permutation invariant operation, we can use Theorem 7 in Zaheer et al. (2017) to show that one can always find two functions $\phi : \mathbb{R}^{|G|+1} \to \mathbb{R}$ and $\rho : \mathbb{R} \to \mathbb{R}^{|G|+1}$ such that $P \circ \boldsymbol{z} = \phi\left(\frac{1}{|G|}\sum_{i=1}^{|G|} \rho(z_i)\right)$. We can provide the following generalization bound for a subset of such representations, namely for positively homogeneous $\phi : \mathbb{R} \to \mathbb{R}$ and $\rho : \mathbb{R} \to \mathbb{R}$.

Theorem 4.1. *Consider the hypothesis space $\mathcal{H}$ defined in eq. 4. If $P(\cdot)$ is the pooling operation represented as $P \circ \boldsymbol{z} = \phi(\frac{1}{|G|}\mathbf{1}^\top \rho(\boldsymbol{z}))$, where the two functions $\rho(\cdot)$, $\phi(\cdot)$ and the activation function $\sigma(\cdot)$ are all 1-Lipschitz positively homogeneous activation function, then with probability at least $1-\delta$ and for all $h \in \mathcal{H}$, we have:*

$$\mathcal{L}(h) \leq \hat{\mathcal{L}}(h) + 2\frac{b_x M_1 M_2}{\sqrt{m}} + 4\sqrt{\frac{2\log(4/\delta)}{m}}.$$

The proof leverages Rademacher complexity analysis and is presented in Appendix C.4. Note that the assumption of positively homogeneity is only needed to utilize the peeling technique of Golowich et al. (2018). We expect that similar techniques from Vardi et al. (2022) can be used to extend the result to Lipschitz activation functions.

Average pooling. Consider now the special case of average pooling operation $P(\boldsymbol{x}) = \frac{1}{|G|}\mathbf{1}^\top \boldsymbol{x}$. This is a linear layer; therefore, it can be combined with the last layer $\boldsymbol{u}$ to yield a standard two-layer neural network. We can utilize the results from Vardi et al. (2022); Golowich et al. (2018). The combination of the layer $\boldsymbol{u}$ and average pooling is a linear layer with the norm $M_1/\sqrt{|G|}$, and the matrix $\boldsymbol{W}$, a circulant matrix, has

[2]For all the results in the paper, we can use a data-dependent bound on the input. Namely, it suffices to assume that $\max_{i\in[m]} \|\boldsymbol{x}_i\| \leq b_x$.

the Frobenius norm $\sqrt{|G|}M_2$. The product of these norms would be bounded by M_1M_2. Being a special case of the model in Vardi et al. (2022), we can use their results off-the-shelf to get an upper bound on the sample complexity that depends only on M_1M_2 for Lipschitz-activation functions (Theorem 2 of Vardi et al. (2022)). We provide an independent proof for positively homogeneous activation functions in Appendix C.2 with a clean form. Note that the authors in Vardi et al. (2022) provide a result for average pooling that contains the term O_ϕ, the maximal number of patches that any single input coordinate appears in. This term is equal to $|G|$ in our case, which is canceled out by the average pooling term. Their bound depends on the spectral norm of the underlying circulant matrix, which can be bigger than the norm of the filter provided here. But, their proof can be reworked with the norm of convolutional filter instead, in which case, their result will be the special case of ours.

Impact of group size. The above theorem is dimension-free, and there is no dependence on the number of input and output channels c_0 and c_1, as well as the group size $|G|$. Note that for average pooling and sufficiently smooth activation functions, we can use even the stronger result (Theorem 4 of Vardi et al. (2022)) and get a bound that depends on $M_1M_{2\to2}/\sqrt{|G|}$, where $M_{2\to2}$ is the spectral norm of $\boldsymbol{W}$. This manifests the impact of group size on the generalization similar to Sokolić et al. (2017a); Behboodi et al. (2022).

Max pooling. We cannot rely on the previous results for Max pooling operation, since the peeling argument would not work. Theorem 7 and 8 of Vardi et al. (2022) provide a bound for max pooling, however their network does not contain the linear aggregation $\boldsymbol{u}$ after max-pooling, and their bound contains dimension dependencies such as $\log(|G|c_1)$ or $\log(m)$. In Appendix C.3, we provide a bound for max pooling that depends merely on $\log(|G|)$ but contains a data dependent term that can have poor scaling.

To summarize, we have established that for a single hidden layer group convolution network, we can have a dimension-free bound that depends merely on the norm of filters.

Remark 4.2 (Frequency Domain Analysis). The authors in Behboodi et al. (2022) improved the PAC-Bayesian generalization bound by conducting their analysis using the representation in the frequency domain. In our Rademacher analysis, such a shift would not bring any additional gain, and we basically recover the same bound. We provide the details in the supplementary materials.

4.1 Bounds for Multi-Layer Equivariant Network

In this section, we study a simple extension to multi-layer group equivariant networks. Consider the following network with L hidden layer:

$$h_{\boldsymbol{u},\{\boldsymbol{w}^{(l)},l\in[L]\}}(\boldsymbol{x}) := \boldsymbol{u}^\top P \circ \sigma(\boldsymbol{W}^{(L)}\sigma(\boldsymbol{W}^{(L-1)}\dots\sigma(\boldsymbol{W}^{(1)})\boldsymbol{x}\dots) \tag{5}$$

where $P(\cdot)$ is the average pooling operation, $\sigma(\cdot)$ is the ReLU function. Each linear layer $\boldsymbol{W}^l$ is the same as the mapping in eq. 2 but with c_{l-1} and c_l as the input and output channels. The new hypothesis space is given by:

$$\mathcal{H}^{(L)} := \left\{h_{\boldsymbol{u},\{\boldsymbol{w}^{(l)},l\in[L]\}} : \|\boldsymbol{u}\| \le M_1, \|\boldsymbol{w}_i\| \le M_{i+1}, i \in [L]\right\}. \tag{6}$$

We have the following theorem.

Theorem 4.3. *Consider the hypothesis space $\mathcal{H}^{(L)}$ defined in eq. 6. With probability at least $1-\delta$ and for all $h \in \mathcal{H}$, we have:*

$$\mathcal{L}(h) \le \hat{\mathcal{L}}(h) + 2\frac{b_x|G|^{\frac{L-1}{2}}M_1M_2\dots M_{L+1}}{\sqrt{m}} + 4\sqrt{\frac{2\log(4/\delta)}{m}}.$$

The proof can be found in Appendix C.5. Although our bound has no dependence on the number of input and hidden layer channels, it still has dependence on $|G|^{(L-1)/2}$ and is not completely dimension-free. Using some other techniques, it can be improved to $(L-1)\log|G|$ for $L>1$; see the proof for the discussion on this point. It is worth pointing out that the generalization bounds for deeper networks are known to suffer from many shortcomings and generally fail to correlate well with the empirical generalization error. See Jiang et al. (2020); Nagarajan and Kolter (2019) for further discussions.

4.2 Lower bound on the Rademacher Complexity Analysis

A natural question that might come up is whether the obtained bound is tight or not. In this section, we provide an answer to this by showing that the Rademacher complexity is lower bounded in a similar fashion for a class of networks.

Theorem 4.4. *Consider the hypothesis space $\mathcal{H}$ defined in eq. 4. If $P(\cdot)$ is the average pooling operation, $\sigma(\cdot)$ is the ReLU activation function, then there is a data distribution such that the Rademacher complexity is lower bounded by $c\frac{b_x M_1 M_2}{\sqrt{m}}$ where c is an independent constant.*

The proof is provided in the Appendix E. Note that Rademacher complexity (RC) bounds are known to be tight for shallow models, for example, for SVMs. Indeed, if one fixes the first layer and only trains the last linear layer with weight decay, the model is equivalent to hard-margin SVM, for which RC bounds are tight. We also provide additional evidence in the numerical result section.

5 General Equivariant Networks

The focus of our analysis in the above section has been on group convolutional networks and related architectures. In particular, we had considered the equivariance for finite Abelian groups for which the filters were implemented using multi-channel convolution operation. We now look at the general equivariant networks w.r.t. a compact group. As we will see, the analysis for these networks would be based on their MLP structure.

We follow the procedure described in Cohen and Welling (2016b); Cesa et al. (2022); Weiler et al. (2018b). We assume a general input space where the action of the compact group G on the space is given by a linear map $\rho_0(g)$ for $g \in G$. For this space, the filters of the first layer, similarly to GCNs, are parametrized in the frequency domain. The generalization of Fourier analysis to compact groups is done via the notion of *irreducible representations* (irreps). An irrep, typically denoted by ψ, can be thought as a frequency component of a signal over the group.

Using tools from the representation theory, the map $\rho_0(g)$ can be represented in the frequency domain as the direct sum of irreps $\boldsymbol{Q}_0^\top \left(\bigoplus_\psi \bigoplus_{i=1}^{m_{0,\psi}} \psi\right) \boldsymbol{Q}_0$ where $m_{0,\psi}$ is the multiplicity of the irrep ψ. The matrix $\boldsymbol{Q}_0$ is a unitary matrix representing the generalized Fourier transform given by $\hat{\boldsymbol{x}} = \boldsymbol{Q}_0 \boldsymbol{x}$. See Appendix A.1 for detailed definitions. A similar frequency domain representation can be obtained for the hidden layer in terms of irreps, each with multiplicity $m_{1,\psi}$. The block diagonal structure of filters in the multi-channel GCNs given in eq. 25 is now obtained by a general block-diagonal structure. The equivariant neural network is represented as

$$h_{\hat{\boldsymbol{u}},\hat{\boldsymbol{W}}} := \hat{\boldsymbol{u}}^\top \boldsymbol{Q}_2 \sigma \left(\boldsymbol{Q}_1 \bigoplus_\psi \bigoplus_{i=1}^{m_{1,\psi}} \sum_{j=1}^{m_{0,\psi}} \hat{\boldsymbol{W}}(\psi, i, j) \hat{\boldsymbol{x}}(\psi, j) \right).$$

Since we are working with the point-wise non-linearity σ in the *spatial domain*, two unitary transformations $\boldsymbol{Q}_1$ and $\boldsymbol{Q}_2$ are applied as Fourier transforms from the frequency domain to the spatial domain. The last layer $\hat{\boldsymbol{u}}$ should be chosen to yield a group invariant function, which means that the vector $\hat{\boldsymbol{u}}$ only aggregates the frequencies of the trivial representation ψ_0, and it is zero otherwise. To use an analogy with group convolutional networks, $\boldsymbol{Q}_1$ and $\boldsymbol{Q}_2$ are the Fourier matrices, and $\hat{\boldsymbol{u}}$ is a combination of the pooling, which projects into the trivial representation of the group, and the last aggregation step. The general equivariant networks are defined in Fourier space as follows:

$$\mathcal{H}_{\hat{\boldsymbol{u}},\hat{\boldsymbol{W}}} := \left\{ h_{\hat{\boldsymbol{u}},\hat{\boldsymbol{W}}} : \|\hat{\boldsymbol{u}}\| \leq M_1, \left\|\hat{\boldsymbol{W}}\right\| \leq M_2 \right\}.$$

Note that the hypothesis space assumes a bounded norm of the filters' parameters in the frequency domain. For this hypothesis space, we can get a similar dimension-free bound.

Theorem 5.1. *Consider the hypothesis space $\mathcal{H}_{\hat{\boldsymbol{u}},\hat{\boldsymbol{W}}}$ of equivariant networks with bounded weight norms. If the activation function $\sigma(\cdot)$ is 1-Lipschitz positively homogeneous, then with probability at least $1-\delta$ for all*

$h \in \mathcal{H}_{\hat{\boldsymbol{u}},\hat{\boldsymbol{W}}}$, we have:

$$\mathcal{L}(h) \leq \hat{\mathcal{L}}(h) + 2\frac{b_x M_1 M_2}{\sqrt{m}} + 4\sqrt{\frac{2\log(4/\delta)}{m}}.$$

The proof is presented in Appendix D. This result provides another dimension-free bounds for equivariant networks that depend merely on the norm of the kernels. Note that the network has a standard MLP structure, so the result can be obtained using techniques used in Golowich et al. (2018). Also, note that constructing equivariant networks in the frequency domain is useful in steerable networks to deal with continuous rotation groups Poulenard and Guibas (2021); Cesa et al. (2022), while the parametrization in the spatial domain is pursued in works like Bekkers (2020); Finzi et al. (2020).

6 Generalization Bounds for Weight Sharing

In this section, we try to answer the question whether the gain of our bound lies in the specific equivariant architecture or weight sharing. The answer is subtle. Indeed, an arbitrary type of weight sharing will not bring out the generalization gain. However, there are weight-sharing schemes that can lead to a similar gain without necessarily being equivariant.

For a fair comparison with the group convolution network explained above, we consider an architecture with the same number of effective parameters shared similarly. The weight-sharing network is specified as follows:

$$h^{w.s.}_{\boldsymbol{u},\boldsymbol{w}}(\boldsymbol{x}) := \boldsymbol{u}^\top P \circ \sigma \begin{pmatrix} \sum_{c=1}^{c_0} \left(\sum_{k=1}^{|G|} \boldsymbol{w}_{(1,c)}(k) \boldsymbol{B}_k \right) \boldsymbol{x}(c) \\ \vdots \\ \sum_{c=1}^{c_0} \left(\sum_{k=1}^{|G|} \boldsymbol{w}_{(c_1,c)}(k) \boldsymbol{B}_k \right) \boldsymbol{x}(c) \end{pmatrix}, \tag{7}$$

where $\boldsymbol{B}_k$'s are fixed $|G| \times |G|$ matrices inducing the weight sharing scheme. These matrices are not trained using data and merely specify how the weights are shared in the network. For example, if $\boldsymbol{B}_k$'s are chosen as the basis for the space of circulant matrices, the setup boils down to the group convolution network.

The corresponding hypothesis space is defined as:

$$\mathcal{H}^{w.s.} = \left\{ h^{w.s.}_{\boldsymbol{u},\boldsymbol{w}}(\boldsymbol{x}) : \|\boldsymbol{u}\| \leq M_1, \|\boldsymbol{w}\|_{\boldsymbol{B}} \leq M_2^{w.s.} \right\}$$

where

$$\|\boldsymbol{w}\|_{\boldsymbol{B}} := \max_{l \in [|G|]} \left\| \left(\sum_{k=1}^{|G|} \boldsymbol{w}_{(j,c)}(k) \boldsymbol{b}_{k,l}^\top \right)_{c \in [c_0], j \in [c_1]} \right\|_F .$$

The following proposition provides a purely norm based generalization bound.

Proposition 6.1. For the class of functions h in the hypothesis space $\mathcal{H}^{w.s.}$ with the average pooling operation P, $\sigma(\cdot)$ as a 1-Lipschitz positively homogeneous activation function, the generalization error is bounded as:

$$\mathcal{L}(h) \leq \hat{\mathcal{L}}(h) + 2\frac{b_x M_1 M_2^{w.s.}}{\sqrt{m}} + 4\sqrt{\frac{2\log(4/\delta)}{m}}.$$

Note that if $\boldsymbol{b}_{k,l}$'s are the rows of the circulant matrices, then we end up with the same result as before with $M_2^{w.s.} = M_2$. Interestingly, if the vectors $\{\boldsymbol{b}_{k,l} : k \in [|G|]\}$'s are orthogonal to each other for each $l \in [|G|]$, and all of them have unit norm, i.e., $\|\boldsymbol{b}_{k,l}\| = 1$, then we also get $M_2^{w.s.} = M_2$. The conclusion is that the weight sharing can impact the generalization similarly to the group convolution, even if the construction does not arise from the group convolution. This does not generally hold, particularly if the row vectors of matrices $\boldsymbol{B}_k$ are not orthogonal. On the other hand, the gain of equivariance shows itself for distributions with built-in symmetries.

7 Generalization Bounds for Local Filters

In previous sections, we observed that the impact of equivariance on the generalization is very similar to that of weight sharing under an appropriately chosen basis. Another argument relates the generalization benefits of convolutional neural networks to the use of local filters, where the same filter is applied to a number of patches. The patches have lower dimensions, and the filters similarly have lower dimensions than the total input dimension. Note that this goes beyond the benefit of weight sharing mentioned in the previous section. One example is Theorem 6 in Vardi et al. (2022); we follow their setup. In their case, each convolution operation $\boldsymbol{w}_{(j,k)} \circledast_G \boldsymbol{x}(k)$ can be represented as $\left(\boldsymbol{w}_{(j,k)}^\top \phi_1(\boldsymbol{x}(k)) \dots \boldsymbol{w}_{(j,k)}^\top \phi_{|G|}(\boldsymbol{x}(k))\right)$, where $\phi_l(\cdot)$ represents the patch l. Each patch selects a subset of input entries. The patches $\Phi = \{\phi_l, l \in [|G|]\}$ are assumed to be *local*, in the sense that each coordinate in $\boldsymbol{x}(k)$ appears at most in O_Φ number of patches with $O_\Phi < |G|$. More formally, for any vector $\boldsymbol{x}$ and a set $S \subset [|G|]$, define the vector $\boldsymbol{x}_S := (x_i)_{i \in S}$, i.e., with entries selected from the index in S. Define the patch $\phi_l : \mathbb{R}^{|G|} \to \mathbb{R}^{n'}$ as $\phi_l(\boldsymbol{x}) := \boldsymbol{x}_{S_l}$ for a subset S_l. The group convolution network with locality is defined as:

$$h^\Phi_{\boldsymbol{u},\boldsymbol{w}}(\boldsymbol{x}) = \boldsymbol{u}^\top P \circ \sigma \begin{pmatrix} \sum_{k=1}^{c_0} \left(\boldsymbol{w}_{(1,k)}^\top \phi_l(\boldsymbol{x}(k))\right)_{l \in [|G|]} \\ \vdots \\ \sum_{k=1}^{c_0} \left(\boldsymbol{w}_{(c_1,k)}^\top \phi_l(\boldsymbol{x}(k))\right)_{l \in [|G|]} \end{pmatrix}.$$

By reorganizing the weights in each row corresponding to each patch, the whole network is presented as $\boldsymbol{u}^\top P \circ \sigma(\boldsymbol{W}\boldsymbol{x})$, where we assume that the matrix $\boldsymbol{W}$ conforms to the set of patches Φ. The hypothesis space with locality is defined as

$$\mathcal{H}^\Phi = \{h^\Phi_{\boldsymbol{u},\boldsymbol{w}}(\boldsymbol{x}) : \|\boldsymbol{u}\| \le M_1, \|\boldsymbol{w}\| \le M_2\}.$$

For this class of functions, it can be shown that there is a generalization benefit in using local filters besides the gain of equivariance or proper weight sharing. This conclusion is captured in the following result.

Proposition 7.1. Consider the hypothesis space of functions $\mathcal{H}^\Phi$ constructed by patches Φ, the average pooling operation P, 1-Lipschitz positively homogeneous activation function σ. Let O_Φ be the maximal number of patches that any input entry appears in. Then, with probability at least $1-\delta$ and for all $h \in \mathcal{H}^\Phi$, we have:

$$\mathcal{L}(h) \le \hat{\mathcal{L}}(h) + 2\sqrt{\frac{O_\Phi}{|G|}} \frac{b_x M_1 M_2}{\sqrt{m}} + 4\sqrt{\frac{2\log(4/\delta)}{m}}.$$

Compared with the result above, the locality assumption brings an additional improvement of $\frac{O_\Phi}{|G|}$. Although the proof focuses on average pooling and group convolution, the same results can be obtained for weight sharing. We should only change the filter parametrization from the matrix $\boldsymbol{B}_k$ basis to the vector basis $\boldsymbol{b}_k$ given as $\left(\sum_{k=1}^{|G|} \boldsymbol{w}_{(j,c)}(k)\boldsymbol{b}_k\right)$.

The architecture considered in Vardi et al. (2022) is a single-channel version of our result (see more discussions in Appendix J). In that case, the difference in their bounds is in using the spectral norm of $\boldsymbol{W}$. However, their proof only needs a bound on the Euclidean norm of weights, which would end in the same result as ours.

The analysis so far has focused on the local filters in the spatial domain. However, the filters are also applied per frequency in the frequency domain and are, therefore, local. This can be seen from the block diagonal structure of filters ($\bigoplus_\psi \hat{w}(\psi)$). In this sense, the filters in the frequency domain are already local. When the filters are band-limited in the frequency domain, we have an additional notion of locality. In practice, this is useful when the input is also band-limited; therefore, not all the frequencies are useful for learning. This introduces a fundamental trade-off for locality benefits arising from the uncertainty principle Donoho and Stark (1989); Folland and Sitaram (1997). According to the uncertainty principle, the band-limited filters with B non-zero components will have at least $|G|/B$ non-zero entries in the spatial domain (see Section I for more details). The trade-off is captured in the following proposition.

Proposition 7.2. Consider the hypothesis space of group convolution networks with band-limited filters. If the filters have B non-zero entries in the frequency domain, then the generalization error term in Proposition 7.1 for the smallest spatial filters is at least of order $\mathcal{O}(b_x M_1 M_2/\sqrt{mB})$.

As it can be seen, the assumption of band-limitedness can potentially bring the gain of order $1/B$ if the filters are spatially local. To summarize, there is a gain in using local filters. However, since band-limited filters are more efficient for band-limited signals, the uncertainty principle imposes a minimum spatial size for band-limited filters.

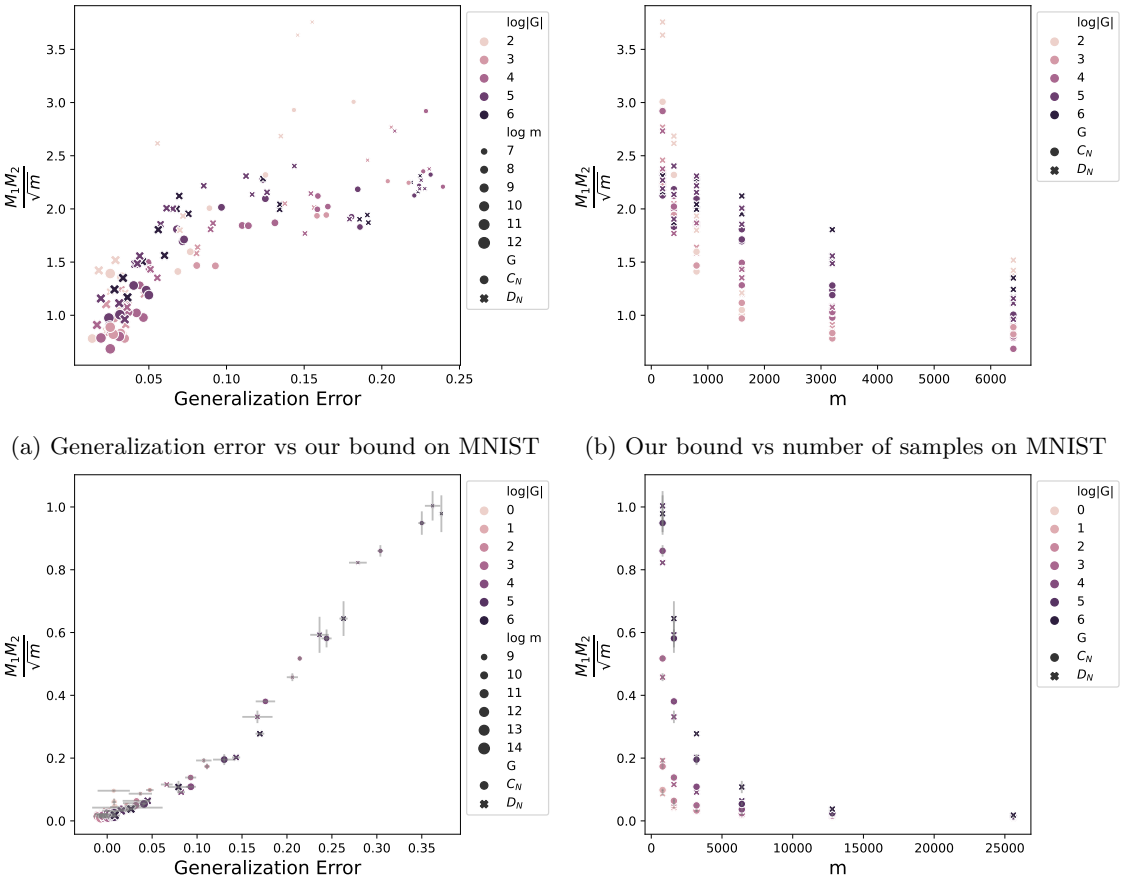

(a) Generalization error vs our bound on MNIST (b) Our bound vs number of samples on MNIST

(c) Generalization error vs our bound on CIFAR10 (d) Our bound vs number of samples on CIFAR10

Figure 2: Numerical results for the generalization error on the rotated MNIST and CIFAR10 datasets. The plots on the left, (a)-(c), confirm that our theoretical bound captures the effect of different configurations - equivariance groups G, training set sizes m and datasets - on the generalization error, i.e. there is a positive correlation between the generalization error and our theoretical bound $\frac{M_1 M_2}{\sqrt{m}}$ across all these cases. On the right, (b)-(d), we verify the bound decreases following a trend similar to $\frac{1}{\sqrt{m}}$ and approaching zero for large training set sizes m.

8 Numerical Results

Let us first introduce the two family of groups we consider in our experiments: the *cyclic group* C_n containing n discrete rotations and the *dihedral group* D_n of n discrete rotations and n reflections (see Def. A.2 and Def. A.3 for precise definitions of these groups).

In this section, we validate our theoretical results on a variation of the rotated MNIST and CIFAR10 datasets where we consider a simpler binary classification task (determining whether a digit is smaller or larger than 4 in MNIST and whether an image belongs to the first 5 classes of CIFAR10 or not). Rather than working

with raw images, we pre-process the dataset by linearly projecting each image via a fixed randomly initialized $G = D_{32}$-steerable convolution layer Weiler and Cesa (2019) to a single 6400-dimensional feature vector[3] - interpreted as a $c_0 = 100$-channels signal over $G = D_{32}$; see Appendix K for more details and Fig. 5 for a visualization of this linear projection. When constructing equivariance to a subgroup $G < D_{32}$, this feature vector is interpreted as a $c_0 = 100 \cdot \frac{|D_{32}|}{|G|}$-channels signal over G. We design our equivariant networks as in Eq. 3 and use $c_1 \cdot |G| \approx 2000$ total intermediate channels for all groups G in the MNIST experiments and $c_1 \cdot |G| \approx 4000$ in the CIFAR10 ones. The dataset is then augmented with random D_{32} transformations to make it symmetric. Hence, we expect that G-equivariant models with G closer to D_{32} to perform best.

In these experiments, we are interested in how well our theoretical bound correlates with the observed trends. In particular, we focus on the $\frac{M_1 M_2}{\sqrt{m}}$ term which is the main component in our bounds. In Fig 2, we evaluate the networks on different values of training set size m and on different equivariance groups G. We first observe that the $\frac{M_1 M_2}{\sqrt{m}}$ term correlates well with the empirical generalization error on both the MNIST dataset in Fig. 2a and the CIFAR10 dataset in Fig. 2c. In particular, larger groups G achieve both lower generalization error and lower value of our norm bound. We also note that this term decreases as $1/\sqrt{m}$ in Fig. 2b, which indicates that our bound becomes non-vacuous as m increases, and we do not suffer from deficiencies of other norm based bounds Nagarajan and Kolter (2019).

Overall, *these results suggest that our bound can explain generalization across different choices of equivariance group G, as well as different training settings.*

Next, we investigate how other equivariant design choices affect generalization and verify if our bound can model this effect. Precisely, when parameterizing the filters over the group G in the frequency (i.e. *irreps*) domain (as in Sec 5), it is common to only use a smaller subset of all frequencies. A bandlimited sub-set of frequencies can be interpreted as a form of locality in the frequency domain, in analogy to the local filters in Sec 7. In Fig.3, we experiments on CIFAR10 with different variations of our equivariant architecture obtained by varying the maximum frequency used to parameterize filters. In these experiments, we keep the training dataset size fixed to $m = 3200$ and we only consider the largest groups (since a wider range of frequencies in $[0, \ldots, N/2]$ can be chosen).

In Fig.3, we find that *our bound captures the effect of locality in the frequency domain on the generalization.*

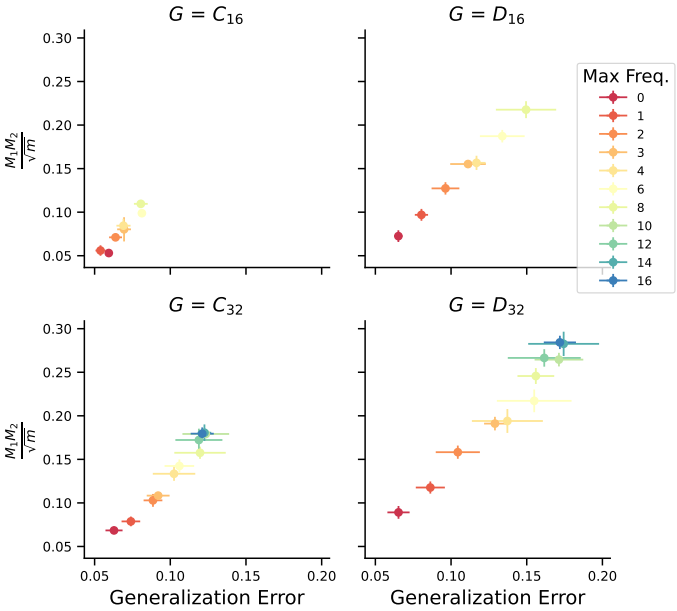

Figure 3: Our bound vs the generalization error on CIFAR10 (trainingset size $m = 3200$) when varying the maximum frequency used to parameterize the filters, which is the locality effect in the frequency domain. Each dot and its error bars represent the mean and standard deviation over at least 3 runs with the same configuration. As expected, *architectures leveraging a lower frequency design achieve lower generalization error* and our bound can exactly capture this effect. Note that increased frequencies are still beneficial for the final test performance: we study the trade-off between generalization and test performance as a function of the model frequency in Fig. 4.

[3]This is a random linear transformation of the input images into feature vectors: the reader can think of this as analogous to reshaping an image before feeding it into an MLP, but with some care to preserve rotation and reflection equivariance. Note also that, since the output (6400) is much larger than the number of input pixels, this transformation is practically invertible and preserves all relevant input information.

In Fig. 3, we observed that higher frequencies typically lead to worse generalization. For this reason, we include a final study to explore the effect of locality in the frequency domain - i.e. band-limitation - on the final test performance of the models and the associated trade-offs between generalization and expressivity.

Fig. 4 compares the generalization error with the final test accuracy of some of our models, when varying the maximum frequency of the filters and the training set size m. This visualization highlights a particular behavior: low-frequency models tend to achieve lower generalization error at the cost of worse data fitting (lower test accuracy). Conversely, higher frequency models often show higher generalization errors (especially in the low data regime) but achieve much higher test performance. Moreover, high frequency models benefit the most from increased dataset size m. These properties lead to the (multiple) U-shaped patterns in Fig. 4: on the smaller datasets (light dots in Fig. 4), while increasing frequencies leads to improved test accuracy, it also increases the generalization error. On the other hand, in the larger dataset (dark dots in Fig. 4), higher frequencies directly improve the test performance and even show minor improvements in generalization error.

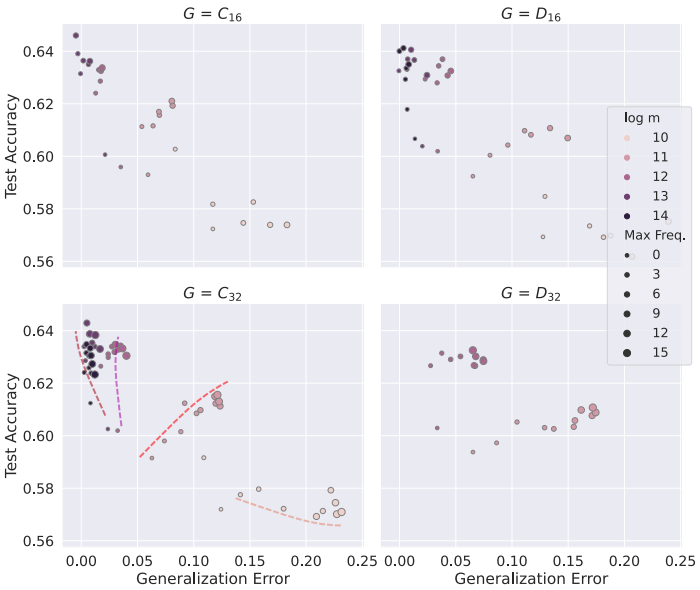

Figure 4: Test accuracy vs Generalization error on CIFAR10 when varying the *maximum frequency* used to parameterize the filters and the training set size m. Each dot is the average performance over at least 3 runs with the same configuration. In Fig. 3, we found that higher frequencies correlated with higher generalization error: here, we study the trade-off between generalization and test performance. For each dataset size m, increasing the frequency improves the test performance until a certain saturation point; beyond that, increased frequencies mostly lead to increased generalization error. We highlight this effect by drawing four dotted lines following the trends for varying frequencies with $G = C_{32}$ on four different dataset sizes m: the different slopes of the curves correspond to the different saturation effects.

9 Conclusion

In this work, we provided various generalization bounds on equivariant networks with a single hidden layer. We have used Rademacher complexity analysis to derive these bounds. They are all dimension-free, as they do not depend on the input and output dimensions. They only depend on the norm of learnable weights. We have considered equivariant models in spatial and in frequency domain, models with weight sharing and local filters. The first insight from our analysis is that the suitable weight-sharing techniques should be able to provide similar guarantees. This is not surprising, as we did not assume any symmetry in the data distribution. Other works in the literature have highlighted the benefit of equivariance if such symmetries exist - see for example Sannai et al. (2021); Sokolić et al. (2017a). Finally, local filters can potentially provide an additional gain, although the story for band-limited filters is more subtle. We also provide a lower bound on Rademacher complexity and showed numerically that our generalization error correlates well with the true error and decreases with m. In future works, it is interesting to generalize the current result to deeper networks. Besides, we have focused on positively homogeneous activation functions. We expect that the result can be extended to general Lipschitz activations using techniques in Vardi et al. (2022). However, the current proof techniques would not work for norm-based nonlinearities used in equivariant literature Worrall et al. (2017); Weiler et al. (2018a); Weiler and Cesa (2019). We encourage readers to consult Appendix J for comparison with other works and future directions.

References

Sanjeev Arora, Rong Ge, Behnam Neyshabur, and Yi Zhang. Stronger Generalization Bounds for Deep Nets via a Compression Approach. In *International Conference on Machine Learning*, pages 254–263, 2018.

Peter L Bartlett and Shahar Mendelson. Rademacher and gaussian complexities: Risk bounds and structural results. *J. Mach. Learn. Res.*, 3(Nov):463–482, 2002.

Peter L Bartlett, Dylan J Foster, and Matus J Telgarsky. Spectrally-normalized margin bounds for neural networks. In I. Guyon, U. V. Luxburg, S. Bengio, H. Wallach, R. Fergus, S. Vishwanathan, and R. Garnett, editors, *Advances in Neural Information Processing Systems 30*, pages 6240–6249. Curran Associates, Inc., 2017.

Arash Behboodi, Gabriele Cesa, and Taco S. Cohen. A pac-bayesian generalization bound for equivariant networks. *Advances in Neural Information Processing Systems*, 35:5654–5668, 2022.

Erik J Bekkers. B-spline CNNs on lie groups. In *International Conference on Learning Representations*, 2020.

Erik J. Bekkers, Maxime W Lafarge, Mitko Veta, Koen A.J. Eppenhof, Josien P.W. Pluim, and Remco Duits. Roto-translation covariant convolutional networks for medical image analysis. In *International Conference on Medical Image Computing and Computer-Assisted Intervention (MICCAI)*, 2018.

Alberto Bietti and Julien Mairal. Group invariance, stability to deformations, and complexity of deep convolutional representations. *J. Mach. Learn. Res.*, 20(1):876–924, January 2019. ISSN 1532-4435.

Felix Biggs and Benjamin Guedj. Non-Vacuous Generalisation Bounds for Shallow Neural Networks. *arXiv:2202.01627 [cs, stat]*, February 2022. URL `http://arxiv.org/abs/2202.01627`. arXiv: 2202.01627.

Johannes Brandstetter, Rob Hesselink, Elise van der Pol, Erik J Bekkers, and Max Welling. Geometric and physical quantities improve e (3) equivariant message passing. *arXiv preprint arXiv:2110.02905*, 2021.

Johann Brehmer, Pim De Haan, Sönke Behrends, and Taco Cohen. Geometric algebra transformers. *arXiv preprint arXiv:2305.18415*, 2023.

Michael M Bronstein, Joan Bruna, Taco Cohen, and Petar Veličković. Geometric deep learning: Grids, groups, graphs, geodesics, and gauges. *arXiv preprint arXiv:2104.13478*, 2021.

Gabriele Cesa, Leon Lang, and Maurice Weiler. A program to build e(n)-equivariant steerable CNNs. In *International Conference on Learning Representations*, 2022. URL `https://openreview.net/forum?id=WE4qe9xlnQw`.

Taco Cohen, Maurice Weiler, Berkay Kicanaoglu, and Max Welling. Gauge equivariant convolutional networks and the icosahedral cnn. In *International conference on Machine learning*, pages 1321–1330. PMLR, 2019.

Taco S. Cohen and Max Welling. Group Equivariant Convolutional Networks. *arXiv:1602.07576 [cs, stat]*, February 2016a. arXiv: 1602.07576.

Taco S. Cohen and Max Welling. Steerable CNNs. In *ICLR 2017*, November 2016b.

Taco S. Cohen, Mario Geiger, and Maurice Weiler. A general theory of equivariant CNNs on homogeneous spaces. *arXiv preprint arXiv:1811.02017*, 2018.

Michaël Defferrard, Martino Milani, Frédérick Gusset, and Nathanaël Perraudin. DeepSphere: a graph-based spherical CNN. In *International Conference on Learning Representations*, 2019.

Sander Dieleman, Jeffrey De Fauw, and Koray Kavukcuoglu. Exploiting cyclic symmetry in convolutional neural networks. In *International Conference on Machine Learning (ICML)*, 2016.

David L. Donoho and Philip B. Stark. Uncertainty Principles and Signal Recovery. *SIAM Journal on Applied Mathematics*, 49(3):906–931, June 1989. ISSN 0036-1399, 1095-712X.

Gintare Karolina Dziugaite and Daniel Roy. Entropy-SGD optimizes the prior of a PAC-Bayes bound: Generalization properties of Entropy-SGD and data-dependent priors. In *International Conference on Machine Learning*, pages 1377–1386, July 2018a.

Gintare Karolina Dziugaite and Daniel M. Roy. Computing nonvacuous generalization bounds for deep (stochastic) neural networks with many more parameters than training data. *arXiv preprint arXiv:1703.11008*, 2017.

Gintare Karolina Dziugaite and Daniel M. Roy. Data-dependent PAC-Bayes priors via differential privacy. In *Advances in Neural Information Processing Systems*, pages 8430–8441, 2018b.

Gintare Karolina Dziugaite, Alexandre Drouin, Brady Neal, Nitarshan Rajkumar, Ethan Caballero, Linbo Wang, Ioannis Mitliagkas, and Daniel M. Roy. In search of robust measures of generalization. *Advances in Neural Information Processing Systems*, 33:11723–11733, 2020.

Bryn Elesedy. Group symmetry in PAC learning. In *ICLR 2022 Workshop on Geometrical and Topological Representation Learning*, page 9, 2022.

Bryn Elesedy and Sheheryar Zaidi. Provably strict generalisation benefit for equivariant models. In *International Conference on Machine Learning*, pages 2959–2969. PMLR, 2021.

Marc Finzi, Samuel Stanton, Pavel Izmailov, and Andrew Gordon Wilson. Generalizing convolutional neural networks for equivariance to lie groups on arbitrary continuous data. In *International Conference on Machine Learning*, pages 3165–3176. PMLR, 2020.

Marc Finzi, Max Welling, and Andrew Gordon Wilson. A practical method for constructing equivariant multilayer perceptrons for arbitrary matrix groups. In *International conference on machine learning*, pages 3318–3328. PMLR, 2021.

Gerald B. Folland and Alladi Sitaram. The uncertainty principle: A mathematical survey. *The Journal of Fourier Analysis and Applications*, 3(3):207–238, May 1997. ISSN 1069-5869, 1531-5851.

Simon Foucart and Holger Rauhut. *A Mathematical Introduction to Compressive Sensing*. Applied and Numerical Harmonic Analysis. Springer New York, New York, NY, 2013. URL `http://link.springer.com/10.1007/978-0-8176-4948-7`.

Fabian Fuchs, Daniel Worrall, Volker Fischer, and Max Welling. Se(3)-transformers: 3d roto-translation equivariant attention networks. In H. Larochelle, M. Ranzato, R. Hadsell, M.F. Balcan, and H. Lin, editors, *Advances in Neural Information Processing Systems*, volume 33, pages 1970–1981. Curran Associates, Inc., 2020. URL `https://proceedings.neurips.cc/paper_files/paper/2020/file/15231a7ce4ba789d13b722cc5c955834-Paper.pdf`.

Noah Golowich, Alexander Rakhlin, and Ohad Shamir. Size-Independent Sample Complexity of Neural Networks. In *Conference On Learning Theory*, pages 297–299, July 2018.

Florian Graf, Sebastian Zeng, Bastian Rieck, Marc Niethammer, and Roland Kwitt. On measuring excess capacity in neural networks. *Advances in Neural Information Processing Systems*, 35:10164–10178, 2022.

Suriya Gunasekar, Jason D Lee, Daniel Soudry, and Nati Srebro. Implicit bias of gradient descent on linear convolutional networks. *Advances in neural information processing systems*, 31, 2018.

Yiding Jiang, Behnam Neyshabur, Dilip Krishnan, Hossein Mobahi, and Samy Bengio. Fantastic Generalization Measures and Where to Find Them. In *International Conference on Learning Representations*, 2020.

Frederic Koehler, Lijia Zhou, Danica J. Sutherland, and Nathan Srebro. Uniform Convergence of Interpolators: Gaussian Width, Norm Bounds and Benign Overfitting. In *Advances in Neural Information Processing Systems*, May 2021. URL `https://openreview.net/forum?id=FyOhThdDBM`.

Risi Kondor and Shubhendu Trivedi. On the generalization of equivariance and convolution in neural networks to the action of compact groups. In *International Conference on Machine Learning (ICML)*, 2018.

Hannah Lawrence, Kristian Georgiev, Andrew Dienes, and Bobak T Kiani. Implicit bias of linear equivariant networks. In *International Conference on Machine Learning*, pages 12096–12125. PMLR, 2022.

Antoine Ledent, Waleed Mustafa, Yunwen Lei, and Marius Kloft. Norm-based generalisation bounds for deep multi-class convolutional neural networks. In *35th AAAI Conference on Artificial Intelligence*, pages 8279–8287. AAAI Press, 2021.

Michel Ledoux and Michel Talagrand. *Probability in Banach spaces: isoperimetry and processes*. Classics in mathematics. Springer, Berlin ; London, 2011. OCLC: ocn751525992.

Zhiyuan Li, Yi Zhang, and Sanjeev Arora. Why Are Convolutional Nets More Sample-Efficient than Fully-Connected Nets? In *International Conference on Learning Representations*, 2021.

Philip M. Long and Hanie Sedghi. Size-free generalization bounds for convolutional neural networks. *arXiv:1905.12600 [cs, math, stat]*, May 2019. arXiv: 1905.12600.

Sanae Lotfi, Marc Finzi, Sanyam Kapoor, Andres Potapczynski, Micah Goldblum, and Andrew G Wilson. Pac-bayes compression bounds so tight that they can explain generalization. *Advances in Neural Information Processing Systems*, 35:31459–31473, 2022.

Clare Lyle, Mark van der Wilk, Marta Kwiatkowska, Yarin Gal, and Benjamin Bloem-Reddy. On the benefits of invariance in neural networks. *arXiv preprint arXiv:2005.00178*, 2020.

Roey Magen and Ohad Shamir. Initialization-Dependent Sample Complexity of Linear Predictors and Neural Networks. In *Thirty-seventh Conference on Neural Information Processing Systems*, 2023.

Stéphane Mallat. Group invariant scattering. *Communications on Pure and Applied Mathematics*, 65(10): 1331–1398, 2012.

Vaishnavh Nagarajan and J. Zico Kolter. Uniform convergence may be unable to explain generalization in deep learning. In H. Wallach, H. Larochelle, A. Beygelzimer, F. d\textquotesingle Alché-Buc, E. Fox, and R. Garnett, editors, *Advances in Neural Information Processing Systems 32*, pages 11615–11626. Curran Associates, Inc., 2019.

Jeffrey Negrea, Gintare Karolina Dziugaite, and Daniel M. Roy. In Defense of Uniform Convergence: Generalization via derandomization with an application to interpolating predictors. Technical Report arXiv:1912.04265, arXiv, September 2021. URL `http://arxiv.org/abs/1912.04265`.

Behnam Neyshabur, Srinadh Bhojanapalli, and Nathan Srebro. A PAC-Bayesian Approach to Spectrally-Normalized Margin Bounds for Neural Networks. In *International Conference on Learning Representations*, 2018.

Mircea Petrache and Shubhendu Trivedi. Approximation-generalization trade-offs under (approximate) group equivariance. *arXiv preprint arXiv:2305.17592*, 2023.

Konstantinos Pitas, Andreas Loukas, Mike Davies, and Pierre Vandergheynst. Some limitations of norm based generalization bounds in deep neural networks. *arXiv:1905.09677 [cs, stat]*, May 2019. arXiv: 1905.09677.

Adrien Poulenard and Leonidas J. Guibas. A functional approach to rotation equivariant non-linearities for tensor field networks. In *2021 IEEE/CVF Conference on Computer Vision and Pattern Recognition (CVPR)*, pages 13169–13178, 2021. doi: 10.1109/CVPR46437.2021.01297.

David Ruhe, Johannes Brandstetter, and Patrick Forré. Clifford group equivariant neural networks. *arXiv preprint arXiv:2305.11141*, 2023.

Sara Sabour, Nicholas Frosst, and Geoffrey E. Hinton. Dynamic routing between capsules. *Advances in neural information processing systems*, 30, 2017.

Akiyoshi Sannai, Masaaki Imaizumi, and Makoto Kawano. Improved generalization bounds of group invariant/equivariant deep networks via quotient feature spaces. In *Uncertainty in Artificial Intelligence*, pages 771–780. PMLR, 2021.

Jean-Pierre Serre. *Linear representations of finite groups*. Springer, 1977.

Shai Shalev-Shwartz and Shai Ben-David. *Understanding machine learning: from theory to algorithms*. Cambridge University Press, New York, NY, USA, 2014.

Han Shao, Omar Montasser, and Avrim Blum. A theory of pac learnability under transformation invariances. *Advances in Neural Information Processing Systems*, 35:13989–14001, 2022.

J. Shawe-Taylor. Building symmetries into feedforward networks. In *1989 First IEE International Conference on Artificial Neural Networks, (Conf. Publ. No. 313)*, page 158–162, 10 1989.

J Shawe-Taylor. Symmetries and discriminability in feedforward network architectures. *IEEE Trans. Neural Netw.*, page 1–25, 1993. ISSN 1045-9227.

John Shawe-Taylor. Threshold network learning in the presence of equivalences. In J. Moody, S. Hanson, and R.P. Lippmann, editors, *Advances in Neural Information Processing Systems*, volume 4. Morgan-Kaufmann, 1991. URL `https://proceedings.neurips.cc/paper_files/paper/1991/file/087408522c31eeb1f982bc0eaf81d35f-Paper.pdf`.

Jure Sokolić, Raja Giryes, Guillermo Sapiro, and Miguel Rodrigues. Generalization Error of Invariant Classifiers. In *Artificial Intelligence and Statistics*, pages 1094–1103, 2017a.

Jure Sokolić, Raja Giryes, Guillermo Sapiro, and Miguel Rodrigues. Robust Large Margin Deep Neural Networks. *IEEE Transactions on Signal Processing*, 65(16):4265–4280, August 2017b. ISSN 1053-587X. doi: 10.1109/TSP.2017.2708039.

Ingo Steinwart and Andreas Christmann. *Support vector machines*. Information science and statistics. Springer, New York, 1st ed edition, 2008.

Nathaniel Thomas, Tess Smidt, Steven M. Kearnes, Lusann Yang, Li Li, Kai Kohlhoff, and Patrick Riley. Tensor field networks: Rotation- and translation-equivariant neural networks for 3d point clouds. *arXiv preprint arXiv:1802.08219*, 2018.

Guillermo Valle-Pérez and Ard A. Louis. Generalization bounds for deep learning, December 2020. URL `http://arxiv.org/abs/2012.04115`. arXiv:2012.04115 [cs, stat].

Gal Vardi, Ohad Shamir, and Nathan Srebro. The Sample Complexity of One-Hidden-Layer Neural Networks. *arXiv:2202.06233 [cs, stat]*, February 2022. URL `http://arxiv.org/abs/2202.06233`.

Zihao Wang and Lei Wu. Theoretical Analysis of Inductive Biases in Deep Convolutional Networks, May 2023. URL `http://arxiv.org/abs/2305.08404`. arXiv:2305.08404 [cs, stat].

Colin Wei and Tengyu Ma. Improved Sample Complexities for Deep Networks and Robust Classification via an All-Layer Margin. *arXiv:1910.04284 [cs, stat]*, October 2019. arXiv: 1910.04284.

Maurice Weiler and Gabriele Cesa. General $E(2)$-Equivariant Steerable CNNs. In *Conference on Neural Information Processing Systems (NeurIPS)*, 2019.

Maurice Weiler, Mario Geiger, Max Welling, Wouter Boomsma, and Taco S. Cohen. 3D steerable CNNs: Learning rotationally equivariant features in volumetric data. In *Conference on Neural Information Processing Systems (NeurIPS)*, 2018a.

Maurice Weiler, Fred A. Hamprecht, and Martin Storath. Learning steerable filters for rotation equivariant CNNs. In *Conference on Computer Vision and Pattern Recognition (CVPR)*, 2018b.

Maurice Weiler, Patrick Forré, Erik Verlinde, and Max Welling. Coordinate Independent Convolutional Networks–Isometry and Gauge Equivariant Convolutions on Riemannian Manifolds. *arXiv preprint arXiv:2106.06020*, 2021.

Daniel E. Worrall, Stephan J. Garbin, Daniyar Turmukhambetov, and Gabriel J. Brostow. Harmonic networks: Deep translation and rotation equivariance. In *Conference on Computer Vision and Pattern Recognition (CVPR)*, 2017.

Manzil Zaheer, Satwik Kottur, Siamak Ravanbakhsh, Barnabas Poczos, Russ R. Salakhutdinov, and Alexander J. Smola. Deep Sets. *Advances in Neural Information Processing Systems*, 30, 2017.

Chiyuan Zhang, Samy Bengio, Moritz Hardt, Benjamin Recht, and Oriol Vinyals. Understanding deep learning requires rethinking generalization. In *ICLR 2017*, 2017.

Sicheng Zhu, Bang An, and Furong Huang. Understanding the Generalization Benefit of Model Invariance from a Data Perspective. In *Advances in Neural Information Processing Systems*, 2021.

A An Overview of Representation Theory and Equivariant Networks

We provide a brief overview of some useful concepts from (compact group) Representation Theory in this supplementary section.

Definition A.1 (Group)**.** A *group* a set G of elements together with a binary operation $\cdot : G \times G \to G$ satisfying the following three group axioms:

- Associativity: $\forall a, b, c \in G \quad a \cdot (b \cdot c) = (a \cdot b) \cdot c$
- Identity: $\exists e \in G : \forall g \in G \quad g \cdot e = e \cdot g = g$
- Inverse: $\forall g \in G \;\; \exists g^{-1} \in G : \quad g \cdot g^{-1} = g^{-1} \cdot g = e$

The inverse elements g^{-1} of an element g, and the identity element e are *unique*. Moreover, if the binary operation $\cdot$ is also *commutative*, the group G is called *abelian group*. To simplify the notation, we commonly write ab instead of $a \cdot b$.

The **order** of a group G is the *cardinality* of its set and is indicated by $|G|$. A group G is **finite** when $|G| \in \mathbb{N}$, i.e., when it has a finite number of elements. A **compact** group is a group that is also a compact topological space with continuous group operation. Every finite groups is also compact (with the discrete topology).

We now present two examples of finite groups which we used throughout our experiments, the *cyclic* and the *dihedral groups*.

Definition A.2 (Cyclic Group)**.** The *cyclic group* C_N of order $N \in \mathbb{N}$ is the group of N discrete rotations by angles which are integer multiples of $\frac{2\pi}{N}$, i.e. $\{R_{p\frac{2\pi}{N}} \mid p \in [0, 1, \ldots, N-1]\}$.

The binary operation combines two rotations to generate the sum of the two rotations. This is represented by integer sum modulo N, i.e.

$$R_{p\frac{2\pi}{N}} \cdot R_{q\frac{2\pi}{N}} = R_{(p+q \mod N)\frac{2\pi}{N}}$$

Definition A.3 (Dihedral Group)**.** The *dihedral group* D_N of order $2N \in \mathbb{N}$ is the group of N discrete rotations (by angles which are integer multiples of $\frac{2\pi}{N}$) and N reflections (generated by a reflection along an axis followed by any of the N rotations), i.e.

$$\{R_{p\frac{2\pi}{N}} \mid p \in [0, 1, \ldots, N-1]\} \cup \{R_{p\frac{2\pi}{N}} F \mid p \in [0, 1, \ldots, N-1]\}$$

where F is a reflection along an axis. Note that the group D_N has size $2N$ and contains the group C_N as a subgroup.

Another important concept is that of *group action*:

Definition A.4 (Group Action)**.** The *action* of a group G on a set $\mathcal{X}$ is a map $. : G \times \mathcal{X} \to \mathcal{X}, \; (g, x) \mapsto g.x$ satisfying the following axioms:

- identity: $\forall x \in \mathcal{X} \quad e.x = x$
- compatibility: $\forall a, b \in G \;\; \forall x \in \mathcal{X} \quad a.(b.x) = (ab).x$

For example, a group can act on functions overs the group's elements: given a signal $x : G \to \mathbb{R}$, the action of $g \in G$ on x is defined as $[g.x](h) := x(g^{-1}h)$, i.e. g "translates" the function x.

The **orbit** of $x \in \mathcal{X}$ through G is the set $G.x := \{g.x | g \in G\}$. The orbits of the elements in $\mathcal{X}$ form a *partition* of $\mathcal{X}$. By considering the equivalence relation $\forall x, y \in \mathcal{X} \quad x \sim_G y \iff x \in G.y$ (or, equivalently, $y \in G.x$), one can define the **quotient space** $\mathcal{X}/G := \{G.x | x \in \mathcal{X}\}$, i.e. the set of all different orbits.

Definition A.5 (Linear Representation)**.** Given a group G and a vector space V, a linear representation of G is a homomorphism $\rho : G \to \mathrm{GL}(V)$ associating to each element of $g \in G$ an invertible matrix acting on V, such that:

$$\forall g, h \in G, \quad \rho(gh) = \rho(g)\rho(h).$$

i.e., the matrix multiplication $\rho(g)\rho(h)$ needs to be compatible with the group composition gh.

The most simple representation is the *trivial representation* $\psi : G \to \mathbb{R}, g \mapsto 1$, mapping all element to the multiplicative identity $1 \in V = \mathbb{R}$. The common 2-dimensional rotation matrices are an example of representation on $V = \mathbb{R}^2$ of the group SO(2):

$$\rho(r_\theta) = \begin{bmatrix} \cos\theta & -\sin\theta \\ \sin\theta & \cos\theta \end{bmatrix}$$

with $\theta \in [0, 2\pi)$. In the complex field $\mathbb{C}$, circular harmonics are other representations of the rotation group:

$$\psi_k(r_\theta) = e^{-ik\theta} \in V = \mathbb{C}^1$$

where $k \in \mathbb{Z}$ is the harmonic's frequency. Similarly, these representations can be constructed also for the finite *cyclic group* $\mathrm{C}_N \cong \mathbb{Z}/N\mathbb{Z}$:

$$\psi_k(p) = e^{-ikp\frac{2\pi}{N}} \in V = \mathbb{C}^1$$

with $p \in \{0, 1, \ldots, N-1\}$.

Regular Representation A particularly important representation is the *regular representation* ρ_{reg} of a *finite* group G. This representation acts on the space $V = \mathbb{R}^{|G|}$ of vectors representing functions over the group G. The regular representation $\rho_{\mathrm{reg}}(g)$ of an element $g \in G$ is a $|G| \times |G|$ *permutation matrix*. Each vector $\boldsymbol{x} \in V = \mathbb{R}^{|G|}$ can be interpreted as a function over the group, $x : G \to \mathbb{R}$, with $x(g_i)$ being i-th entries of $\boldsymbol{x}$. Then, the matrix-vector multiplication $\rho_{\mathrm{reg}}(g)\boldsymbol{x}$ represents the action of g on the function x which generates the "translated" function $g.x$. These representations are of high importance because they describe the features of group convolution networks.

Direct Sum Given two representations $\rho_1 : G \to \mathrm{GL}(\mathbb{R}^{n_1})$ and $\rho_2 : G \to \mathrm{GL}(\mathbb{R}^{n_2})$, their *direct sum* $\rho_1 \oplus \rho_2 : G \to \mathrm{GL}(\mathbb{R}^{n_1+n_2})$ is a representation obtained by stacking the two representations as follows:

$$(\rho_1 \oplus \rho_2)(g) = \begin{bmatrix} \rho_1(g) & 0 \\ 0 & \rho_2(g) \end{bmatrix} .$$

Note that this representation acts on $\mathbb{R}^{n_1+n_2}$ which contains the concatenation of the vectors in $\mathbb{R}^{n_1}$ and $\mathbb{R}^{n_2}$. By combining c copies of the *regular representation* via the direct sum, one obtains a representation of G acting on the features of a group convolution network with c channels.

Fourier Transform The classical Fourier analysis of periodic discrete functions can be framed as the representation theory of the $\mathbb{Z}/N\mathbb{Z}$ group. This is summarised by the following result: the regular representation of $G = \mathbb{Z}/N\mathbb{Z}$ is equivalent to the direct sum of all circular harmonics with frequency $k \in \{0, \ldots, N-1\}$, i.e. there exists a unitary matrix $\boldsymbol{F} \in \mathbb{C}^{N \times N}$ such that:

$$\rho_{\mathrm{reg}}(p) = \boldsymbol{F}^* \left(\bigoplus_k \psi_k(p) \right) \boldsymbol{F}$$

for $p \in \{0, \ldots, N-1\} = \mathbb{Z}/N\mathbb{Z}$ and where ψ_k is the circular harmonic of frequency k as defined earlier in this section. The unitary matrix $\boldsymbol{F}$ is what is typically referred to as the (unitary)*discrete Fourier Transform* operator, while its conjugate transpose $\boldsymbol{F}^*$ is the *Inverse Fourier Transform* one.

By indexing the dimensions of the vector space $V \cong \mathbb{C}^N$ on which ρ_{reg} acts with the elements $p \in \{0, \ldots, N-1\}$ of $G = \mathbb{Z}/N\mathbb{Z}$, the Fourier transform matrix can be explicitly constructed as

$$F_{k,p} = \frac{1}{\sqrt{N}} \psi_k(p) = \frac{1}{\sqrt{N}} e^{-ikp\frac{2\pi}{N}} \tag{8}$$

One can verify that the matrix is indeed unitary.

In representation theoretic terms, the circular harmonics $\{\psi_k\}_k$ are referred to as the **irreducible representations** (or *irreps*) of the group $G = \mathbb{Z}/N\mathbb{Z}$. While we are mostly interested in commutative (abelian) finite groups in this work, this construction can be easily extended to square-integrable signals over non-abelian compact groups by using the more general concept of irreducible representations Behboodi et al. (2022); Cesa et al. (2022). See also Serre (1977) for rigorous details about representation theory.

Notation Given a signal $x : G \to \mathbb{C}$, we typically write $\boldsymbol{x} \in V = \mathbb{C}^{|G|}$ to refer to the vector containing the values of x at each group element. Note that this is the vector space on which ρ_{reg} acts. We also use $\hat{\boldsymbol{x}} = \boldsymbol{F}\boldsymbol{x}$ to indicate the vector of Fourier coefficients and $\hat{x}$ to indicate the function associating to each frequency k (or, equivalently, irrep ψ_k) the corresponding Fourier coefficient $\hat{x}(\psi_k) \in \mathbb{C}$.

Group Convolution Given a vector space V associated with a representation $\rho : G \to \text{GL}(V)$ of a group G, the *group convolution* $\boldsymbol{w} \circledast_G \boldsymbol{x} \in \mathbb{C}^{|G|}$ of two elements $\boldsymbol{x}, \boldsymbol{w} \in V$ is defined as

$$\forall g \in G \quad (\boldsymbol{w} \circledast_G \boldsymbol{x})(g) := \boldsymbol{w}^T \rho(g)^T \boldsymbol{x} \ . \tag{9}$$

What we defined is technically a **group cross-correlation** and so it differs from the usual definitions of convolution over groups. We still refer to it as group convolution to follow the common terminology in the Deep Learning literature. One can prove that group convolution is **equivariant** to G, i.e.:

$$\boldsymbol{w} \circledast_G \rho(g)\boldsymbol{x} = \rho_{\text{reg}}(g)\,(\boldsymbol{w} \circledast_G \boldsymbol{x})$$

If $V = \mathbb{C}^{|G|}$, then $x, w : G \to \mathbb{C}$ can be interpreted as signals over the group and group convolution takes the more familiar form

$$(w \circledast_G x)(g) = \sum_{h \in G} w(g^{-1}h)x(h) \tag{10}$$

Finally, we recall two important properties of the Fourier transform: given two signals $w, x : G \to \mathbb{C}$, the following properties hold

$$\widehat{g.x}(\psi) = \psi(g)\hat{x}(\psi) \tag{11}$$

$$\widehat{w \circledast_G x}(\psi) = \hat{w}(\psi)\hat{x}(\psi) \tag{12}$$

Eq. 11 guarantees that a transformation by g of x does not mix the coefficients associated to different irreps / frequencies. Eq. 12 is the typical *convolution theorem*.

Finally, some of these results related to the Fourier transform are generalized by the following theorems. This last property is related to the more general result expressed by *Schur's Lemma*:

Theorem A.6 (Schur's Lemma)**.** *Let G be a compact group (not necessarily abelian) and ψ_1 and ψ_2 two irreps of G. Then, there exists a non-zero linear map $\boldsymbol{W}$ such that*

$$\psi_1(g)\boldsymbol{W} = \boldsymbol{W}\psi_2(g)$$

for any $g \in G$ (i.e. an equivariant *linear map) if and only if ψ_1 and ψ_2 are equivalent representations, i.e. they differ at most by a change of basis Q: $\psi_1(g) = Q\psi_2(g)Q^{-1}$ for all $g \in G$.*

A second result generalizes the notion of Fourier transform to representations beyond the regular one:

Theorem A.7 (Peter-Weyl Theorem)**.** *Let G be a compact group and ρ a unitary representation of G. Then, ρ decomposes into a direct sum of irreducible representations of G, up to a change of basis, i.e.*

$$\rho(g) = U \left(\bigoplus_{\psi} \bigoplus_{i}^{m_\psi} \psi \right) U^T$$

Each irrep ψ can appear in the decomposition with a multiplicity $m_\psi \geq 0$.

In particular, in the case of a regular representation, the change of basis is given precisely by the Fourier transform matrix $\boldsymbol{F}$.

The combination of these two results is typically used in steerable CNNs and other equivariant designs to characterize arbitrary equivariant networks by reducing the study to individual irreducible components. See also the next section.

A.1 Equivariant Networks

We now discuss some popular equivariant neural network designs.

In this work, we consider *real* valued networks with 2 layers, i.e. we limit our discussion to an hypothesis class of the form

$$\mathcal{H} := \left\{ \boldsymbol{u}^T \sigma(\boldsymbol{W}\boldsymbol{x}) \right\}.$$

In a G-equivariant network, the group G carries an *action* on the intermediate features of the model; these actions are specified by *group representations*, which we introduced in the previous section. We assume the action of an element $g \in G$ on the input and the output of the first layer is given respectively by the matrices $\rho_0(g)$ and $\rho_1(g)$. The first layer, including the activation function, is **equivariant** with respect to G if:

$$\forall g \in G, \quad \sigma(\boldsymbol{W}\rho_0(g)\boldsymbol{x}) = \rho_1(g)\sigma(\boldsymbol{W}\boldsymbol{x})$$

Instead, the last layer of the network is invariant with respect to the action of the group G on the input data via ρ_0, which means that:

$$\forall g \in G, \quad \boldsymbol{u}^T\sigma(\boldsymbol{W}\boldsymbol{x}) = \boldsymbol{u}^T\rho_1(g)\sigma(\boldsymbol{W}\boldsymbol{x}) = \boldsymbol{u}^T\sigma(\boldsymbol{W}\rho_0(g)\boldsymbol{x})$$

GCNNs A typical way to construct networks equivariant to a finite group G is via **group convolution**, which we introduced in the previous section; this is the *Group Convolution neural network* (GCNN) design Cohen and Welling (2016a). Indeed, if the representation ρ_1 is chosen to be the *direct sum* of c_1 copies of the *regular representation* ρ_{reg} of G, i.e. $\rho_1 = \bigoplus^{c_1} \rho_{\text{reg}}$ and the input $\rho_0 = \bigoplus^{c_0} \rho_{\text{reg}}$ also consists of c_0 copies of the regular representation, then the linear layer $\boldsymbol{W}$ can always be expressed as $c_1 \times c_0$ group-convolution linear operators as in eq. 9:

$$\boldsymbol{W} = \left[\begin{array}{c|c|c|c} \boldsymbol{W}_{(1,1)} & \boldsymbol{W}_{(2,1)} & \cdots & \boldsymbol{W}_{(c_0,1)} \\ \hline \boldsymbol{W}_{(1,2)} & \boldsymbol{W}_{(2,2)} & \cdots & \boldsymbol{W}_{(c_0,2)} \\ \hline \vdots & \vdots & \ddots & \vdots \\ \hline \boldsymbol{W}_{(1,c_1)} & \boldsymbol{W}_{(2,c_1)} & \cdots & \boldsymbol{W}_{(c_0,c_1)} \end{array}\right]$$

where each $\boldsymbol{W}_{(i,j)} \in \mathbb{R}^{|G|\times|G|}$ is a G-circular matrix (i.e. rows are "rotations" of each others via ρ_{reg}) of the form:

$$\boldsymbol{W}_{(i,j)} = \begin{bmatrix} \boldsymbol{w}_{(i,j)}^T \rho_{\text{reg}}(g_1) \\ \vdots \\ \boldsymbol{w}_{(i,j)}^T \rho_{\text{reg}}(g_{|G|}) \end{bmatrix}$$

In this case, note that the representation ρ_1 acts via permutation and, therefore, any activation function σ which is applied to each entry of $\boldsymbol{W}\boldsymbol{x}$ entry-wise is equivariant: this includes the typical activations used in deep learning (e.g. ReLU).

General linear layer The representation theoretic tools we introduced earlier allow for a quite general framework to describe a wide family of equivariant networks beyond group-convolution, by considering the generalization of the Fourier transform we discussed in the previous section. By using Theorem A.7, a representation ρ_l (for $l = 0, 1$) decomposes into direct sum of irreps as follows:

$$\rho_l = U_l \left(\bigoplus_{\psi} \bigoplus_{i=1}^{m_{l,\psi}} \psi \right) U_l^\top,$$

Activation function	Definition
Norm ReLU Weiler et al. (2018b); Worrall et al. (2017)	$\eta(\|\boldsymbol{x}\|) = \mathrm{ReLU}(\|\boldsymbol{x}\| - b) \quad (b <= 0)$
Squashing Sabour et al. (2017)	$\eta(\|\boldsymbol{x}\|) = \frac{\|\boldsymbol{x}\|^2}{\|\boldsymbol{x}\|^2+1}$
Gated Weiler et al. (2018b)	$\eta(\|\boldsymbol{x}\|) = \frac{1}{1+e^{-s(\boldsymbol{x})}} \|\boldsymbol{x}\|$

Table 1: Equivariant activation functions

where U_l is an orthogonal matrix, and $m_{l,\psi}$ is the multiplicity of the irrep ψ in the representation ρ_l. If $\dim_\psi$ is the dimensionality of the irrep ψ, the width of the network n is equal to $\sum m_{1,\psi} \dim_\psi$, and the input dimension d is given by $\sum m_{0,\psi} \dim_\psi$.

Next, by combining this result with Theorem A.6, an equivariant network can be parameterized entirely in terms of irreps, which is analogous to a Fourier space parameterization of a convolutional network. Defining $\widehat{\boldsymbol{W}}_l = U_l^{-1} \boldsymbol{W}_l U_{l-1}$, the equivariance condition writes as

$$\forall g \in G, \quad \widehat{\boldsymbol{W}}_l \left(\bigoplus_\psi \bigoplus_{i=1}^{m_{l-1,\psi}} \psi(g) \right) = \left(\bigoplus_\psi \bigoplus_{i=1}^{m_{l,\psi}} \psi(g) \right) \widehat{\boldsymbol{W}}_l.$$

This induces a block structure in $\hat{\boldsymbol{W}}_l$, where the $(\psi, i; \psi', j)$-th block block maps the i-th input block transforming according to ψ to the j-th output block transforming under ψ', with $i \in [m_{l-1,\psi}]$ and $j \in [m_{l,\psi'}]$. By Theorem A.6, there are no linear maps equivariant to ψ and ψ' whenever these representations are in-equivalent; this implies the matrix $\hat{\boldsymbol{W}}_l$ is sparse, since its $(\psi, i; \psi', j)$-th block is non-zero only when $\psi \cong \psi'$. Then, the *non-zero* (ψ, i, j)-th block (here, we drop the redundant ψ' index) is denoted by $\hat{w}_{i,j}(\psi)$ and should commute with $\psi(g)$ for any $g \in G$. This is achieved by expressing this matrix as a linear combination of a few fixed basis matrices spanning the space; see Behboodi et al. (2022); Cesa et al. (2022) for more details.

In the special case of GCNN with abelian group G, each irrep in the intermediate features occurs exactly c_1 times. Similarly, if the input representation ρ_0 consists of c_0 copies of the regular representation, each irrep appears exactly c_0 times in ρ_0. Then, $\hat{w}_{i,j}(\psi)$ is the Fourier transform of the filter $\boldsymbol{w}_{(i,j)} \in \mathbb{R}^{|G|}$ at the frequency/irrep ψ.

Activation function σ Each module in an equivariant network should commute with the action of the group on its on input in order to guarantee the overall equivariance of the model. Hence, the activation function σ used in the intermediate layer should be equivariant with respect to $\rho_1(g)$ as well, i.e. $\sigma(\rho_1(g)\boldsymbol{x}) = \rho_2(g)\sigma(\boldsymbol{x}), \forall g \in G$. There are different activation functions used in the literature. As we use unitary representations, one can use norm nonlinearities, $\sigma(\boldsymbol{x}) = \eta(\|\boldsymbol{x}\|)\frac{\boldsymbol{x}}{\|\boldsymbol{x}\|}$ for a suitable function $\eta : \mathbb{R}_0^+ \to \mathbb{R}_0^+$. It can be seen that $\sigma(\rho_1(g)\boldsymbol{x}) = \rho_1(g)\sigma(\boldsymbol{x})$. Some examples are norm ReLU Worrall et al. (2017), squashing Sabour et al. (2017) and gated nonlinearities Weiler et al. (2018b).

As introduced in the GCNN paragraph, when the intermediate representation is built from the regular representation, any pointwise activation is admissible: since the group's action permutes the features' entries in the spatial domain, it intertwines with the non-linearity applied entry-wise. There exist also other type of activations, such as tensor-product non-linearities (based on the Clebsh-Gordan transform) but we do not consider them here.

Last layer $\boldsymbol{u}$ The last layer maps the features after the activation to a single scalar and is assumed to be invariant. This linear layer can be thought as a special case of the general framework above with the choice of output representation ρ_2 being a collection of *trivial representations*, i.e. $\rho_2(g) = I$ is the identity. Since the trivial representation is an irrep, by Theorem A.6, this linear map only captures the invariant information in the output of the activation function. In the case of a GCNN with pointwise activation σ, this layer acts as an averaging pooling operator over the $|G|$ entries of each channel and learns the weights to linearly combines the c_1 independent channels. Note that, one can also include a custom **pooling operator** $P(\cdot)$ (e.g. max-pooling) between the activation layer σ and the final layer $\boldsymbol{u}$ like in eq. 3: this gives additional freedom to construct the final invariant features beyond just average pooling.

B Mathematical Preliminaries

This section gathers the main tools we will use throughout the proofs.

First, we introduce the decoupling technique Foucart and Rauhut (2013), which will be used in the proof of the next lemma.

Theorem B.1. *Let $\boldsymbol{\epsilon} = (\epsilon_1, \ldots, \epsilon_m)$ be a sequence of independent random variables with $\mathbb{E}\epsilon_i = 0$ for all $i \in [m]$. Let $\boldsymbol{x}_{j,k}$, $j, k \in [m]$ be a double sequence of elements in a finite-dimensional vector space V. If $F : V \to \mathbb{R}$ is a convex function, then:*

$$\mathbb{E}F\left(\sum_{\substack{j,k=1\\ j\neq k}}^{m} \epsilon_j \epsilon_k \boldsymbol{x}_{j,k}\right) \leq \mathbb{E}F\left(4\sum_{j,k=1}^{m} \epsilon_j \epsilon'_k \boldsymbol{x}_{j,k}\right), \tag{13}$$

where $\boldsymbol{\epsilon}'$ is an independent copy of $\boldsymbol{\epsilon}$.

The following lemma can be found in Foucart and Rauhut (2013), namely inequality (8.22), within the proof of Proposition 8.13. We re-state the lemma and the proof here, as it is of independent interest.

Lemma B.2. *For any positive semidefinite matrix $\boldsymbol{B}$, for $8\beta \|\boldsymbol{B}\|_{2\to 2} < 1$, and Rademacher vector $\boldsymbol{\epsilon}$, we have*

$$\mathbb{E}_{\boldsymbol{\epsilon}}\left(\exp\left(\beta \boldsymbol{\epsilon}^\top \boldsymbol{B}\boldsymbol{\epsilon}\right)\right) \leq \exp\left(\frac{\beta \operatorname{Tr}(\boldsymbol{B})}{1 - 8\beta \|\boldsymbol{B}\|_{2\to 2}}\right).$$

Proof. We start by using Theorem B.1:

$$\begin{aligned}
\mathbb{E}\left(\exp\left(\beta \boldsymbol{\epsilon}^\top \boldsymbol{B}\boldsymbol{\epsilon}\right)\right) &= \mathbb{E}\left(\exp\left(\beta \sum_{j=1} B_{jj} + \beta \sum_{j\neq k} \epsilon_j \epsilon_k B_{jk}\right)\right) \\
&\leq \left(\exp\left(\beta \operatorname{Tr}(\boldsymbol{B})\right)\right) \mathbb{E}\left(\exp\left(4\beta \sum_{j,k} \epsilon_j \epsilon'_k B_{jk}\right)\right)
\end{aligned}$$

Then using the inequality $\mathbb{E}\exp(\beta \sum_{l=1}^m a_1 \epsilon_l) \leq \mathbb{E}\exp(\beta^2 \sum_{l=1}^m a_1^2/2)$, we have:

$$\mathbb{E}\left(\exp\left(4\beta \sum_{j,k} \epsilon_j \epsilon'_k B_{jk}\right)\right) \leq \mathbb{E}\left(\exp\left(8\beta^2 \sum_{k}\left(\sum_{j} \epsilon_j B_{jk}\right)^2\right)\right)$$

Next, we can see that:

$$\begin{aligned}
\sum_{k}\left(\sum_{j} \epsilon_j B_{jk}\right)^2 &= \|\boldsymbol{B}\boldsymbol{\epsilon}\|^2 = \left\|\boldsymbol{B}^{1/2}\boldsymbol{B}^{1/2}\boldsymbol{\epsilon}\right\|^2 \\
&\leq \left\|\boldsymbol{B}^{1/2}\right\|_{2\to 2}^2 \left\|\boldsymbol{B}^{1/2}\boldsymbol{\epsilon}\right\|^2 = \|\boldsymbol{B}\|_{2\to 2} \boldsymbol{\epsilon}^\top \boldsymbol{B}\boldsymbol{\epsilon}.
\end{aligned}$$

Therefore, for $8\beta \|\boldsymbol{B}\|_{2\to 2} < 1$, we get:

$$\begin{aligned}
\mathbb{E}\left(\exp\left(\beta \boldsymbol{\epsilon}^\top \boldsymbol{B}\boldsymbol{\epsilon}\right)\right) &\leq \exp\left(\beta \operatorname{Tr}(\boldsymbol{B})\right)\mathbb{E}\left(\exp\left(8\beta^2 \|\boldsymbol{B}\|_{2\to 2} \boldsymbol{\epsilon}^\top \boldsymbol{B}\boldsymbol{\epsilon}\right)\right) \\
&\leq \exp\left(\beta \operatorname{Tr}(\boldsymbol{B})\right)\mathbb{E}\left(\left(\exp\left(\beta \boldsymbol{\epsilon}^\top \boldsymbol{B}\boldsymbol{\epsilon}\right)\right)\right)^{8\beta\|\boldsymbol{B}\|_{2\to 2}}.
\end{aligned}$$

Rearranging the terms yields the final result. □

B.1 Rademacher Complexity Bounds

The generalization analysis of this paper is based on the Rademacher analysis. We summarize the main theorems here. The terms $\mathcal{L}(h)$ and $\hat{\mathcal{L}}(h)$ denotes, respectively, the test and the training error, formally defined as follows:

$$\mathcal{L}(h) = \mathbb{E}_{\boldsymbol{x}\sim\mathbb{P}_{\boldsymbol{x}}}\left(\ell \circ h(\boldsymbol{x})\right), \quad \hat{\mathcal{L}}(h) = \frac{1}{m}\sum_{i=1}^{m} \ell \circ h(\boldsymbol{x}_i). \tag{14}$$

The empirical Rademacher complexity is defined as:

$$\mathcal{R}_{\mathcal{S}}(\mathcal{G}) = \mathbb{E}_{\epsilon} \sup_{h\in\mathcal{G}} \frac{1}{m}\sum_{i=1}^{m} \epsilon_i g(\boldsymbol{x}_i), \tag{15}$$

Theorem B.3 (Theorem 26.5, Shalev-Shwartz and Ben-David (2014))**.** *Let $\mathcal{H}$ be a family of functions, and let $\mathcal{S}$ be the training sequence of m samples drawn from the distribution $\mathcal{D}^m$. Let ℓ be a real-valued loss function satisfying $|\ell| \leq c$. Then, for $\delta \in (0,1)$, with probability at least $1-\delta$ we have, for all $h \in \mathcal{H}$,*

$$\mathcal{L}(h) \leq \hat{\mathcal{L}}(h) + 2\mathcal{R}_{\mathcal{S}}(\ell \circ \mathcal{H}) + 4c\sqrt{\frac{2\log(4/\delta)}{m}}. \tag{16}$$

Using Theorem B.3, we can focus on finding upper bounds for the empirical Rademacher complexity of $\ell \circ \mathcal{H}$. Below, we show how to remove the loss function $\ell(\cdot)$ and focus on $\mathcal{H}$.

A function $\phi : \mathbb{R} \to \mathbb{R}$ is called a contraction if $|\phi(x) - \phi(y)| \leq |x - y|$ for all $x, y \in \mathbb{R}$, or equivalently if the function is 1-Lipschitz. The contraction lemma is a standard result in equation 4.20 of Ledoux and Talagrand (2011). We will use that for the Rademacher complexity analysis.

Lemma B.4. *Let $\phi_i : \mathbb{R} \to \mathbb{R}$ be contractions such that $\phi_i(0) = 0$. If $G : \mathbb{R} \to \mathbb{R}$ is a convex and increasing function, then*

$$\mathbb{E}G\left(\sup_{t\in T}\sum_{i=1}^{m}\epsilon_i\phi_i(t_i)\right) \leq \mathbb{E}G\left(\sup_{t\in T}\sum_{i=1}^{m}\epsilon_i t_i\right). \tag{17}$$

Let's rewrite the Rademacher term, including the loss function explicitly:

$$\mathcal{R}_{\mathcal{S}}(\ell \circ \mathcal{H}) = \mathbb{E}_{\boldsymbol{\epsilon}}\left[\sup_{h\in\mathcal{H}} \frac{1}{m}\sum_{i=1}^{m}\epsilon_i \ell \circ h(\boldsymbol{x}_i)\right].$$

We assume a 1-Lipschitz loss function, for which we can use the contraction lemma, 4.20 in Ledoux and Talagrand (2011), to get:

$$\mathcal{R}_{\mathcal{S}}(\ell \circ \mathcal{H}) \leq \mathcal{R}_{\mathcal{S}}(\mathcal{H}).$$

So finding an upper bound on $\mathcal{R}_{\mathcal{S}}(\mathcal{H})$ is sufficient for the generalization error analysis.

C Proof of Main Theorems

C.1 Rademacher Complexity Bounds for Group Convolutional Networks

Consider the group convolutional network with c_0 input channel, c_1 intermediate channels, and a last layer with pooling and aggregation. The input space is assumed to be $\mathbb{R}^{|G|\times c_0}$. Remember that the network was given as follows:

$$h_{\boldsymbol{u},\boldsymbol{w}}(\boldsymbol{x}) = \boldsymbol{u}^\top P \circ \sigma \begin{pmatrix} \sum_{k=1}^{c_0} \boldsymbol{w}_{(1,k)} \circledast_G \boldsymbol{x}(k) \\ \vdots \\ \sum_{k=1}^{c_0} \boldsymbol{w}_{(c_1,k)} \circledast_G \boldsymbol{x}(k) \end{pmatrix} = \boldsymbol{u}^\top P \circ \sigma(\boldsymbol{W}\boldsymbol{x}),$$

where $P(\cdot)$ is the pooling operation. We denote the first convolution layer with the circulant matrix $\boldsymbol{W}\boldsymbol{x}$.

To find a bound on the Rademacher complexity, We start with the following inequality, which is shared across the proofs of some of the other theorems in the paper:

$$\mathbb{E}_{\boldsymbol{\epsilon}}\left(\sup_{\boldsymbol{u},\boldsymbol{w}}\frac{1}{m}\sum_{i=1}^{m}\epsilon_i\boldsymbol{u}^\top P\circ\sigma\left(\boldsymbol{W}\boldsymbol{x}_i\right)\right)=\frac{M_1}{m}\mathbb{E}_{\boldsymbol{\epsilon}}\left(\sup_{\boldsymbol{w}}\left\|\sum_{i=1}^{m}\epsilon_i P\circ\sigma(\boldsymbol{W}\boldsymbol{x}_i)\right\|\right). \tag{18}$$

The above result follows from the Cauchy-Schwartz inequality and peels off the last aggregation layer. We continue the proofs from this step.

C.2 Proof for Positively Homogeneous Activation Functions with Average Pooling (Theorem C.1)

Theorem C.1. *Consider the hypothesis space $\mathcal{H}$ defined in eq. 4. If $P(\cdot)$ is the average pooling operation, $\sigma(\cdot)$ is a 1-Lipschitz positively homogeneous activation function, then with probability at least $1-\delta$ and for all $h\in\mathcal{H}$, we have:*

$$\mathcal{L}(h)\leq\hat{\mathcal{L}}(h)+2\frac{b_x M_1 M_2}{\sqrt{m}}+4\sqrt{\frac{2\log(4/\delta)}{m}}.$$

Proof. For an input $\boldsymbol{x}\in\mathbb{R}^{|G|\times c_0}$, the action of the group G on each channel is given by the permutation of the entries. Suppose that the $G-$permutations are given by $\Pi_1,\ldots,\Pi_{|G|}$. We have:

$$\begin{aligned}
\mathbb{E}_{\boldsymbol{\epsilon}}\left(\sup_{\boldsymbol{w}}\left\|\sum_{i=1}^{m}\epsilon_i P\circ\sigma(\boldsymbol{W}\boldsymbol{x}_i)\right\|\right)&=\mathbb{E}_{\boldsymbol{\epsilon}}\left(\sup_{\boldsymbol{w}}\left\|\sum_{i=1}^{m}\epsilon_i\begin{pmatrix}\frac{1}{|G|}\mathbf{1}^\top\sigma\left(\sum_{k=1}^{c_0}\boldsymbol{w}_{(1,k)}\circledast_G\boldsymbol{x}_i(k)\right)\\ \vdots\\ \frac{1}{|G|}\mathbf{1}^\top\sigma\left(\sum_{k=1}^{c_0}\boldsymbol{w}_{(c_1,k)}\circledast_G\boldsymbol{x}_i(k)\right)\end{pmatrix}\right\|\right)\\
&=\mathbb{E}_{\boldsymbol{\epsilon}}\left(\sup_{\boldsymbol{w}}\left\|\sum_{i=1}^{m}\epsilon_i\sum_{l=1}^{|G|}\frac{1}{|G|}\begin{pmatrix}\sigma\left(\sum_{k=1}^{c_0}\boldsymbol{w}_{(1,k)}^\top\Pi_l\boldsymbol{x}_i(k)\right)\\ \vdots\\ \sigma\left(\sum_{k=1}^{c_0}\boldsymbol{w}_{(c_1,k)}^\top\Pi_l\boldsymbol{x}_i(k)\right)\end{pmatrix}\right\|\right)\\
&\leq\mathbb{E}_{\boldsymbol{\epsilon}}\left(\sup_{\boldsymbol{w}}\sum_{l=1}^{|G|}\frac{1}{|G|}\left\|\sum_{i=1}^{m}\epsilon_i\begin{pmatrix}\sigma\left(\sum_{k=1}^{c_0}\boldsymbol{w}_{(1,k)}^\top\Pi_l\boldsymbol{x}_i(k)\right)\\ \vdots\\ \sigma\left(\sum_{k=1}^{c_0}\boldsymbol{w}_{(c_1,k)}^\top\Pi_l\boldsymbol{x}_i(k)\right)\end{pmatrix}\right\|\right)\\
&\leq\sum_{l=1}^{|G|}\frac{1}{|G|}\mathbb{E}_{\boldsymbol{\epsilon}}\left(\sup_{\boldsymbol{w}}\left\|\sum_{i=1}^{m}\epsilon_i\begin{pmatrix}\sigma\left(\sum_{k=1}^{c_0}\boldsymbol{w}_{(1,k)}^\top\Pi_l\boldsymbol{x}_i(k)\right)\\ \vdots\\ \sigma\left(\sum_{k=1}^{c_0}\boldsymbol{w}_{(c_1,k)}^\top\Pi_l\boldsymbol{x}_i(k)\right)\end{pmatrix}\right\|\right)
\end{aligned}$$

where we used triangle inequalities for the first inequality. The second inequality follows from swapping the supremum and the sum. Consider an arbitrary summand for a given l. We first use the moment inequality to get:

$$\begin{aligned}
&\mathbb{E}_{\boldsymbol{\epsilon}}\left(\sup_{\boldsymbol{w}}\left\|\sum_{i=1}^{m}\epsilon_i\begin{pmatrix}\sigma\left(\sum_{k=1}^{c_0}\boldsymbol{w}_{(1,k)}^\top\Pi_l\boldsymbol{x}_i(k)\right)\\ \vdots\\ \sigma\left(\sum_{k=1}^{c_0}\boldsymbol{w}_{(c_1,k)}^\top\Pi_l\boldsymbol{x}_i(k)\right)\end{pmatrix}\right\|\right)\\
&\leq\sqrt{\mathbb{E}_{\boldsymbol{\epsilon}}\left(\sup_{\boldsymbol{w}}\left\|\sum_{i=1}^{m}\epsilon_i\begin{pmatrix}\sigma\left(\sum_{k=1}^{c_0}\boldsymbol{w}_{(1,k)}^\top\Pi_l\boldsymbol{x}_i(k)\right)\\ \vdots\\ \sigma\left(\sum_{k=1}^{c_0}\boldsymbol{w}_{(c_1,k)}^\top\Pi_l\boldsymbol{x}_i(k)\right)\end{pmatrix}\right\|^2\right)}.
\end{aligned}\tag{19}$$

We can continue the derivation as follows. First, define $\boldsymbol{w}_{(j,:)} := (\boldsymbol{w}_{j,i})_{i\in[c_0]}$, which is the weights used for generating the channel j. Now, using the assumption of positively homogeneity, we have:

$$\mathbb{E}_{\boldsymbol{\epsilon}}\left(\sup_{\boldsymbol{w}}\left\|\sum_{i=1}^{m}\epsilon_i\begin{pmatrix}\sigma\left(\sum_{k=1}^{c_0}\boldsymbol{w}_{(1,k)}^{\top}\Pi_l\boldsymbol{x}_i(k)\right)\\ \vdots\\ \sigma\left(\sum_{k=1}^{c_0}\boldsymbol{w}_{(c_1,k)}^{\top}\Pi_l\boldsymbol{x}_i(k)\right)\end{pmatrix}\right\|^2\right) = \mathbb{E}_{\boldsymbol{\epsilon}}\left(\sup_{\boldsymbol{w}}\sum_{j=1}^{c_1}\left(\sum_{i=1}^{m}\epsilon_i\sigma\left(\sum_{k=1}^{c_0}\boldsymbol{w}_{(j,k)}^{\top}\Pi_l\boldsymbol{x}_i(k)\right)\right)^2\right)$$

$$= \mathbb{E}_{\boldsymbol{\epsilon}}\left(\sup_{\boldsymbol{w}}\sum_{j=1}^{c_1}\left\|\boldsymbol{w}_{(j,:)}\right\|^2\left(\sum_{i=1}^{m}\epsilon_i\sigma\left(\frac{1}{\left\|\boldsymbol{w}_{(j,:)}\right\|}\sum_{k=1}^{c_0}\boldsymbol{w}_{(j,k)}^{\top}\Pi_l\boldsymbol{x}_i(k)\right)\right)^2\right),$$

Since $\|\boldsymbol{w}\|^2 \leq M_2^2$, we have

$$\sum_{j=1}^{c_1}\left\|\boldsymbol{w}_{(j,:)}\right\|^2 \leq M_2^2.$$

We use a similar trick to the paper Golowich et al. (2018) to focus only on one channel for the rest:

$$\begin{aligned}
&\mathbb{E}_{\boldsymbol{\epsilon}}\left(\sup_{\boldsymbol{w}}\sum_{j=1}^{c_1}\left\|\boldsymbol{w}_{(j,:)}\right\|^2\left(\sum_{i=1}^{m}\epsilon_i\sigma\left(\frac{1}{\left\|\boldsymbol{w}_{(j,:)}\right\|}\sum_{k=1}^{c_0}\boldsymbol{w}_{(j,k)}^{\top}\Pi_l\boldsymbol{x}_i(k)\right)\right)^2\right)\\
&\leq M_2^2\mathbb{E}_{\boldsymbol{\epsilon}}\left(\sup_{\boldsymbol{w}}\sup_{j\in[c_l]}\left(\sum_{i=1}^{m}\epsilon_i\sigma\left(\frac{1}{\left\|\boldsymbol{w}_{(j,:)}\right\|}\sum_{k=1}^{c_0}\boldsymbol{w}_{(j,k)}^{\top}\Pi_l\boldsymbol{x}_i(k)\right)\right)^2\right)\\
&\leq M_2^2\mathbb{E}_{\boldsymbol{\epsilon}}\left(\sup_{\tilde{\boldsymbol{w}}:\|\tilde{\boldsymbol{w}}\|\leq 1}\left(\sum_{i=1}^{m}\epsilon_i\sigma\left(\sum_{k=1}^{c_0}\tilde{\boldsymbol{w}}_{(k)}^{\top}\Pi_l\boldsymbol{x}_i(k)\right)\right)^2\right).
\end{aligned}$$

Now, we can use the contraction lemma and get:

$$\begin{aligned}
\mathbb{E}_{\boldsymbol{\epsilon}}\left(\sup_{\tilde{\boldsymbol{w}}:\|\tilde{\boldsymbol{w}}\|\leq 1}\left(\sum_{i=1}^{m}\epsilon_i\sigma\left(\sum_{k=1}^{c_0}\tilde{\boldsymbol{w}}_{(k)}^{\top}\Pi_l\boldsymbol{x}_i(k)\right)\right)^2\right) &\leq \mathbb{E}_{\boldsymbol{\epsilon}}\left(\sup_{\tilde{\boldsymbol{w}}:\|\tilde{\boldsymbol{w}}\|\leq 1}\left(\sum_{i=1}^{m}\epsilon_i\sum_{k=1}^{c_0}\tilde{\boldsymbol{w}}_{(k)}^{\top}\Pi_l\boldsymbol{x}_i(k)\right)^2\right)\\
&\leq \mathbb{E}_{\boldsymbol{\epsilon}}\left(\sup_{\tilde{\boldsymbol{w}}:\|\tilde{\boldsymbol{w}}\|\leq 1}\left(\sum_{k=1}^{c_0}\tilde{\boldsymbol{w}}_{(k)}^{\top}\left(\sum_{i=1}^{m}\epsilon_i\Pi_l\boldsymbol{x}_i(k)\right)\right)^2\right)\\
&\leq \mathbb{E}_{\boldsymbol{\epsilon}}\left(\left\|\sum_{i=1}^{m}\epsilon_i\Pi_l\boldsymbol{x}_i\right\|^2\right) \leq mb_x^2,
\end{aligned} \tag{20}$$

where we used the fact that the permutation matrix Π_l is unitary. Putting all this together, we get:

$$\sum_{l=1}^{|G|}\frac{1}{|G|}\mathbb{E}_{\boldsymbol{\epsilon}}\left(\sup_{\boldsymbol{w}}\left\|\sum_{i=1}^{m}\epsilon_i\begin{pmatrix}\sigma\left(\sum_{k=1}^{c_0}\boldsymbol{w}_{(1,k)}^{\top}\Pi_l\boldsymbol{x}_i(k)\right)\\ \vdots\\ \sigma\left(\sum_{k=1}^{c_0}\boldsymbol{w}_{(c_1,k)}^{\top}\Pi_l\boldsymbol{x}_i(k)\right)\end{pmatrix}\right\|\right) \leq \sum_{l=1}^{|G|}\frac{1}{|G|}\frac{b_xM_1M_2}{\sqrt{m}} = \frac{b_xM_1M_2}{\sqrt{m}},$$

which finalizes the desired results. □

C.3 Homogeneous non-decreasing activation with max pooling

The following result provides a similar upper bound for max-pooling. A bit of notation: fix the training data matrix $\boldsymbol{X}$. Denote the permutation action of the group element $l \in G$ by Π_l. The vector $\boldsymbol{l} = (l_1, \ldots, l_m) \in [|G|]^m$ determines the group permutation index individually applied to each training data points. For each $\boldsymbol{l}$, we get the group-augmented version of the dataset denoted as $\boldsymbol{X}_{\boldsymbol{l}} = (\Pi_{l_1}\boldsymbol{x}_1 \ldots \Pi_{l_m}\boldsymbol{x}_m)$.

Theorem C.2. *Consider the hypothesis space $\mathcal{H}$ defined in eq. 4. Suppose that $P(\cdot)$ is the max pooling operation, and $\sigma(\cdot)$ is a 1-Lipschitz and non-decreasing positively homogeneous activation function. Fix the training data matrix $\boldsymbol{X}$. Then with probability at least $1-\delta$ and for all $h \in \mathcal{H}$, we have:*

$$\mathcal{L}(h) \leq \hat{\mathcal{L}}(h) + 2\frac{M_1 M_2 g(\boldsymbol{X})}{\sqrt{m}} + 4\sqrt{\frac{2\log(4/\delta)}{m}},$$

with $g(\boldsymbol{X})$ defined as:

$$g(\boldsymbol{X}) = \sqrt{8\log(|G|)M_{2,X}^{\max} + b_x^2 + \sqrt{8\log(|G|)M_{2,X}^{\max} b_x^2}}$$

where $M_{2,X}^{\max} = \max_{\boldsymbol{l}} \left\|\boldsymbol{X}_{\boldsymbol{l}}^\top \boldsymbol{X}_{\boldsymbol{l}}\right\|_{2\to 2}$ for the group-augmented training data matrix $\boldsymbol{X}_{\boldsymbol{l}}$.

The proof for max pooling leverages new techniques and is presented in Appendix C.3. The generalization bound in the above theorem is completely dimension-free (apart from a logarithmic dependence on the group size in $g(\boldsymbol{X})$). The norm dependency is also quite minimal. The bound merely depends on the Euclidean norm of parameters per layer. Note that the norm is computed for the convolutional kernel $\boldsymbol{w}$, which is tighter than both spectral and Frobenius norm of the respective matrix $\boldsymbol{W}$. Finally, there is no dependency on the dimension or the number of input and output channels (c_0, c_1). The term $M_{2,X}^{\max}$ is new compared to other results in the literature. This term essentially captures the covariance of the data in the quotient feature space. The term $M_{2,X}^{\max}$ is defined in terms of the spectral norm, which is lower-bounded by the norm of column vectors, namely b_x. See Appendix C.3 for more discussions on $M_{2,X}^{\max}$.

We start from eq. 18, where the first layer is peeled off. One of the key ideas behind the proof is that if $\sigma(\cdot)$ is positively homogeneous and non-decreasing, the activation $\sigma(\cdot)$ and the max operation can swap their place. We have:

$$\begin{aligned}
\mathbb{E}_{\boldsymbol{\epsilon}}\left(\sup_{\boldsymbol{w}}\left\|\sum_{i=1}^m \epsilon_i P\circ\sigma(\boldsymbol{W}\boldsymbol{x}_i)\right\|\right) &= \mathbb{E}_{\boldsymbol{\epsilon}}\left(\sup_{\boldsymbol{w}}\left\|\sum_{i=1}^m \epsilon_i \begin{pmatrix}\max\sigma\left(\sum_{k=1}^{c_0}\boldsymbol{w}_{(1,k)}\circledast_G \boldsymbol{x}_i(k)\right)\\ \vdots \\ \max\sigma\left(\sum_{k=1}^{c_0}\boldsymbol{w}_{(c_1,k)}\circledast_G \boldsymbol{x}_i(k)\right)\end{pmatrix}\right\|\right)\\
&= \mathbb{E}_{\boldsymbol{\epsilon}}\left(\sup_{\boldsymbol{w}}\left\|\sum_{i=1}^m \epsilon_i \begin{pmatrix}\sigma\left(\max\sum_{k=1}^{c_0}\boldsymbol{w}_{(1,k)}\circledast_G \boldsymbol{x}_i(k)\right)\\ \vdots \\ \sigma\left(\max\sum_{k=1}^{c_0}\boldsymbol{w}_{(c_1,k)}\circledast_G \boldsymbol{x}_i(k)\right)\end{pmatrix}\right\|\right)
\end{aligned}$$

Then, similar to the previous proof, we use the following moment inequality:

$$\begin{aligned}
&\mathbb{E}_{\boldsymbol{\epsilon}}\left(\sup_{\boldsymbol{w}}\left\|\sum_{i=1}^m \epsilon_i \begin{pmatrix}\sigma\left(\max\sum_{k=1}^{c_0}\boldsymbol{w}_{(1,k)}\circledast_G \boldsymbol{x}_i(k)\right)\\ \vdots \\ \sigma\left(\max\sum_{k=1}^{c_0}\boldsymbol{w}_{(c_1,k)}\circledast_G \boldsymbol{x}_i(k)\right)\end{pmatrix}\right\|\right)\\
&\leq \sqrt{\mathbb{E}_{\boldsymbol{\epsilon}}\left(\sup_{\boldsymbol{w}}\left\|\sum_{i=1}^m \epsilon_i \begin{pmatrix}\sigma\left(\max\sum_{k=1}^{c_0}\boldsymbol{w}_{(1,k)}\circledast_G \boldsymbol{x}_i(k)\right)\\ \vdots \\ \sigma\left(\max\sum_{k=1}^{c_0}\boldsymbol{w}_{(c_1,k)}\circledast_G \boldsymbol{x}_i(k)\right)\end{pmatrix}\right\|^2\right)}
\end{aligned}$$

We can then use the peeling-off technique similar to the proof above for the term inside the square root:

$$
\begin{aligned}
&\mathbb{E}_{\boldsymbol{\epsilon}}\left(\sup_{\boldsymbol{w}}\left\|\sum_{i=1}^{m}\epsilon_i\begin{pmatrix}\sigma\left(\max\sum_{k=1}^{c_0}\boldsymbol{w}_{(1,k)}\circledast_G\boldsymbol{x}_i(k)\right)\\ \vdots\\ \sigma\left(\max\sum_{k=1}^{c_0}\boldsymbol{w}_{(c_1,k)}\circledast_G\boldsymbol{x}_i(k)\right)\end{pmatrix}\right\|^2\right)\\
&=\mathbb{E}_{\boldsymbol{\epsilon}}\left(\sup_{\boldsymbol{w}}\left\|\sum_{i=1}^{m}\epsilon_i\begin{pmatrix}\sigma\left(\max_{l\in[|G|]}\sum_{k=1}^{c_0}\boldsymbol{w}_{(1,k)}^{\top}\Pi_l\boldsymbol{x}_i(k)\right)\\ \vdots\\ \sigma\left(\max_{l\in[|G|]}\sum_{k=1}^{c_0}\boldsymbol{w}_{(c_1,k)}^{\top}\Pi_l\boldsymbol{x}_i(k)\right)\end{pmatrix}\right\|^2\right)\\
&=\mathbb{E}_{\boldsymbol{\epsilon}}\left(\sup_{\boldsymbol{w}}\sum_{j=1}^{c_1}\left(\sum_{i=1}^{m}\epsilon_i\sigma\left(\max_{l\in[|G|]}\sum_{k=1}^{c_0}\boldsymbol{w}_{(j,k)}^{\top}\Pi_l\boldsymbol{x}_i(k)\right)\right)^2\right)\\
&\leq M_2^2\mathbb{E}_{\boldsymbol{\epsilon}}\left(\sup_{\boldsymbol{w}:\|\boldsymbol{w}\|\leq 1}\left(\sum_{i=1}^{m}\epsilon_i\sigma\left(\max_{l\in[|G|]}\sum_{k=1}^{c_0}\boldsymbol{w}_{(k)}^{\top}\Pi_l\boldsymbol{x}_i(k)\right)\right)^2\right)
\end{aligned}
$$

To continue, we define $\boldsymbol{l}\in[|G|]^m$ as the vector of $(l_1,\ldots,l_m)$ with $l_i\in[|G|]$. Now, we can first use the contraction inequality and some other standard techniques to get the following:

$$
\begin{aligned}
&\mathbb{E}_{\boldsymbol{\epsilon}}\left(\sup_{\boldsymbol{w}:\|\boldsymbol{w}\|\leq 1}\left(\sum_{i=1}^{m}\epsilon_i\sigma\left(\max_{l\in[|G|]}\sum_{k=1}^{c_0}\boldsymbol{w}_{(k)}^{\top}\Pi_l\boldsymbol{x}_i(k)\right)\right)^2\right)\\
&\leq\mathbb{E}_{\boldsymbol{\epsilon}}\left(\sup_{\boldsymbol{w}:\|\boldsymbol{w}\|\leq 1}\left(\sum_{i=1}^{m}\epsilon_i\max_{l\in[|G|]}\left(\sum_{k=1}^{c_0}\boldsymbol{w}_{(k)}^{\top}\Pi_l\boldsymbol{x}_i(k)\right)\right)^2\right)\\
&\leq\mathbb{E}_{\boldsymbol{\epsilon}}\left(\sup_{\boldsymbol{w}:\|\boldsymbol{w}\|\leq 1}\max_{\boldsymbol{l}}\left(\sum_{i=1}^{m}\epsilon_i\left(\sum_{k=1}^{c_0}\boldsymbol{w}_{(k)}^{\top}\Pi_{l_i}\boldsymbol{x}_i(k)\right)\right)^2\right)\\
&=\mathbb{E}_{\boldsymbol{\epsilon}}\left(\sup_{\boldsymbol{w}:\|\boldsymbol{w}\|\leq 1}\max_{\boldsymbol{l}}\left(\sum_{k=1}^{c_0}\boldsymbol{w}_{(k)}^{\top}\left(\sum_{i=1}^{m}\epsilon_i\Pi_{l_i}\boldsymbol{x}_i(k)\right)\right)^2\right)\\
&\leq\mathbb{E}_{\boldsymbol{\epsilon}}\left(\max_{\boldsymbol{l}}\left\|\sum_{i=1}^{m}\epsilon_i\Pi_{l_i}\boldsymbol{x}_i\right\|^2\right)
\end{aligned}
\tag{21}
$$

where we abuse the notation $\Pi_{l_i}\boldsymbol{x}_i$ to denote the channel-wise application of the permutation to $\boldsymbol{x}_i$ (assuming $\boldsymbol{x}_i$ is shaped as $|G|\times c_0$). We use the same term $\Pi_{l_i}\boldsymbol{x}_i$ to denote its vectorized version to avoid the notation overhead.

Now, see that for $\beta>0$, :

$$
\begin{aligned}
\beta\mathbb{E}_{\boldsymbol{\epsilon}}\left(\max_{\boldsymbol{l}}\left\|\sum_{i=1}^{m}\epsilon_i\Pi_{l_i}\boldsymbol{x}_i\right\|^2\right)&=\mathbb{E}_{\boldsymbol{\epsilon}}\left(\log\exp\max_{\boldsymbol{l}}\beta\left\|\sum_{i=1}^{m}\epsilon_i\Pi_{l_i}\boldsymbol{x}_i\right\|^2\right)\\
&\leq\log\mathbb{E}_{\boldsymbol{\epsilon}}\left(\max_{\boldsymbol{l}}\exp\beta\left\|\sum_{i=1}^{m}\epsilon_i\Pi_{l_i}\boldsymbol{x}_i\right\|^2\right)\\
&\leq\log\mathbb{E}_{\boldsymbol{\epsilon}}\left(\sum_{\boldsymbol{l}}\exp\beta\left\|\sum_{i=1}^{m}\epsilon_i\Pi_{l_i}\boldsymbol{x}_i\right\|^2\right)
\end{aligned}
$$

We can now use the Lemma B.2. Note that, in our case, we have:

$$\left\| \sum_{i=1}^{m} \epsilon_i \Pi_{l_i} \boldsymbol{x}_i \right\|^2 = \|\boldsymbol{X_l}\boldsymbol{\epsilon}\|^2 = \boldsymbol{\epsilon}^\top \boldsymbol{X_l}^\top \boldsymbol{X_l}\boldsymbol{\epsilon},$$

where $\boldsymbol{\epsilon} = (\epsilon_1, \ldots, \epsilon_m)$, $\boldsymbol{l} = (l_1, \ldots, l_m)$, and $\boldsymbol{X_l} = (\Pi_{l_1}\boldsymbol{x}_1 \ldots \Pi_{l_m}\boldsymbol{x}_m)$. We now choose $\boldsymbol{B} = \boldsymbol{X_l}^\top \boldsymbol{X_l}$ in Lemma B.2 to get:

$$\begin{aligned}
\log \mathbb{E}_{\boldsymbol{\epsilon}} \left(\sum_{\boldsymbol{l}} \exp \beta \left\| \sum_{i=1}^{m} \epsilon_i \Pi_{l_i} \boldsymbol{x}_i \right\|^2 \right) &\leq \log \left(\sum_{\boldsymbol{l}} \exp \left(\frac{\beta \operatorname{Tr}(\boldsymbol{X_l}^\top \boldsymbol{X_l})}{1 - 8\beta \left\| \boldsymbol{X_l}^\top \boldsymbol{X_l} \right\|_{2\to 2}} \right) \right) \\
&= \log \left(\sum_{\boldsymbol{l}} \exp \left(\frac{\beta \operatorname{Tr}(\boldsymbol{X}^\top \boldsymbol{X})}{1 - 8\beta \left\| \boldsymbol{X_l}^\top \boldsymbol{X_l} \right\|_{2\to 2}} \right) \right) \\
&\leq \log \left(\sum_{\boldsymbol{l}} \exp \left(\frac{\beta m b_x^2}{1 - 8\beta M_{2,X}^{\max}} \right) \right) \\
&\leq \log \left(|G|^m \exp \left(\frac{\beta m b_x^2}{1 - 8\beta M_{2,X}^{\max}} \right) \right)
\end{aligned}$$

where $M_{2,X}^{\max} = \max_{\boldsymbol{l}} \left\| \boldsymbol{X_l}^\top \boldsymbol{X_l} \right\|_{2\to 2}$. Note that we have assumed $8\beta M_{2,X}^{\max} \leq 1$. We then have:

$$\mathbb{E}_{\boldsymbol{\epsilon}} \left(\max_{\boldsymbol{l}} \left\| \sum_{i=1}^{m} \epsilon_i \Pi_{l_i} \boldsymbol{x}_i \right\|^2 \right) \leq \frac{m \log(|G|)}{\beta} + \frac{m b_x^2}{1 - 8\beta M_{2,X}^{\max}}$$

Note that

$$\max_{\beta} \frac{a}{\beta} + \frac{b}{1 - c\beta} = ac + b + 2\sqrt{abc},$$

obtained for $\beta = 1/\left(c + \sqrt{bc/a}\right)$. We need to assume that $8\beta M_{2,X}^{\max} \leq 1$, which means:

$$8M_{2,X}^{\max} \leq \left(8M_{2,X}^{\max} + \sqrt{8M_{2,X}^{\max} b_x^2 / \log|G|} \right).$$

This is always true, so choosing β accordingly, we have:

$$\mathbb{E}_{\boldsymbol{\epsilon}} \left(\max_{\boldsymbol{l}} \left\| \sum_{i=1}^{m} \epsilon_i \Pi_{l_i} \boldsymbol{x}_i \right\|^2 \right) \leq 8m \log(|G|) M_{2,X}^{\max} + m b_x^2 + m\sqrt{8 \log(|G|) M_{2,X}^{\max} b_x^2},$$

which gives us the total bound:

$$\frac{M_1 M_2 \sqrt{8 \log(|G|) M_{2,X}^{\max} + b_x^2 + \sqrt{8 \log(|G|) M_{2,X}^{\max} b_x^2}}}{\sqrt{m}}$$

Remark C.3. Ignoring the term $M_{2,X}^{\max}$, the bound is dimension-free. The term $M_{2,X}^{\max}$ depends on the data matrix's spectral norm with normalized columns. Remember that:

$$M_{2,X}^{\max} = \max_{\boldsymbol{l}} \left\| \boldsymbol{X_l}^\top \boldsymbol{X_l} \right\|_{2\to 2}.$$

The spectral norm of $\boldsymbol{X}^\top \boldsymbol{X}$ is the spectral norm of the sample covariance matrix of the data. Consider an extreme case of i.i.d data samples with the diagonal covariance matrix; the spectral norm of $\boldsymbol{X}^\top \boldsymbol{X}$ will be $\mathcal{O}(m)$ as $m \to \infty$. The situation remains the same for an arbitrary covariance matrix. In other words, this bound is loose for large samples. However, in small samples, the spectral norm can be smaller (for example, assume $\boldsymbol{X}$ is approximately an orthogonal matrix).

It is important to note that the term $M_{2,X}^{\max}$ appears for bounding $\mathbb{E}_{\boldsymbol{\epsilon}}\left(\max_{\boldsymbol{l}} \|\sum_{i=1}^m \epsilon_i \Pi_{l_i} \boldsymbol{x}_i\|^2\right)$, which itself appeared in the step eq. 21. We can consider max-pooling as a Lipschitz pooling operation and use techniques similar to Vardi et al. (2022); Graf et al. (2022) to bound the term. However, this would incur an additional logarithmic dependence on the input dimension and m, but it will be tighter as $m \to \infty$. Ideally, the ultimate generalization bound should be the minimum of these two cases.

C.4 General Pooling

In this section, we consider the case of general pooling. The proof steps are similar to the classical average pooling case, so we present it more compactly. We first peel off the last layer and use the moment inequality:

$$\mathbb{E}_{\boldsymbol{\epsilon}}\left(\sup_{\boldsymbol{w}}\left\|\sum_{i=1}^m \epsilon_i P\circ\sigma(\boldsymbol{W}\boldsymbol{x}_i)\right\|\right) = \mathbb{E}_{\boldsymbol{\epsilon}}\left(\sup_{\boldsymbol{w}}\left\|\sum_{i=1}^m \epsilon_i \begin{pmatrix}\phi\left(\frac{1}{|G|}\mathbf{1}^\top\sigma\left(\sum_{k=1}^{c_0}\boldsymbol{w}_{(1,k)}\circledast_G \boldsymbol{x}_i(k)\right)\right)\\ \vdots \\ \phi\left(\frac{1}{|G|}\mathbf{1}^\top\sigma\left(\sum_{k=1}^{c_0}\boldsymbol{w}_{(c_1,k)}\circledast_G \boldsymbol{x}_i(k)\right)\right)\end{pmatrix}\right\|\right)$$

$$\leq \sqrt{\mathbb{E}_{\boldsymbol{\epsilon}}\left(\sup_{\boldsymbol{w}}\left\|\sum_{i=1}^m \epsilon_i \begin{pmatrix}\phi\left(\frac{1}{|G|}\mathbf{1}^\top\sigma\left(\sum_{k=1}^{c_0}\boldsymbol{w}_{(1,k)}\circledast_G \boldsymbol{x}_i(k)\right)\right)\\ \vdots \\ \phi\left(\frac{1}{|G|}\mathbf{1}^\top\sigma\left(\sum_{k=1}^{c_0}\boldsymbol{w}_{(c_1,k)}\circledast_G \boldsymbol{x}_i(k)\right)\right)\end{pmatrix}\right\|^2\right)}.$$

The next step is to use the peeling argument and contraction inequality step by step:

$$\begin{aligned}
&\mathbb{E}_{\boldsymbol{\epsilon}}\left(\sup_{\boldsymbol{w}}\left\|\sum_{i=1}^m \epsilon_i \begin{pmatrix}\phi\left(\frac{1}{|G|}\mathbf{1}^\top\sigma\left(\sum_{k=1}^{c_0}\boldsymbol{w}_{(1,k)}\circledast_G \boldsymbol{x}_i(k)\right)\right)\\ \vdots \\ \phi\left(\frac{1}{|G|}\mathbf{1}^\top\sigma\left(\sum_{k=1}^{c_0}\boldsymbol{w}_{(c_1,k)}\circledast_G \boldsymbol{x}_i(k)\right)\right)\end{pmatrix}\right\|^2\right)\\
&= \mathbb{E}_{\boldsymbol{\epsilon}}\left(\sup_{\boldsymbol{w}}\sum_{j=1}^{c_1}\left(\sum_{i=1}^m \epsilon_i\phi\left(\frac{1}{|G|}\mathbf{1}^\top\sigma\left(\sum_{k=1}^{c_0}\boldsymbol{w}_{(j,k)}\circledast_G \boldsymbol{x}_i(k)\right)\right)\right)^2\right)\\
&= \mathbb{E}_{\boldsymbol{\epsilon}}\left(\sup_{\boldsymbol{w}}\sum_{j=1}^{c_1}\left\|\boldsymbol{w}_{(j,:)}\right\|^2\left(\sum_{i=1}^m \epsilon_i\phi\left(\frac{1}{|G|}\mathbf{1}^\top\sigma\left(\frac{1}{\left\|\boldsymbol{w}_{(j,:)}\right\|}\sum_{k=1}^{c_0}\boldsymbol{w}_{(j,k)}\circledast_G \boldsymbol{x}_i(k)\right)\right)\right)^2\right)\\
&\leq M_2^2\mathbb{E}_{\boldsymbol{\epsilon}}\left(\sup_{\boldsymbol{w}}\left(\sum_{i=1}^m \epsilon_i\phi\left(\frac{1}{|G|}\mathbf{1}^\top\sigma\left(\frac{1}{\|\boldsymbol{w}\|}\sum_{k=1}^{c_0}\boldsymbol{w}_{(k)}\circledast_G \boldsymbol{x}_i(k)\right)\right)\right)^2\right)\\
&\leq M_2^2\mathbb{E}_{\boldsymbol{\epsilon}}\left(\sup_{\boldsymbol{w}}\left(\sum_{i=1}^m \epsilon_i\frac{1}{|G|}\mathbf{1}^\top\sigma\left(\frac{1}{\|\boldsymbol{w}\|}\sum_{k=1}^{c_0}\boldsymbol{w}_{(k)}\circledast_G \boldsymbol{x}_i(k)\right)\right)^2\right)\\
&\leq M_2^2\frac{1}{|G|}\sum_{l=1}^{|G|}\mathbb{E}_{\boldsymbol{\epsilon}}\left(\sup_{\boldsymbol{w}}\left(\sum_{i=1}^m \epsilon_i\sigma\left(\frac{1}{\|\boldsymbol{w}\|}\sum_{k=1}^{c_0}\boldsymbol{w}_{(k)}^\top\Pi_l\boldsymbol{x}_i(k)\right)\right)^2\right)
\end{aligned}$$

And then we can re-use what we proved in eq. 20 to get:

$$\begin{aligned}
&\mathbb{E}_{\boldsymbol{\epsilon}}\left(\sup_{\boldsymbol{w}}\left(\sum_{i=1}^m \epsilon_i\sigma\left(\frac{1}{\|\boldsymbol{w}\|}\sum_{k=1}^{c_0}\boldsymbol{w}_{(k)}^\top\Pi_l\boldsymbol{x}_i(k)\right)\right)^2\right)\\
&\quad= \mathbb{E}_{\boldsymbol{\epsilon}}\left(\sup_{\boldsymbol{w}}\left(\sum_{i=1}^m \epsilon_i\left(\frac{1}{\|\boldsymbol{w}\|}\sum_{k=1}^{c_0}\boldsymbol{w}_{(k)}^\top\Pi_l\boldsymbol{x}_i(k)\right)\right)^2\right) \leq mb_x^2.
\end{aligned}$$

Putting all of this together, we get the final theorem.

C.5 Proof for Multi-Layer Group Convolutional Networks

In this section, we prove Theorem 4.3. We start again by simply peeling off the last layer:

$$\mathbb{E}_{\boldsymbol{\epsilon}}\left(\sup_{\boldsymbol{u},\{\boldsymbol{w}^{(l)},l\in[L]\}}\frac{1}{m}\sum_{i=1}^{m}\epsilon_i\boldsymbol{u}^\top P\circ\sigma\left(\boldsymbol{W}^L\boldsymbol{x}_i^{(L-1)}\right)\right)=\frac{M_1}{m}\mathbb{E}_{\boldsymbol{\epsilon}}\left(\sup_{\{\boldsymbol{w}^{(l)},l\in[L]\}}\left\|\sum_{i=1}^{m}\epsilon_i P\circ\sigma(\boldsymbol{W}\boldsymbol{x}_i^{(L-1)})\right\|\right), \quad (22)$$

where, for brevity, we use $\boldsymbol{x}^{(L-1)}$ to denote the output of the hidden layer $L-1$. We can expand the average pooling operation and use the positive homogeneity property of ReLU function to

$$\mathbb{E}_{\boldsymbol{\epsilon}}\left(\sup_{\{\boldsymbol{w}^{(l)},l\in[L]\}}\left\|\sum_{i=1}^{m}\epsilon_i P\circ\sigma(\boldsymbol{W}\boldsymbol{x}_i^{(L-1)})\right\|\right)\leq\sum_{g=1}^{|G|}\frac{1}{|G|}\mathbb{E}_{\boldsymbol{\epsilon}}\left(\sup_{\{\boldsymbol{w}^{(l)},l\in[L]\}}\left\|\sum_{i=1}^{m}\epsilon_i\begin{pmatrix}\sigma\left(\sum_{k=1}^{c_{L-1}}\boldsymbol{w}_{(1,k)}^{(L),\top}\Pi_g\boldsymbol{x}_i^{(L-1)}(k)\right)\\ \vdots\\ \sigma\left(\sum_{k=1}^{c_{L-1}}\boldsymbol{w}_{(c_L,k)}^{(L),\top}\Pi_g\boldsymbol{x}_i^{(L-1)}(k)\right)\end{pmatrix}\right\|\right)$$

and then, we focus on a single term and use simple Jensen to get:

$$\begin{aligned}&\mathbb{E}_{\boldsymbol{\epsilon}}\left(\sup_{\{\boldsymbol{w}^{(l)},l\in[L]\}}\left\|\sum_{i=1}^{m}\epsilon_i\begin{pmatrix}\sigma\left(\sum_{k=1}^{c_{L-1}}\boldsymbol{w}_{(1,k)}^{(L),\top}\Pi_g\boldsymbol{x}_i^{(L-1)}(k)\right)\\ \vdots\\ \sigma\left(\sum_{k=1}^{c_{L-1}}\boldsymbol{w}_{(c_L,k)}^{(L),\top}\Pi_g\boldsymbol{x}_i^{(L-1)}(k)\right)\end{pmatrix}\right\|\right)\\ &\leq\sqrt{\mathbb{E}_{\boldsymbol{\epsilon}}\left(\sup_{\{\boldsymbol{w}^{(l)},l\in[L]\}}\left\|\sum_{i=1}^{m}\epsilon_i\begin{pmatrix}\sigma\left(\sum_{k=1}^{c_{L-1}}\boldsymbol{w}_{(1,k)}^{(L),\top}\Pi_g\boldsymbol{x}_i^{(L-1)}(k)\right)\\ \vdots\\ \sigma\left(\sum_{k=1}^{c_{L-1}}\boldsymbol{w}_{(c_L,k)}^{(L),\top}\Pi_g\boldsymbol{x}_i^{(L-1)}(k)\right)\end{pmatrix}\right\|^2\right)},\end{aligned}$$

and we can continue with a similar approach to simplify this further:

$$\begin{aligned}&\mathbb{E}_{\boldsymbol{\epsilon}}\left(\sup_{\{\boldsymbol{w}^{(l)},l\in[L]\}}\left\|\sum_{i=1}^{m}\epsilon_i\begin{pmatrix}\sigma\left(\sum_{k=1}^{c_{L-1}}\boldsymbol{w}_{(1,k)}^{(L),\top}\Pi_g\boldsymbol{x}_i^{(L-1)}(k)\right)\\ \vdots\\ \sigma\left(\sum_{k=1}^{c_{L-1}}\boldsymbol{w}_{(c_L,k)}^{(L),\top}\Pi_g\boldsymbol{x}_i^{(L-1)}(k)\right)\end{pmatrix}\right\|^2\right)\\ &=\mathbb{E}_{\boldsymbol{\epsilon}}\left(\sup_{\{\boldsymbol{w}^{(l)},l\in[L]\}}\sum_{j=1}^{c_L}\left\|\boldsymbol{w}_{(j,:)}^{(L)}\right\|^2\left(\sum_{i=1}^{m}\epsilon_i\sigma\left(\frac{1}{\left\|\boldsymbol{w}_{(j,:)}^{(L)}\right\|}\sum_{k=1}^{c_{L-1}}\boldsymbol{w}_{(j,k)}^{(L),\top}\Pi_g\boldsymbol{x}_i^{(L-1)}(k)\right)\right)^2\right)\\ &\leq M_L^2\mathbb{E}_{\boldsymbol{\epsilon}}\left(\sup_{\{\boldsymbol{w}^{(l)},l\in[L-1],\boldsymbol{w}^{\tilde{(L)}}:\left\|\boldsymbol{w}^{\tilde{(L)}}\right\|\leq1\}}\left(\sum_{i=1}^{m}\epsilon_i\sigma\left(\sum_{k=1}^{c_{L-1}}\tilde{\boldsymbol{w}}_{(k)}^{(L),\top}\Pi_g\boldsymbol{x}_i^{(L-1)}(k)\right)\right)^2\right)\\ &\leq M_L^2\mathbb{E}_{\boldsymbol{\epsilon}}\left(\sup_{\{\boldsymbol{w}^{(l)},l\in[L-1]\}}\left\|\sum_{i=1}^{m}\epsilon_i\left(\boldsymbol{x}_i^{(L-1)}\right)\right\|^2\right),\end{aligned}$$

where Π_g is a unitary matrix and was removed. Now, we have removed the last layer from the bound, and we can focus on the rest of layers.

$$
\begin{aligned}
&\mathbb{E}_{\boldsymbol{\epsilon}}\left(\sup_{\{\boldsymbol{w}^{(l)}, l\in[L-1]\}}\left\|\sum_{i=1}^{m}\epsilon_i\left(\boldsymbol{x}_i^{(L-1)}\right)\right\|^2\right)\\
&=\mathbb{E}_{\boldsymbol{\epsilon}}\left(\sup_{\{\boldsymbol{w}^{(l)}, l\in[L-1]\}}\left\|\sum_{i=1}^{m}\epsilon_i\begin{pmatrix}\sigma\left(\sum_{k=1}^{c_{L-2}}\boldsymbol{w}_{(1,k)}^{(L-1),\top}\circledast\boldsymbol{x}_i^{(L-2)}(k)\right)\\ \vdots\\ \sigma\left(\sum_{k=1}^{c_{L-2}}\boldsymbol{w}_{(c_{L-1},k)}^{(L-1),\top}\circledast\boldsymbol{x}_i^{(L-2)}(k)\right)\end{pmatrix}\right\|^2\right)\\
&=\mathbb{E}_{\boldsymbol{\epsilon}}\left(\sup_{\{\boldsymbol{w}^{(l)}, l\in[L-1]\}}\sum_{g=1}^{|G|}\sum_{j=1}^{c_{L-1}}\left\|\boldsymbol{w}_{(j,:)}^{(L-1)}\right\|^2\left(\sum_{i=1}^{m}\epsilon_i\sigma\left(\frac{1}{\left\|\boldsymbol{w}_{(j,:)}^{(L-1)}\right\|}\sum_{k=1}^{c_{L-2}}\boldsymbol{w}_{(j,k)}^{(L-1),\top}\Pi_g\boldsymbol{x}_i^{(L-2)}(k)\right)\right)^2\right)\\
&\leq\sum_{g=1}^{|G|}\mathbb{E}_{\boldsymbol{\epsilon}}\left(\sup_{\{\boldsymbol{w}^{(l)}, l\in[L-1]\}}\sum_{j=1}^{c_{L-1}}\left\|\boldsymbol{w}_{(j,:)}^{(L-1)}\right\|^2\left(\sum_{i=1}^{m}\epsilon_i\sigma\left(\frac{1}{\left\|\boldsymbol{w}_{(j,:)}^{(L-1)}\right\|}\sum_{k=1}^{c_{L-2}}\boldsymbol{w}_{(j,k)}^{(L-1),\top}\Pi_g\boldsymbol{x}_i^{(L-2)}(k)\right)\right)^2\right)\\
&\leq|G|M_{L-1}^2\mathbb{E}_{\boldsymbol{\epsilon}}\left(\sup_{\{\boldsymbol{w}^{(l)}, l\in[L-2]\}}\left\|\sum_{i=1}^{m}\epsilon_i\left(\boldsymbol{x}_i^{(L-2)}\right)\right\|^2\right).
\end{aligned}
$$

Note that the last step involves the very same peeling argument for each term in the sum, and we removed it. Doing this iteratively, we can peel off all the layers, and get the final result. It is worth noting that the authors Golowich et al. (2018) provide a way of converting exponential depth dependence to polynomial dependence. Using this technique we can change the depth dependence from $|G|^{L-1/2}$ to $(L-1)\log|G|$ for $L>1$. See Section 3 of Golowich et al. (2018) for more discussions.

D General Equivariant Networks

The general equivariant networks are defined in Fourier space as follows:

$$\mathcal{H}_{\hat{\boldsymbol{u}},\hat{\boldsymbol{w}}} := \left\{\hat{\boldsymbol{u}}^\top\boldsymbol{Q}_2\sigma(\boldsymbol{Q}_1\hat{\boldsymbol{W}}\hat{\boldsymbol{x}})\right\}.$$

Here, we assumed that the input is already represented in the Fourier space $\hat{\boldsymbol{x}}$. The input and hidden layer representations are the direct sums of the group irreps ψ each, respectively, with the multiplicity $m_{0,\psi}$ and $m_{1,\psi}$. Since we are working with the point-wise non-linearity σ in the *spatial domain*, two unitary transformations $\boldsymbol{Q}_1$ and $\boldsymbol{Q}_2$ are applied as Fourier transforms from the irrep space to the spatial domain. Finally, to get an invariant function, the vector $\hat{\boldsymbol{u}}$ only mixes the frequencies of the trivial representation ψ_0, and it is zero otherwise. To use an analogy with group convolutional networks, $\boldsymbol{Q}_1$ and $\boldsymbol{Q}_2$ are the Fourier matrices, and $\hat{\boldsymbol{u}}$ is a combination of the pooling, which projects into the trivial representation of the group, and the last aggregation step. The hypothesis space is represented as

$$\mathcal{H} := \left\{\hat{\boldsymbol{u}}^\top\boldsymbol{Q}_2\sigma\left(\boldsymbol{Q}_1\bigoplus_{\psi}\bigoplus_{i=1}^{m_{1,\psi}}\sum_{j=1}^{m_{0,\psi}}\hat{\boldsymbol{W}}(\psi,i,j)\hat{\boldsymbol{x}}(\psi,j)\right)\right\}.$$

We start the proof as follows:

$$
\begin{aligned}
\mathbb{E}_{\boldsymbol{\epsilon}}\left(\sup_{\hat{\boldsymbol{u}},\hat{\boldsymbol{W}}}\frac{1}{m}\sum_{i=1}^{m}\epsilon_i\hat{\boldsymbol{u}}^\top\boldsymbol{Q}_2\sigma(\boldsymbol{Q}_1\hat{\boldsymbol{W}}\hat{\boldsymbol{x}}_i)\right) &\leq \frac{M_1}{m}\mathbb{E}_{\boldsymbol{\epsilon}}\left(\sup_{\hat{\boldsymbol{W}}}\left\|\sum_{i=1}^{m}\epsilon_i\sigma(\boldsymbol{Q}_1\hat{\boldsymbol{W}}\hat{\boldsymbol{x}}_i)\right\|\right).\\
&\leq \frac{M_1}{m}\left(\mathbb{E}_{\boldsymbol{\epsilon}}\left(\sup_{\hat{\boldsymbol{W}}}\left\|\sum_{i=1}^{m}\epsilon_i\sigma(\boldsymbol{Q}_1\hat{\boldsymbol{W}}\hat{\boldsymbol{x}}_i)\right\|^2\right)\right)^{1/2}
\end{aligned}
$$

From this step, we can re-use the pooling operation:

$$
\begin{aligned}
&\mathbb{E}_{\boldsymbol{\epsilon}}\left(\sup_{\hat{\boldsymbol{W}}}\left\|\sum_{i=1}^{m}\epsilon_i\sigma(\boldsymbol{Q}_1\hat{\boldsymbol{W}}\hat{\boldsymbol{x}}_i)\right\|^2\right)\\
&=\mathbb{E}_{\boldsymbol{\epsilon}}\left(\sup_{\hat{\boldsymbol{W}}}\sum_j\left(\sum_{i=1}^{m}\epsilon_i\sigma\left(\boldsymbol{q}_{1,j}^\top\hat{\boldsymbol{W}}\hat{\boldsymbol{x}}_i\right)\right)^2\right)\\
&=\mathbb{E}_{\boldsymbol{\epsilon}}\left(\sup_{\hat{\boldsymbol{W}}}\sum_j\left\|\boldsymbol{q}_{1,j}^\top\hat{\boldsymbol{W}}\right\|^2\left(\sum_{i=1}^{m}\epsilon_i\sigma\left(\frac{1}{\left\|\boldsymbol{q}_{1,j}^\top\hat{\boldsymbol{W}}\right\|}\boldsymbol{q}_{1,j}^\top\hat{\boldsymbol{W}}\hat{\boldsymbol{x}}_i\right)\right)^2\right)\\
&\leq\mathbb{E}_{\boldsymbol{\epsilon}}\left(\sup_{\hat{\boldsymbol{W}}}\sum_j\left\|\boldsymbol{q}_{1,j}^\top\hat{\boldsymbol{W}}\right\|^2\sup_{\hat{\boldsymbol{W}},j}\left(\sum_{i=1}^{m}\epsilon_i\sigma\left(\frac{1}{\left\|\boldsymbol{q}_{1,j}^\top\hat{\boldsymbol{W}}\right\|}\boldsymbol{q}_{1,j}^\top\hat{\boldsymbol{W}}\hat{\boldsymbol{x}}_i\right)\right)^2\right)\\
&\leq M_2^2\mathbb{E}_{\boldsymbol{\epsilon}}\left(\sup_{\hat{\boldsymbol{W}},j}\left(\sum_{i=1}^{m}\epsilon_i\sigma\left(\frac{1}{\left\|\boldsymbol{q}_{1,j}^\top\hat{\boldsymbol{W}}\right\|}\boldsymbol{q}_{1,j}^\top\hat{\boldsymbol{W}}\hat{\boldsymbol{x}}_i\right)\right)^2\right)
\end{aligned}
$$

Note that we used the following:

$$
\sum_{j=1}^{c_1}\left\|\boldsymbol{q}_{1,j}^\top\hat{\boldsymbol{W}}\right\|^2=\left\|\boldsymbol{Q}_1\hat{\boldsymbol{W}}\right\|^2=\left\|\hat{\boldsymbol{W}}\right\|^2\leq M_2^2.
$$

Then, using the contraction lemma, we obtain:

$$
\begin{aligned}
&\mathbb{E}_{\boldsymbol{\epsilon}}\left(\sup_{\hat{\boldsymbol{W}},j}\left(\sum_{i=1}^{m}\epsilon_i\sigma\left(\frac{1}{\left\|\boldsymbol{q}_{1,j}^\top\hat{\boldsymbol{W}}\right\|}\boldsymbol{q}_{1,j}^\top\hat{\boldsymbol{W}}\hat{\boldsymbol{x}}_i\right)\right)^2\right)\\
&\leq\mathbb{E}_{\boldsymbol{\epsilon}}\left(\sup_{\hat{\boldsymbol{W}},j}\left(\sum_{i=1}^{m}\epsilon_i\left(\frac{1}{\left\|\boldsymbol{q}_{1,j}^\top\hat{\boldsymbol{W}}\right\|}\boldsymbol{q}_{1,j}^\top\hat{\boldsymbol{W}}\hat{\boldsymbol{x}}_i\right)\right)^2\right)\\
&=\mathbb{E}_{\boldsymbol{\epsilon}}\left(\sup_{\hat{\boldsymbol{W}},j}\left(\frac{1}{\left\|\boldsymbol{q}_{1,j}^\top\hat{\boldsymbol{W}}\right\|}\boldsymbol{q}_{1,j}^\top\hat{\boldsymbol{W}}\left(\sum_{i=1}^{m}\epsilon_i\hat{\boldsymbol{x}}_i\right)\right)^2\right)\\
&\leq\mathbb{E}_{\boldsymbol{\epsilon}}\left(\left\|\sum_{i=1}^{m}\epsilon_i\hat{\boldsymbol{x}}_i\right\|^2\right)\leq mb_x^2.
\end{aligned}
$$

E Lower Bound on Rademacher Complexity - Proof of Theorem 4.4

We now provide a lower bound on the Rademacher complexity for average pooling and ReLU activation function. The authors in Bartlett et al. (2017) and Golowich et al. (2018) provide lower bounds on the Rademacher complexity. Their results, however, do not apply for group equivariant architectures given the underlying structure of weight kernels. Similar to Golowich et al. (2018), our result holds for a class of data distributions.

As the starting point, we can again peel off of the last layer:

$$
\mathbb{E}_{\boldsymbol{\epsilon}}\left(\sup_{\boldsymbol{u},\boldsymbol{w}}\frac{1}{m}\sum_{i=1}^{m}\epsilon_i\boldsymbol{u}^\top P\circ\sigma\left(\boldsymbol{W}\boldsymbol{x}\right)\right)=\frac{M_1}{m}\mathbb{E}_{\boldsymbol{\epsilon}}\left(\sup_{\boldsymbol{w}}\left\|\sum_{i=1}^{m}\epsilon_i P\circ\sigma(\boldsymbol{W}\boldsymbol{x}_i)\right\|\right). \tag{23}
$$

The next step is to find a lower bound on the right hand side. For that, we consider only weight kernels that are non-zero in the first channel and zero otherwise. Plugging in the average pooling, this means:

$$\mathbb{E}_{\boldsymbol{\epsilon}}\left(\sup_{\boldsymbol{w}}\left\|\sum_{i=1}^{m}\epsilon_i P\circ\sigma(\boldsymbol{W}\boldsymbol{x}_i)\right\|\right)\geq\mathbb{E}_{\boldsymbol{\epsilon}}\left(\sup_{\boldsymbol{w}\in\mathcal{W}_1}\left\|\sum_{i=1}^{m}\epsilon_i\begin{pmatrix}\frac{1}{|G|}\mathbf{1}^\top\sigma\left(\sum_{k=1}^{c_0}\boldsymbol{w}_{(1,k)}\circledast_G\boldsymbol{x}_i(k)\right)\\ \mathbf{0}\\ \vdots\\ \mathbf{0}\end{pmatrix}\right\|\right) \tag{24}$$

where $\mathcal{W}_1$ is the set of weight kernels with zero channels everywhere except the first channel. This can be further simplified to:

$$\begin{aligned}
&\mathbb{E}_{\boldsymbol{\epsilon}}\left(\sup_{\boldsymbol{w}\in\mathcal{W}_1}\left\|\sum_{i=1}^{m}\epsilon_i\begin{pmatrix}\frac{1}{|G|}\mathbf{1}^\top\sigma\left(\sum_{k=1}^{c_0}\boldsymbol{w}_{(1,k)}\circledast_G\boldsymbol{x}_i(k)\right)\\ \mathbf{0}\\ \vdots\\ \mathbf{0}\end{pmatrix}\right\|\right)\\
&=\mathbb{E}_{\boldsymbol{\epsilon}}\left(\sup_{\boldsymbol{w}\in\mathcal{W}_1}\left\|\sum_{i=1}^{m}\epsilon_i\sum_{l=1}^{|G|}\frac{1}{|G|}\begin{pmatrix}\sigma\left(\sum_{k=1}^{c_0}\boldsymbol{w}_{(1,k)}^\top\Pi_l\boldsymbol{x}_i(k)\right)\\ \mathbf{0}\\ \vdots\\ \mathbf{0}\end{pmatrix}\right\|\right)\\
&=\mathbb{E}_{\boldsymbol{\epsilon}}\left(\sup_{\boldsymbol{w}\in\mathcal{W}_1}\left|\sum_{i=1}^{m}\epsilon_i\sum_{l=1}^{|G|}\frac{1}{|G|}\sigma\left(\sum_{k=1}^{c_0}\boldsymbol{w}_{(1,k)}^\top\Pi_l\boldsymbol{x}_i(k)\right)\right|\right)
\end{aligned}$$

We assume data distributions over $\boldsymbol{x}$ such that each channel $\boldsymbol{x}(k)$ is supported in a single orthant. Without loss of generality assume that $\boldsymbol{x}(k)$'s are supported over the positive orthant, which means that $\mathbf{1}^\top\boldsymbol{x}(k)=\|\boldsymbol{x}(k)\|_1$. We also assume that the data points have maximum norm $\|\boldsymbol{x}_i\|=B$. Now consider a subset $\hat{\mathcal{W}}_1^+$ of $\mathcal{W}_1$ such that $\boldsymbol{w}_{(1,k)}=w_{(1,k)}\mathbf{1}$, where $w_{(1,k)}$ is a positive scalar value. With all these assumptions, we get:

$$\begin{aligned}
\mathbb{E}_{\boldsymbol{\epsilon}}\left(\sup_{\boldsymbol{w}\in\mathcal{W}_1}\left|\sum_{i=1}^{m}\epsilon_i\sum_{l=1}^{|G|}\frac{1}{|G|}\sigma\left(\sum_{k=1}^{c_0}\boldsymbol{w}_{(1,k)}^\top\Pi_l\boldsymbol{x}_i(k)\right)\right|\right)&\geq\mathbb{E}_{\boldsymbol{\epsilon}}\left(\sup_{\boldsymbol{w}\in\hat{\mathcal{W}}_1^+}\left|\sum_{i=1}^{m}\epsilon_i\sum_{l=1}^{|G|}\frac{1}{|G|}\sigma\left(\sum_{k=1}^{c_0}\boldsymbol{w}_{(1,k)}^\top\Pi_l\boldsymbol{x}_i(k)\right)\right|\right)\\
&=\mathbb{E}_{\boldsymbol{\epsilon}}\left(\sup_{\boldsymbol{w}\in\hat{\mathcal{W}}_1^+}\left|\sum_{i=1}^{m}\epsilon_i\sum_{l=1}^{|G|}\frac{1}{|G|}\sigma\left(\sum_{k=1}^{c_0}w_{(1,k)}\mathbf{1}^\top\Pi_l\boldsymbol{x}_i(k)\right)\right|\right)\\
&=\mathbb{E}_{\boldsymbol{\epsilon}}\left(\sup_{\boldsymbol{w}\in\hat{\mathcal{W}}_1^+}\left|\sum_{i=1}^{m}\epsilon_i\sum_{l=1}^{|G|}\frac{1}{|G|}\sigma\left(\sum_{k=1}^{c_0}w_{(1,k)}\mathbf{1}^\top\boldsymbol{x}_i(k)\right)\right|\right)\\
&=\mathbb{E}_{\boldsymbol{\epsilon}}\left(\sup_{\boldsymbol{w}\in\hat{\mathcal{W}}_1^+}\left|\sum_{i=1}^{m}\epsilon_i\left(\sum_{k=1}^{c_0}w_{(1,k)}\mathbf{1}^\top\boldsymbol{x}_i(k)\right)\right|\right),
\end{aligned}$$

where the last step follows from the positiveness of $w_{(1,k)}$'s and the assumption on the data distribution. We can now simplify the last bound further to get:

$$\begin{aligned}
\mathbb{E}_{\boldsymbol{\epsilon}}\left(\sup_{\boldsymbol{w}\in\hat{\mathcal{W}}_1^+}\left|\sum_{i=1}^{m}\epsilon_i\left(\sum_{k=1}^{c_0}w_{(1,k)}\mathbf{1}^\top\boldsymbol{x}_i(k)\right)\right|\right)&=\mathbb{E}_{\boldsymbol{\epsilon}}\left(\sup_{\boldsymbol{w}\in\hat{\mathcal{W}}_1^+}\left|\sum_{k=1}^{c_0}w_{(1,k)}\left(\sum_{i=1}^{m}\epsilon_i\mathbf{1}^\top\boldsymbol{x}_i(k)\right)\right|\right)\\
&=M_2\mathbb{E}_{\boldsymbol{\epsilon}}\left(\left\|\sum_{i=1}^{m}\epsilon_i\begin{pmatrix}\mathbf{1}^\top\boldsymbol{x}_i(1)\\ \vdots\\ \mathbf{1}^\top\boldsymbol{x}_i(c_0)\end{pmatrix}\right\|\right).
\end{aligned}$$

Using Khintchine's inequality, we can conclude that there is a constant $c > 0$ such that

$$\begin{aligned}
\mathbb{E}_{\boldsymbol{\epsilon}}\left(\left\|\sum_{i=1}^{m}\epsilon_i\begin{pmatrix}\mathbf{1}^\top\boldsymbol{x}_i(1)\\ \vdots\\ \mathbf{1}^\top\boldsymbol{x}_i(c_0)\end{pmatrix}\right\|\right) &\geq c\sqrt{\sum_{i=1}^{m}\left\|\begin{pmatrix}\mathbf{1}^\top\boldsymbol{x}_i(1)\\ \vdots\\ \mathbf{1}^\top\boldsymbol{x}_i(c_0)\end{pmatrix}\right\|_2^2}\\
&= c\sqrt{\sum_{i=1}^{m}\sum_{k=1}^{c_0}(\mathbf{1}^\top\boldsymbol{x}_i(k))^2}\\
&= c\sqrt{\sum_{i=1}^{m}\sum_{k=1}^{c_0}\|\boldsymbol{x}_i(k)\|_1^2}\\
&\geq c\sqrt{\sum_{i=1}^{m}\sum_{k=1}^{c_0}\|\boldsymbol{x}_i(k)\|_2^2} = c\sqrt{\sum_{i=1}^{m}\|\boldsymbol{x}_i\|_2^2} = B\sqrt{m}.
\end{aligned}$$

For the last steps, we have used the assumptions on the data distribution. This yields the intended lower bound.

Remark E.1. The lower bounds on the sample complexity are commonly obtained via fat-shattering dimension as in Vardi et al. (2022). The construction of input-label samples shattered by non-equivariant networks would not extend to equivariant networks (ENs), as the ENs can only shatter data points that satisfy the exact symmetry. There are works on VC dimension of ENs, however they are not dimension-free and do not include norm bounds similar to ours.

F Frequency Domain Analysis

Let's consider the representation in the frequency domain. The Fourier transform is given by a unitary matrix $\boldsymbol{F}$. For simplicity, here we assume the simplest setting of a *commutative compact group* G, for which we have:

$$\boldsymbol{F}(\boldsymbol{w} \circledast_G \boldsymbol{x}) = \mathrm{diag}(\hat{\boldsymbol{w}})\hat{\boldsymbol{x}},$$

where $\hat{\boldsymbol{x}} = \boldsymbol{F}\boldsymbol{x}$, and $\mathrm{diag}(\hat{\boldsymbol{w}})$ arises from the Fourier based decomposition of the circulant matrix $\boldsymbol{W}$. Each frequency component in $\hat{\boldsymbol{w}}$ is an irreducible representation of the group G denoted by ψ. Commutativity implies that each irrep has a multiplicity equal to 1 in the Fourier transform. Therefore, using the direct sum notation, we have:

$$\mathrm{diag}(\hat{\boldsymbol{w}}) = \bigoplus_{\psi}\hat{w}(\psi), \tag{25}$$

See the Supplementary Materials A for more details. Note that the point-wise non-linearity should be applied in the spatial domain, so we need an inverse Fourier transform before activation. The network representation in the Fourier space is given by:

$$h_{\boldsymbol{u},\boldsymbol{w}}(\boldsymbol{x}) := \boldsymbol{u}^\top P \circ \sigma\begin{pmatrix}\boldsymbol{F}^*\sum_{i=1}^{c_0}\left(\bigoplus_{\psi}\hat{w}_{(1,i)}(\psi)\right)\hat{\boldsymbol{x}(i)})\\ \vdots\\ \boldsymbol{F}^*\sum_{i=1}^{c_0}\left(\bigoplus_{\psi}\hat{w}_{(c_1,i)}(\psi)\right)\hat{\boldsymbol{x}(i)})\end{pmatrix} \tag{26}$$

where $\boldsymbol{F}^*$ denotes the conjugate transpose of the unitary matrix $\boldsymbol{F}$. Note that we have not touched the last layers. The last layer merely focuses on getting an invariant representation.

We show that conducting the Rademacher analysis in the frequency domain brings no additional gain. The situation may be different if the input is bandlimited. We summarize this result in the following proposition.

Proposition F.1. For the hypothesis space $\mathcal{H}$ defined in eq. 4, the average pooling operation, $\sigma(\cdot)$ as a 1-Lipschitz positively homogeneous activation function, the generalization error is bounded as $\mathcal{O}(\frac{b_x M_1 M_2}{\sqrt{m}})$.

Proof. Consider the network represented in the frequency domain as follows:

$$h_{\boldsymbol{u},\boldsymbol{w}}(\boldsymbol{x}) := \boldsymbol{u}^\top P \circ \sigma \begin{pmatrix} \boldsymbol{F}^* \sum_{i=1}^{c_0} \left(\bigoplus_\psi \hat{w}_{(1,i)}(\psi)\right) \hat{\boldsymbol{x}(i)}) \\ \vdots \\ \boldsymbol{F}^* \sum_{i=1}^{c_0} \left(\bigoplus_\psi \hat{w}_{(c_1,i)}(\psi)\right) \hat{\boldsymbol{x}(i)}) \end{pmatrix} \tag{27}$$

A few clarifications before continuing further. Consider the circular convolution $\boldsymbol{w} \circledast_G \boldsymbol{x}$. Note that the decomposition $\left(\bigoplus_\psi \hat{w}(\psi)\right)$ is obtained by using the Fourier decomposition of the equivalent circulant matrix:

$$\boldsymbol{F}^* \left(\bigoplus_\psi \hat{w}(\psi)\right) \boldsymbol{F} = \boldsymbol{W},$$

and therefore, when using Parseval's relation, we should be careful to include the group size as follows:

$$\sum_\psi \hat{w}(\psi)^2 = \|\boldsymbol{W}\|_F = |G| \, \|\boldsymbol{w}\|^2 .$$

Now, let's continue the proof. For average pooling, we can start by peeling off the last linear layers and average pooling and continue from there, namely from eq. 19. Note that l'th entry can be computed using an inner product with the l'th row of $\boldsymbol{F}^*$, represented by $\boldsymbol{f}_l^*$. We have:

$$\begin{aligned}
&\mathbb{E}_{\boldsymbol{\epsilon}} \left(\sup_{\boldsymbol{w}} \left\| \sum_{i=1}^m \epsilon_i \begin{pmatrix} \sigma\left(\boldsymbol{f}_l^* \sum_{k=1}^{c_0} \left(\bigoplus_\psi \hat{w}_{(1,k)}(\psi)\right) \hat{\boldsymbol{x}_i(k)})\right) \\ \vdots \\ \sigma\left(\boldsymbol{f}_l^* \sum_{k=1}^{c_0} \left(\bigoplus_\psi \hat{w}_{(c_1,k)}(\psi)\right) \hat{\boldsymbol{x}_i(k)})\right) \end{pmatrix} \right\|^2 \right) \\
&= \mathbb{E}_{\boldsymbol{\epsilon}} \left(\sup_{\boldsymbol{w}} \sum_{j=1}^{c_1} \left(\sum_{i=1}^m \epsilon_i \sigma \left(\boldsymbol{f}_l^* \sum_{k=1}^{c_0} \left(\bigoplus_\psi \hat{w}_{(j,k)}(\psi) \right) \hat{\boldsymbol{x}_i(k)}) \right) \right)^2 \right) \\
&= \mathbb{E}_{\boldsymbol{\epsilon}} \left(\sup_{\boldsymbol{w}} \sum_{j=1}^{c_1} \left\|\hat{\boldsymbol{w}}_{(j,:)}\right\|^2 \left(\sum_{i=1}^m \epsilon_i \sigma \left(\frac{1}{\left\|\hat{\boldsymbol{w}}_{(j,:)}\right\|} \boldsymbol{f}_l^* \sum_{k=1}^{c_0} \left(\bigoplus_\psi \hat{w}_{(j,k)}(\psi) \right) \hat{\boldsymbol{x}_i(k)}) \right) \right)^2 \right),
\end{aligned}$$

where we used the positively homogeneity property of the activation function, and we defined:

$$\left\|\hat{\boldsymbol{w}}_{(j,:)}\right\|^2 = \sum_{\psi,k\in[c_0]} \hat{w}_{(j,k)}(\psi)^2.$$

We can use Parseval's theorem, and based on the discussion above, we know that:

$$\sum_{j\in[c_1]} \left\|\hat{\boldsymbol{w}}_{(j,:)}\right\|^2 = |G| \sum_{j\in[c_1]} \left\|\boldsymbol{w}_{(j,:)}\right\|^2 \leq |G| M_2^2.$$

And then, we can continue similarly to the proof of average pooling:

$$\begin{aligned}
&\mathbb{E}_{\boldsymbol{\epsilon}} \left(\sup_{\boldsymbol{w}} \sum_{j=1}^{c_1} \left\|\hat{\boldsymbol{w}}_{(j,:)}\right\|^2 \left(\sum_{i=1}^m \epsilon_i \sigma \left(\frac{1}{\left\|\hat{\boldsymbol{w}}_{(j,:)}\right\|} \boldsymbol{f}_l^* \sum_{k=1}^{c_0} \left(\bigoplus_\psi \hat{w}_{(j,k)}(\psi) \right) \hat{\boldsymbol{x}_i(k)}) \right) \right)^2 \right) \\
&\leq |G| M_2^2 \mathbb{E}_{\boldsymbol{\epsilon}} \left(\sup_{\hat{\boldsymbol{w}}:\|\hat{\boldsymbol{w}}\|\leq 1} \left(\sum_{i=1}^m \epsilon_i \sigma \left(\boldsymbol{f}_l^* \sum_{k=1}^{c_0} \left(\bigoplus_\psi \hat{w}_{(k)}(\psi) \right) \hat{\boldsymbol{x}_i(k)}) \right) \right)^2 \right)
\end{aligned}$$

From which we can continue using contraction inequality:

$$
\begin{aligned}
&\mathbb{E}_{\boldsymbol{\epsilon}}\left(\sup_{\hat{\boldsymbol{w}}:\|\hat{\boldsymbol{w}}\|\leq 1}\left(\sum_{i=1}^{m}\epsilon_i\sigma\left(\boldsymbol{f}_l^*\sum_{k=1}^{c_0}\left(\bigoplus_{\psi}\hat{w}_{(k)}(\psi)\right)\hat{\boldsymbol{x}_i(k)}\right)\right)^2\right)\\
&\leq \mathbb{E}_{\boldsymbol{\epsilon}}\left(\sup_{\hat{\boldsymbol{w}}:\|\hat{\boldsymbol{w}}\|\leq 1}\left(\sum_{i=1}^{m}\epsilon_i\left(\boldsymbol{f}_l^*\sum_{k=1}^{c_0}\left(\bigoplus_{\psi}\hat{w}_{(k)}(\psi)\right)\hat{\boldsymbol{x}_i(k)}\right)\right)^2\right)\\
&\leq \mathbb{E}_{\boldsymbol{\epsilon}}\left(\sup_{\hat{\boldsymbol{w}}:\|\hat{\boldsymbol{w}}\|\leq 1}\left(\boldsymbol{f}_l^*\sum_{k=1}^{c_0}\left(\bigoplus_{\psi}\hat{w}_{(k)}(\psi)\right)\left(\sum_{i=1}^{m}\epsilon_i\hat{\boldsymbol{x}_i(k)}\right)\right)^2\right)\\
&\leq \sup_{\hat{\boldsymbol{w}}:\|\hat{\boldsymbol{w}}\|\leq 1}\left\|\left(\boldsymbol{f}_l^*\left(\bigoplus_{\psi}\hat{w}_{(k)}(\psi)\right)\right)_{k\in[c_0]}\right\|_F^2\mathbb{E}_{\boldsymbol{\epsilon}}\left(\left\|\sum_{i=1}^{m}\epsilon_i\hat{\boldsymbol{x}}_i\right\|^2\right)\\
&\leq \sup_{\hat{\boldsymbol{w}}:\|\hat{\boldsymbol{w}}\|\leq 1}\left\|\left(\boldsymbol{f}_l^*\left(\bigoplus_{\psi}\hat{w}_{(k)}(\psi)\right)\right)_{k\in[c_0]}\right\|_F^2 mb_x^2.
\end{aligned}
$$

To simplify the norm on the left-hand side, it is important to note that each entry of $\boldsymbol{f}_l^*$ has the modulus $1/\sqrt{|G|}$, which means that

$$
\sup_{\hat{\boldsymbol{w}}:\|\hat{\boldsymbol{w}}\|\leq 1}\left\|\left(\boldsymbol{f}_l^*\left(\bigoplus_{\psi}\hat{w}_{(k)}(\psi)\right)\right)_{k\in[c_0]}\right\|_F^2\leq\frac{1}{|G|}.
$$

The term $1/|G|$ cancels the term $|G|$ in the previous inequality and yields the bound. The result shows that there is no gain in the frequency domain analysis. □

G Proofs for Weight Sharing

Consider the network:

$$
h_{\boldsymbol{u},\boldsymbol{w}}(\boldsymbol{x}) := \boldsymbol{u}^\top P\circ\sigma\begin{pmatrix}\sum_{c=1}^{c_0}\left(\sum_{k=1}^{|G|}\boldsymbol{w}_{(1,c)}(k)\boldsymbol{B}_k\right)\boldsymbol{x}(c)\\ \vdots\\ \sum_{i=1}^{c_0}\left(\sum_{k=1}^{|G|}\boldsymbol{w}_{(c_1,c)}(k)\boldsymbol{B}_k\right)\boldsymbol{x}(c)\end{pmatrix}.
$$

For the pooling operation $P(\cdot)$, we consider the average pooling operation. The Rademacher complexity analysis starts similarly to the proof of group convolution networks. This means that we can peel off the first

layer $\boldsymbol{u}$ and consider a single term in the average pooling operation, namely:

$$\mathbb{E}_{\boldsymbol{\epsilon}}\left(\sup_{\boldsymbol{w}}\left\|\sum_{i=1}^{m}\epsilon_i P\circ\sigma\begin{pmatrix}\sum_{c=1}^{c_0}\left(\sum_{k=1}^{|G|}\boldsymbol{w}_{(1,c)}(k)\boldsymbol{B}_k\right)\boldsymbol{x}_i(c)\\ \vdots\\ \sum_{c=1}^{c_0}\left(\sum_{k=1}^{|G|}\boldsymbol{w}_{(c_1,c)}(k)\boldsymbol{B}_k\right)\boldsymbol{x}_i(c)\end{pmatrix}\right\|\right)$$
$$=\mathbb{E}_{\boldsymbol{\epsilon}}\left(\frac{1}{|G|}\sup_{\boldsymbol{w}}\left\|\sum_{l=1}^{|G|}\sum_{i=1}^{m}\epsilon_i\sigma\begin{pmatrix}\sum_{c=1}^{c_0}\left(\sum_{k=1}^{|G|}\boldsymbol{w}_{(1,c)}(k)\boldsymbol{b}_{k,l}^{\top}\right)\boldsymbol{x}_i(c)\\ \vdots\\ \sum_{c=1}^{c_0}\left(\sum_{k=1}^{|G|}\boldsymbol{w}_{(c_1,c)}(k)\boldsymbol{b}_{k,l}^{\top}\right)\boldsymbol{x}_i(c)\end{pmatrix}\right\|\right)$$
$$\leq\frac{1}{|G|}\sum_{l=1}^{|G|}\mathbb{E}_{\boldsymbol{\epsilon}}\left(\sup_{\boldsymbol{w}}\left\|\sum_{i=1}^{m}\epsilon_i\sigma\begin{pmatrix}\sum_{c=1}^{c_0}\left(\sum_{k=1}^{|G|}\boldsymbol{w}_{(1,c)}(k)\boldsymbol{b}_{k,l}^{\top}\right)\boldsymbol{x}_i(c)\\ \vdots\\ \sum_{c=1}^{c_0}\left(\sum_{k=1}^{|G|}\boldsymbol{w}_{(c_1,c)}(k)\boldsymbol{b}_{k,l}^{\top}\right)\boldsymbol{x}_i(c)\end{pmatrix}\right\|\right),$$

where $\boldsymbol{b}_{k,l}^{\top}$ is the l'th row of $\boldsymbol{B}_k$. From here, we can continue similarly. First, we use the following moment inequality:

$$\mathbb{E}_{\boldsymbol{\epsilon}}\left(\sup_{\boldsymbol{w}}\left\|\sum_{i=1}^{m}\epsilon_i\sigma\begin{pmatrix}\sum_{c=1}^{c_0}\left(\sum_{k=1}^{|G|}\boldsymbol{w}_{(1,c)}(k)\boldsymbol{b}_{k,l}^{\top}\right)\boldsymbol{x}_i(c)\\ \vdots\\ \sum_{c=1}^{c_0}\left(\sum_{k=1}^{|G|}\boldsymbol{w}_{(c_1,c)}(k)\boldsymbol{b}_{k,l}^{\top}\right)\boldsymbol{x}_i(c)\end{pmatrix}\right\|\right)$$
$$\leq\sqrt{\mathbb{E}_{\boldsymbol{\epsilon}}\left(\sup_{\boldsymbol{w}}\left\|\sum_{i=1}^{m}\epsilon_i\sigma\begin{pmatrix}\sum_{c=1}^{c_0}\left(\sum_{k=1}^{|G|}\boldsymbol{w}_{(1,c)}(k)\boldsymbol{b}_{k,l}^{\top}\right)\boldsymbol{x}_i(c)\\ \vdots\\ \sum_{c=1}^{c_0}\left(\sum_{k=1}^{|G|}\boldsymbol{w}_{(c_1,c)}(k)\boldsymbol{b}_{k,l}^{\top}\right)\boldsymbol{x}_i(c)\end{pmatrix}\right\|^2\right)}$$
$$=\sqrt{\mathbb{E}_{\boldsymbol{\epsilon}}\left(\sup_{\boldsymbol{w}}\sum_{j=1}^{c_1}\left(\sum_{i=1}^{m}\epsilon_i\sigma\left(\sum_{c=1}^{c_0}\left(\sum_{k=1}^{|G|}\boldsymbol{w}_{(j,c)}(k)\boldsymbol{b}_{k,l}^{\top}\right)\boldsymbol{x}_i(c)\right)\right)^2\right)}.$$

For the rest, denote (by abuse of notation, we drop the index l when it is evident in context):

$$\left\|\boldsymbol{w}_{(j,:)}\right\|_{\boldsymbol{B}}:=\left\|\left(\sum_{k=1}^{|G|}\boldsymbol{w}_{(j,c)}(k)\boldsymbol{b}_{k,l}^{\top}\right)_{c\in[c_0]}\right\|_F,\ \|\boldsymbol{w}\|_{\boldsymbol{B}}:=\max_{l\in[|G|]}\left\|\left(\sum_{k=1}^{|G|}\boldsymbol{w}_{(j,c)}(k)\boldsymbol{b}_{k,l}^{\top}\right)_{c\in[c_0],j\in[c_1]}\right\|_F$$

Note that:

$$\sum_{j=1}^{c_1}\left\|\boldsymbol{w}_{(j,:)}\right\|_{\boldsymbol{B}}^2=\left\|\left(\sum_{k=1}^{|G|}\boldsymbol{w}_{(j,c)}(k)\boldsymbol{b}_{k,l}^{\top}\right)_{c\in[c_0],j\in[c_1]}\right\|_F^2\leq\max_{l\in[|G|]}\left\|\left(\sum_{k=1}^{|G|}\boldsymbol{w}_{(j,c)}(k)\boldsymbol{b}_{k,l}^{\top}\right)_{c\in[c_0],j\in[c_1]}\right\|_F^2\leq(M_2^{w.s.})^2.$$

We can continue the proof as follows:

$$
\begin{aligned}
&\mathbb{E}_{\boldsymbol{\epsilon}}\left(\sup_{\boldsymbol{w}}\sum_{j=1}^{c_1}\left(\sum_{i=1}^{m}\epsilon_i\sigma\left(\sum_{c=1}^{c_0}\left(\sum_{k=1}^{|G|}\boldsymbol{w}_{(j,c)}(k)\boldsymbol{b}_{k,l}^{\top}\right)\boldsymbol{x}_i(c)\right)\right)^2\right)\\
&\leq \mathbb{E}_{\boldsymbol{\epsilon}}\left(\sup_{\boldsymbol{w}}\sum_{j=1}^{c_1}\left\|\boldsymbol{w}_{(j,:)}\right\|_{\boldsymbol{B}}^2\left(\sum_{i=1}^{m}\epsilon_i\sigma\left(\frac{1}{\left\|\boldsymbol{w}_{(j,:)}\right\|_{\boldsymbol{B}}}\sum_{c=1}^{c_0}\left(\sum_{k=1}^{|G|}\boldsymbol{w}_{(j,c)}(k)\boldsymbol{b}_{k,l}^{\top}\right)\boldsymbol{x}_i(c)\right)\right)^2\right)\\
&\leq \mathbb{E}_{\boldsymbol{\epsilon}}\left(\sup_{\boldsymbol{w}}\sum_{j=1}^{c_1}\left\|\boldsymbol{w}_{(j,:)}\right\|_{\boldsymbol{B}}^2\left(\sum_{i=1}^{m}\epsilon_i\sigma\left(\frac{1}{\left\|\boldsymbol{w}_{(j,:)}\right\|_{\boldsymbol{B}}}\sum_{c=1}^{c_0}\left(\sum_{k=1}^{|G|}\boldsymbol{w}_{(j,c)}(k)\boldsymbol{b}_{k,l}^{\top}\right)\boldsymbol{x}_i(c)\right)\right)^2\right)\\
&\leq (M_2^{w.s.})^2\mathbb{E}_{\boldsymbol{\epsilon}}\left(\sup_{\boldsymbol{w}}\sup_{j}\left(\sum_{i=1}^{m}\epsilon_i\sigma\left(\frac{1}{\left\|\boldsymbol{w}_{(j,:)}\right\|_{\boldsymbol{B}}}\sum_{c=1}^{c_0}\left(\sum_{k=1}^{|G|}\boldsymbol{w}_{(j,c)}(k)\boldsymbol{b}_{k,l}^{\top}\right)\boldsymbol{x}_i(c)\right)\right)^2\right)\\
&\leq (M_2^{w.s.})^2\mathbb{E}_{\boldsymbol{\epsilon}}\left(\sup_{\hat{\boldsymbol{w}}}\left(\sum_{i=1}^{m}\epsilon_i\sigma\left(\sum_{c=1}^{c_0}\left(\sum_{k=1}^{|G|}\hat{\boldsymbol{w}}_{(c)}(k)\boldsymbol{b}_{k,l}^{\top}\right)\boldsymbol{x}_i(c)\right)\right)^2\right),
\end{aligned}
$$

where the supremum is taked over all vectors $\hat{\boldsymbol{w}}$ satisfying:

$$
\left\|\left(\sum_{k=1}^{|G|}\hat{\boldsymbol{w}}_{(c)}(k)\boldsymbol{b}_{k,l}^{\top}\right)_{c\in[c_0]}\right\|_F\leq 1.
$$

We can use the contraction inequality and the Cauchy-Schwartz inequality to obtain the following:

$$
\begin{aligned}
&\mathbb{E}_{\boldsymbol{\epsilon}}\left(\sup_{\hat{\boldsymbol{w}}}\left(\sum_{i=1}^{m}\epsilon_i\sigma\left(\sum_{c=1}^{c_0}\left(\sum_{k=1}^{|G|}\hat{\boldsymbol{w}}_{(c)}(k)\boldsymbol{b}_{k,l}^{\top}\right)\boldsymbol{x}_i(c)\right)\right)^2\right)\\
&\leq \mathbb{E}_{\boldsymbol{\epsilon}}\left(\sup_{\hat{\boldsymbol{w}}}\left(\sum_{i=1}^{m}\epsilon_i\left(\sum_{c=1}^{c_0}\left(\sum_{k=1}^{|G|}\hat{\boldsymbol{w}}_{(c)}(k)\boldsymbol{b}_{k,l}^{\top}\right)\boldsymbol{x}_i(c)\right)\right)^2\right)\\
&= \mathbb{E}_{\boldsymbol{\epsilon}}\left(\sup_{\hat{\boldsymbol{w}}}\left(\sum_{c=1}^{c_0}\left(\sum_{k=1}^{|G|}\hat{\boldsymbol{w}}_{(c)}(k)\boldsymbol{b}_{k,l}^{\top}\right)\left(\sum_{i=1}^{m}\epsilon_i\boldsymbol{x}_i(c)\right)\right)^2\right)\\
&\leq \sup_{\hat{\boldsymbol{w}}}\left\|\left(\sum_{k=1}^{|G|}\hat{\boldsymbol{w}}_{(c)}(k)\boldsymbol{b}_{k,l}^{\top}\right)_{c\in[c_0]}\right\|_F^2\mathbb{E}_{\boldsymbol{\epsilon}}\left(\left\|\sum_{i=1}^{m}\epsilon_i\boldsymbol{x}_i\right\|^2\right)\leq mb_x^2.
\end{aligned}
$$

H Proofs for Local Filters - Proposition 7.1

Consider the network defined as:

$$
h_{\boldsymbol{u},\boldsymbol{w}}(\boldsymbol{x})=\boldsymbol{u}^{\top}P\circ\sigma\begin{pmatrix}\sum_{k=1}^{c_0}\left(\boldsymbol{w}_{(1,k)}^{\top}\phi_l(\boldsymbol{x}(k))\right)_{l\in[|G|]}\\ \vdots\\ \sum_{k=1}^{c_0}\left(\boldsymbol{w}_{(c_1,k)}^{\top}\phi_l(\boldsymbol{x}(k))\right)_{l\in[|G|]}\end{pmatrix}=\boldsymbol{u}^{\top}P\circ\sigma(\boldsymbol{W}\boldsymbol{x}),
$$

where similar to Vardi et al. (2022), $\boldsymbol{W}$ is the matrix *conforming* to the patches Φ and the weights. The first steps for average pooling are similar to what we have done in Section C.2. The only difference is that $\Pi_l \boldsymbol{x}(k)$ is replaced with $\phi_l(\boldsymbol{x}(k))$. We will not repeat the arguments and condense them in the following steps:

$$\mathbb{E}_{\boldsymbol{\epsilon}}\left(\sup_{\boldsymbol{u},\boldsymbol{w}} \frac{1}{m}\sum_{i=1}^{m} \epsilon_i \boldsymbol{u}^\top P \circ \sigma\left(\boldsymbol{W}\boldsymbol{x}\right)\right) \leq \frac{M_1}{m}\mathbb{E}_{\boldsymbol{\epsilon}}\left(\sup_{\boldsymbol{w}} \left\|\sum_{i=1}^{m} \epsilon_i P \circ \sigma(\boldsymbol{W}\boldsymbol{x}_i)\right\|\right).$$

$$\leq \frac{M_1}{m}\sum_{l=1}^{|G|}\frac{1}{|G|}\mathbb{E}_{\boldsymbol{\epsilon}}\left(\sup_{\boldsymbol{w}} \left\|\sum_{i=1}^{m} \epsilon_i \begin{pmatrix} \sigma\left(\sum_{k=1}^{c_0} \boldsymbol{w}_{(1,k)}^\top \phi_l(\boldsymbol{x}_i(k))\right) \\ \vdots \\ \sigma\left(\sum_{k=1}^{c_0} \boldsymbol{w}_{(c_1,k)}^\top \phi_l(\boldsymbol{x}_i(k))\right) \end{pmatrix}\right\|\right)$$

And, we can repeat the peeling arguments to get:

$$\mathbb{E}_{\boldsymbol{\epsilon}}\left(\sup_{\boldsymbol{w}} \left\|\sum_{i=1}^{m} \epsilon_i \begin{pmatrix} \sigma\left(\sum_{k=1}^{c_0} \boldsymbol{w}_{(1,k)}^\top \phi_l(\boldsymbol{x}_i(k))\right) \\ \vdots \\ \sigma\left(\sum_{k=1}^{c_0} \boldsymbol{w}_{(c_1,k)}^\top \phi_l(\boldsymbol{x}_i(k))\right) \end{pmatrix}\right\|\right) \leq M_2\sqrt{\mathbb{E}_{\boldsymbol{\epsilon}}\left(\sup_{\tilde{\boldsymbol{w}}:\|\tilde{\boldsymbol{w}}\|\leq 1}\left(\sum_{i=1}^{m}\epsilon_i \sigma\left(\sum_{k=1}^{c_0}\tilde{\boldsymbol{w}}_{(k)}^\top \phi_l(\boldsymbol{x}_i(k))\right)\right)^2\right)}.$$

The only change in the proof is about the way we simplify the term in the square root:

$$\begin{aligned}
\mathbb{E}_{\boldsymbol{\epsilon}}\left(\sup_{\tilde{\boldsymbol{w}}:\|\tilde{\boldsymbol{w}}\|\leq 1}\left(\sum_{i=1}^{m}\epsilon_i \sigma\left(\sum_{k=1}^{c_0}\tilde{\boldsymbol{w}}_{(k)}^\top \phi_l(\boldsymbol{x}_i(k))\right)\right)^2\right) &\leq \mathbb{E}_{\boldsymbol{\epsilon}}\left(\sup_{\tilde{\boldsymbol{w}}:\|\tilde{\boldsymbol{w}}\|\leq 1}\left(\sum_{i=1}^{m}\epsilon_i \sum_{k=1}^{c_0}\tilde{\boldsymbol{w}}_{(k)}^\top \phi_l(\boldsymbol{x}_i(k))\right)^2\right) \\
&\leq \mathbb{E}_{\boldsymbol{\epsilon}}\left(\sup_{\tilde{\boldsymbol{w}}:\|\tilde{\boldsymbol{w}}\|\leq 1}\left(\sum_{k=1}^{c_0}\tilde{\boldsymbol{w}}_{(k)}^\top \left(\sum_{i=1}^{m}\epsilon_i \phi_l(\boldsymbol{x}_i(k))\right)\right)^2\right) \\
&\leq \mathbb{E}_{\boldsymbol{\epsilon}}\left(\left\|\sum_{i=1}^{m}\epsilon_i \phi_l(\boldsymbol{x}_i)\right\|^2\right) = \sum_{i=1}^{m}\|\phi_l(\boldsymbol{x}_i)\|^2. \qquad (28)
\end{aligned}$$

Now we use Jensen inequality to get the proof:

$$\begin{aligned}
\mathbb{E}_{\boldsymbol{\epsilon}}\left(\sup_{\boldsymbol{u},\boldsymbol{w}} \frac{1}{m}\sum_{i=1}^{m} \epsilon_i \boldsymbol{u}^\top P \circ \sigma\left(\boldsymbol{W}\boldsymbol{x}\right)\right) &\leq \frac{M_1 M_2}{m}\frac{1}{|G|}\sum_{l=1}^{|G|}\sqrt{\sum_{i=1}^{m}\|\phi_l(\boldsymbol{x}_i)\|^2} \\
&\leq \frac{M_1 M_2}{m}\sqrt{\frac{1}{|G|}\sum_{l=1}^{|G|}\sum_{i=1}^{m}\|\phi_l(\boldsymbol{x}_i)\|^2} \\
&\leq \frac{M_1 M_2}{m}\sqrt{\frac{m O_\Phi b_x^2}{|G|}} = \frac{M_1 M_2 b_x}{\sqrt{m}}\sqrt{\frac{O_\Phi}{|G|}}.
\end{aligned}$$

I Uncertainty Principle for Local Filters - Proposition 7.2

We start by stating the uncertainty principle for finite Abelian groups.

Theorem I.1. *Let G be a finite Abelian group. Suppose the function $f : G \to \mathbb{C}$ is non-zero, and $\hat{f}$ is its Fourier transform. We have*

$$|\text{supp}(f)|.|\text{supp}(\hat{f})| \geq |G|.$$

If the filters have B non-zero entries in the frequency domain, then the uncertainty principle implies that the filter in the spatial domain has at least $|G|/B$ non-zero entries. In other words, the smallest filter size will have $|G|/B$ non-zero elements. Therefore, the smallest possible upper bound we can obtain using our approach will use $O_\Phi = |G|/B$. Plugging this in Proposition 7.1 yields the proposition.

Reference	Bound
Equivariance (Theorem 4.1)	$\frac{b_x M_1 M_2}{\sqrt{m}}$
Weight sharing (Proposition 6.1)	$\frac{b_x M_1 M_2^{w.s.}}{\sqrt{m}}$
Locality (Proposition 7.1)	$\sqrt{\frac{O_\Phi}{\lvert G\rvert}} \frac{b_x M_1 M_2}{\sqrt{m}}$
Non-Equivariant Networks Golowich et al. (2018)	$\frac{b_x M_1 \lVert \boldsymbol{W}\rVert_F}{\sqrt{m}}$
Weight sharing, orthogonal $\boldsymbol{b}_{k,l}, k \in [\lvert G\rvert]$	$\frac{b_x M_1 M_2}{\sqrt{m}}$
B-sparse filters (Proposition 7.2	$b_x M_1 M_2/\sqrt{mB}$
Linear convolution Vardi et al. (2022)	$\sqrt{O_\Phi} \frac{b_x M_1 \lVert \boldsymbol{W}\rVert_{2\to 2}}{\sqrt{m}}$
CNN with Pooling Vardi et al. (2022)	$\frac{b_x \lVert \boldsymbol{W}\rVert_{2\to 2} \log m \sqrt{\log(mc_1\lvert G\rvert)}}{\sqrt{m}}$
Graf et al. (2022)	$\mathcal{O}\left(\frac{b_x M_2 \log(\lvert G\rvert \max(c_0,c_1)) \sqrt{\lVert \boldsymbol{W}\rVert_{2\to 2} + \lVert \boldsymbol{w}\rVert_{2,1}}}{\sqrt{m}}\right)$

Table 2: The table summarizes the main results of the paper and compares with the selected prior works. The top three rows are the main results of the paper expressed in their full generality (Reminder : $M_2^{w.s.} = \max_{l\in[|G|]} \left\| \left(\sum_{k=1}^{|G|} \boldsymbol{w}_{(j,c)}(k) \boldsymbol{b}_{k,l}^\top \right)_{c\in[c_0], j\in[c_1]} \right\|_F$). Next three rows summarize the result for the case where the network is not equivariant, the optimal weight sharing and the band-limited filters. The bound from the most relevant results are also summarized in the last rows of the table. The explicit dimension dependency of these bounds are highlighted with a different color.

J Comparison with other existing bounds

The following works do not consider the generalization error for equivariant networks. However, the convolutional networks, which are studied in their work, are closely related to our results. We have also summarized our results and their comparison in Table 2.

Comparison with Vardi et al. (2022). Our work is closely related to Vardi et al. (2022). We focus on equivariant networks and upper bounds on the sample complexity. The networks considered in this work are slightly more general with per-channel linear and non-linear pooling operations. They also provide a bound in Theorem 7 of their paper for pooling operations $\rho : \mathbb{R}^{|G|} \to \mathbb{R}$ that are 1-Lipschitz with respect to the ℓ_∞ norm. This class includes average and max pooling operations. Their bound has logarithmic dimension dependence, the artifact of using the covering number-based arguments (see below for more discussions). The bound is also dependent on the spectral norm of the matrix $\boldsymbol{W}$ instead of the norm of the weight $\boldsymbol{w}$. It is not clear if the dependence on the spectral norm can be removed in their proof. For local filters, they provide a dimension-free bound that also depends on the spectral norm of $\boldsymbol{W}$. However, this time, the dependence on the spectral norm can be substituted with the norm of the weight vector, as it is evident from their proof. In general, all our bounds depend only on the norms of the weight vector, which is tighter that using Frobenius or spectral norm of $\boldsymbol{W}$. The authors in Vardi et al. (2022) provide lower bounds on the sample complexity, which we relegate to future works.

Comparison with Graf et al. (2022). The paper of Graf et al. (2022) relies mainly on Maurey's empirical lemma and covering number arguments. Rademacher complexity bounds either work directly on bounding the Rademacher sum through a set of inequalities or utilize chaining arguments and Dudley's integral inequality. Dudley's integral requires the covering number estimate. The main techniques of finding the covering number, like volumetric, Sudakov, and Maurey's lemma techniques, manifest different dimension dependencies, with the latter usually providing the mildest dependence. Completely dimension-free bounds are obtained mainly via the direct analysis of the Rademacher sum. Therefore, the bounds in Graf et al. (2022) are a mixture of dimension-dependent and norm-dependent terms. Their bounds are, however, quite general and consider different activation functions and residual connections.

To investigate their bound further, let's consider their setup, focusing on what matters for the current paper. They consider a network with L residual blocks, where the residual block i has L_i layers. That is:

$$f = \sigma_L \circ f_L \circ \cdots \circ \sigma_1 \circ f_1 \text{ with } f_i(x) = g_i(x) + \sigma_{iL_i} \circ h_{iL_i} \circ \cdots \circ \sigma_{i1} \circ h_{i1}(x).$$

The activation functions σ_i and σ_{ij} have respectively the Lipschitz constants of ρ_i and ρ_{ij}. The function $g_i(\cdot)$ represents the residual connection with $g_i(0) = 0$. The map h_{ij} represents the convolutional operation with the Kernel K_{ij}. The Lipschitz constant of the layer is given by s_{ij}, which corresponds to the spectral norm of the matrix that *conforms* with the layer (similar to the spectral norm of $\boldsymbol{W}$). The $\ell_{2,1}$ norm of the kernels K_{ij} is bounded by b_{ij} (this can be initialization dependent or independent). The norm of $K \in \mathbb{R}^{c_1 \times c_0 \times d}$is defined as

$$\|K\|_{2,1} = \sum_{i,j} \|K(i,:,j)\|_2 .$$

Define $s_i = \text{Lip}(g_i) + \prod_{j=1}^{L_i} \rho_{ij} s_{ij}$. Denote the total number of layers by $\overline{L}$, W_{ij} is the number of weights in the j-th layer in the i-th residual block. Set $W = \max W_{ij}$. And C_{ij} represents the dependence on the weight and data norms:

$$C_{ij} = \frac{2\|\boldsymbol{X}\|}{\sqrt{m}} \left(\prod_{l=1}^{L} s_l \rho_l \right) \frac{\prod_{k=1}^{L_i} s_{ik}\rho_{ik}}{s_i} \frac{b_{ij}}{s_{ij}}.$$

Define $\tilde{C}_{ij} = 2C_{ij}/\gamma$ where γ is the margin. The authors have two bounds where the dependence on W appears logarithmically or directly. We focus on the former. The equation (16) gives the generalization error as

$$\mathcal{O}\left(\sqrt{\frac{\log(2W) \sum_{i,j} \overline{L}^2 \tilde{C}_{ij}^2}{m}} \right)$$

First, we have $W = |G| \max(c_0, c_1)$. Secondly, for the first layer, we have:

$$C_{11} \leq b_x \left(s_{11}s_{12}\right) \frac{s_{11}s_{12}}{s_{11}s_{12}} \frac{b_{11}}{s_{11}} = b_x b_{11} s_{12} \leq b_x M_2 \|\boldsymbol{w}\|_{2,1} ,$$

with

$$\|\boldsymbol{w}\|_{2,1} = \sum_{j=1}^{c_0} \|\boldsymbol{w}_{:,j}\|_2 .$$

Finally, for the last layer, we get:

$$C_{12} \leq b_x \left(s_{11}s_{12}\right) \frac{s_{11}s_{12}}{s_{11}s_{12}} \frac{b_{11}}{s_{11}} = b_x b_{12} s_{11} \leq b_x M_2 \|\boldsymbol{W}\|_{2\to 2}$$

Ignoring the constants and margins, the generalization error will be:

$$\mathcal{O}\left(\frac{b_x M_2 \log(|G| \max(c_0, c_1)) \sqrt{\|\boldsymbol{W}\|_{2\to 2} + \|\boldsymbol{w}\|_{2,1}}}{\sqrt{m}} \right).$$

Apart from its dimension dependence, both norms $\|\boldsymbol{W}\|_{2\to 2}$ and $\|\boldsymbol{w}\|_{2,1}$ are bigger than $\|\boldsymbol{w}\|$ used in our bounds. Therefore, our bound is tighter. However, they consider more general and exhaustive scenarios, including deep networks with residual connections and general Lipschitz activations.

Comparison with Wang and Wu (2023). In Wang and Wu (2023), they study the same set of problems as ours, related to locality and weight sharing, but from different perspectives. First, the approximation theory perspective, studying the class of functions a model can approximate, is complementary to our paper on the generalization error using statistical learning theory. The learning theory part of the paper is focused on a particular "separation task" (see (5)) with a fixed input distribution. They also use Rademacher complexity but bound it with a covering number. We work with general input distributions and arbitrary tasks. Besides, our bounds are dimension independent, while their bound has explicit dependence on the input dimension, an artifact of using covering number for bounding RC.

Comparison with Li et al. (2021). In Li et al. (2021), the authors consider the sample complexity of convolutional and fully connected models and constructs a distribution for which there is a fundamental gap between them in the sample complexity. Their analysis is based on the VC dimension and uses Benedek-Itai's lower bound. Their final bound is, therefore, dependent on the input dimension. In contrast, one of the main interests of our paper was to explore dimension-free bounds. We additionally study the impact of locality and weight sharing.

J.1 Regarding Norm-based bounds and Other Desiderata of Learning Theory

Dimension Free and Norm Based Bounds. Dimension-free bounds are interesting because they hint at why the generalization error is not affected by over-parametrizing the model. In this sense, the notion of dimension refers mainly to the input dimension, the number of channels, the width of a layer, and the number of layers. The same motivation existed for obtaining norm-based bounds for RKHS SVM models. The works of Golowich et al. (2018) and Vardi et al. (2022) are two recent examples, with the former work providing an extensive review of other dimension-free bounds. The choice of a proper norm to get dimension-free bounds is one of the main questions in learning theory. Naturally, this is easier to get for larger norms like Frobenius norms, and the question is if we can have similar dimension-free results for smaller norms like spectral or, as we show in the paper, the norm of effective parameters.

Tighteness of Rademacher Complexity. In the literature around deep learning theory, there are many works around questioning the relevance of classical learning theoretic results, for example using Rademacher complexity, norm-based bounds, and uniform convergence. We can refer for example to works such as Nagarajan and Kolter (2019); Jiang et al. (2020); Zhang et al. (2017); Zhu et al. (2021). It is fair to ask if Rademacher complexity analysis, in light of this criticisms, can provide tight bounds for our case. First of all, the preceding works focused on state of the art deep neural networks with large number of layers. Our study is limited to single-hidden layer neural networks. Second, Rademacher complexity is indeed tight for support vector machines Steinwart and Christmann (2008); Shalev-Shwartz and Ben-David (2014); Bartlett and Mendelson (2002). If we fix the first layer of our network and only train the last layer, then we have a linear model, and it is known that training it with Gradient descent with lead to minimum ℓ_2-norm solutions. For these sub-class of learning algorithms, the analysis boils to previous works on minimum norm classifiers as in Shalev-Shwartz and Ben-David (2014) for which the Rademacher complexity analysis is tight. Therefore, we believe that Rademacher complexity can still be a relevant tool for shallower models including those discussed in this paper.

Implicit Bias of Linear Networks Previous works also tried to characterize the effect of equivairance on the training dynamics. Lawrence et al. (2022) showed that deep equivariant linear networks trained with gradient descent provably converge to solutions which are sparse in the Fourier domain. While this work focuses on the effect of equivariance on optimization, the authors suggest that this implicit bias towards sparse Fourier solutions can be beneficial towards generalization in bandlimited datasets - which is common for non-discrete compact groups such as rotation groups and a common assumption in steerable CNNs. Similar results were also previously obtained in Gunasekar et al. (2018) for standard convolutional networks, which can be seen as an instance of GCNN with discrete abelian groups.

Discussions on the Limitations. In this paper, we provided a Rademacher complexity based bound for single-hidden layer equivariant networks. We obtained a lower bound showing the tightness of our analysis. The numerical results showed compelling scaling behaviors for our bound. However, there is still a gap between our bound and the generalization error. Our conjecture is that the gap is related to the idea of implicit bias. We conjecture that stochastic gradient descent training implicitly biases toward only a subset of the hypothesis space even smaller than norm-bounded functions. It is an important next step to tie these two analysis together by characterizing the implicit bias, for example in terms of some kind of norms, and then use Rademacher complexity analysis to find a bound on the generalization error based on the implicit bias.

On the other hand, we provided a lower bound on the Rademacher complexity. It would be, however, interesting to obtain such bounds by finding the fat-shattering dimension. If two points in the dataset can be transformed into each other by the action of group G, then the space of G-invariant functions cannot shatter

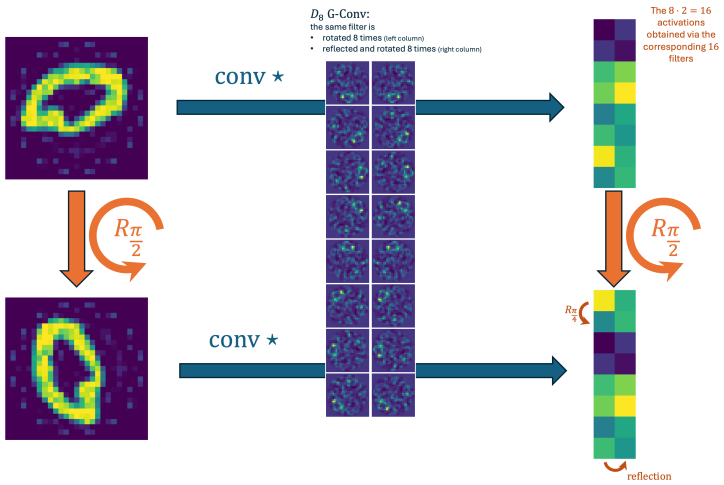

Figure 5: Graphical representation of the equivariant linear projection used to preprocess the image data. An example image is projected with a single filter rotated 8 times and mirrored and rotated 8 more times. The output is a $8 \cdot 2 = 16$ dimensional vector representing a signal over $G = D_8$. A rotation or mirroring of the input image results in a periodic shift or permutation of the output channels.

such datasets. Therefore, the data points should be picked on different orbits, so they can be shattered. Such a construction is an interesting future work.

K Experiment Setup

To pre-process the MNIST and the CIFAR10 datasets, we first create a single D_{32} steerable convolution layer with `kernel size` equal to the images' size, one input channel and $100 \times |D_{32}| = 6400$ output channels. In particular, under the steerable CNNs framework, we use 100 copies of the *regular representation* of the group D_{32} as output feature type. Alternatively, in the group-convolution framework, this steerable convolution layer corresponds to *lifting convolution* with 100 output channels, mapping a 1-channel scalar image to a 100-channels signal over the whole $\mathbb{R}^2 \rtimes D_{32}$ group; because the `kernel size` is as large as the input image (because we use no padding), the spatial resolution of the output of the convolution is a single pixel, leaving only a feature vector over $G = D_{32}$.

This construction guarantees that a rotation of the raw image by an element of D_{32} (and, therefore, of any of its subgroups) results in a corresponding shift of the projected 100-channels signal over D_{32}.

Fig. 5 shows an example of an input image projected with a single filter rotated 8 times and mirrored and rotated 8 more times (i.e. encoded via a $G = D_8$ steerable convolution). The output is a $8 \cdot 2 = 16$ dimensional vector representing a signal over $G = D_8$. A rotation or mirroring of the input image results in a periodic shift or permutation of the output channels.

Finally, to avoid interpolation artifacts, we augment our dataset by directly transforming the projected features (which happens via simple permutation matrices since the group D_{32} is discrete), rather than pre-rotating the raw images.

Our equivariant networks consist of a linear layer (i.e. a group convolution), followed by a ReLU activation and a final pooling and invariant linear layer as in eq. 3. All MNIST models are trained using the Adam optimizer with a learning rate of $1e-2$ for 30 epochs, while the CIFAR10 models are trained using with a learning rate of $1e-3$ for 50 epochs. Precisely, we use the MNIST12K dataset, which has 12K images in the training split and 50K in the test split.

All experiments were run on a single GPU NVIDIA GeForce RTX 2080 Ti.

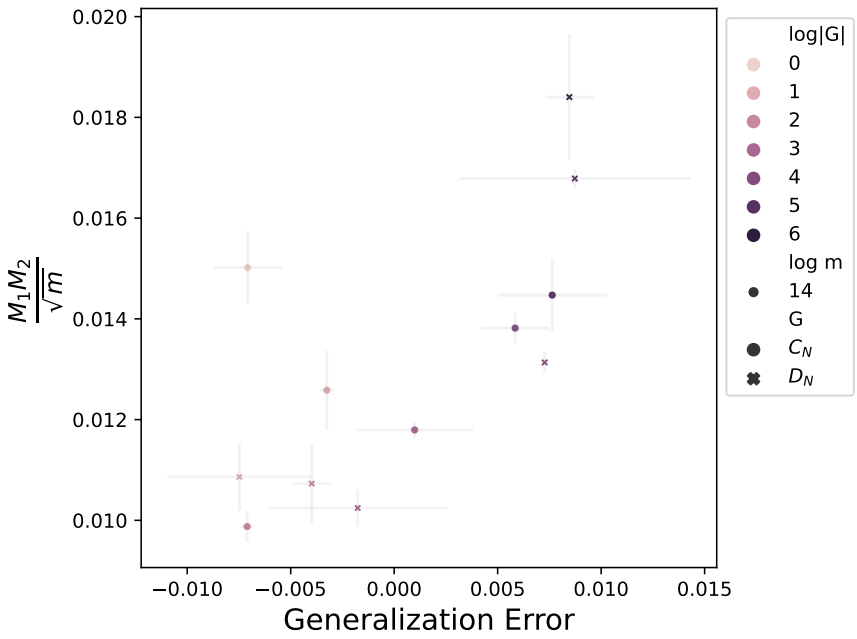

Figure 6: Subset of Fig. 2c focusing on the models training with the largest dataset size $m = 25600$. The models using the smallest equivariance groups show increased norms.